DLR-IB-FL-BS-2021-18

Development of an RNP AR APCH approach procedure within tight airspace constraints

Richard M. Unkelbach

Deutsches Zentrum
DLR für Luft- und Raumfahrt

Document properties

Title	Development of an RNP AR APCH procedure within tight airspace constraints
Subject	Designing an RNP AR approach for OBBS, simulator assessment in A320 FFS Level D (ground validation)
Institute	Institute of Flight Guidance
Compiled by	Richard M. Unkelbach
Participants	Dr. Thomas Dautermann
Classification	C/II (only for use in the Institute of Flight Guidance)
Date	28 January 2021
Version	1
File Path	Dokument5
Release Note	Document is released in accordance to Document Control Sheet

Abstract

Required navigation performance authorization required (RNP AR) approach (APCH) procedures are a special form of approaches with vertical guidance (APVs) where tougher navigation system requirements in terms of accuracy, integrity and functionalities allow smaller obstacle clearance areas and the use of curved legs in all approach segments. That leads to very flexible approach design possibilities compared to other instrument approach procedures and becomes especially valuable at airports surrounded by limiting terrain and/or airspace. This paper guides through the development of an RNP AR approach on runway 15L at Isa Air Base in Bahrain. The establishment of instrument approaches on this runway has been complicated so far as the final approach would have led straight through the controlled traffic region (CTR) of an adjacent air base. We show that entering the CTR, which ends less than 3.3 NM before the runway threshold, can be avoided with an RNP AR approach by employing a curved leg in the final approach segment and the highest possible navigation accuracy of RNP 0.1 – two unique features of RNP AR APCH. We then fly and test the procedure in an Airbus A320 level D full flight simulator under the wind and weather conditions considered by the procedure design rules. The results show that the actual navigation performance met the required one, so that we can prove that our approach is safe to fly.

Index of contents

1. Introduction

Despite their low importance for global air traffic, airports like Cristiano Ronaldo International of Funchal, Madeira or Innsbruck Airport in Austria are known worldwide for their challenging approaches [1]. Rapidly rising terrain but also surrounding airspace can prevent the operation of an instrument landing system (ILS), which still is predominantly used for precision approach (PA) procedures. Non-precision approaches (NPAs) based on radio navigation aids are often offered alternatively instead. However, because of the higher minima and lower precision associated with those procedures, the ability to approach an airport in unfavorable conditions (e.g. low visibility) becomes severely restricted. [2]

With the evolution of area navigation (RNAV) and especially since the ICAO introduced the performance-based navigation (PBN) concept, many navigation applications have been increasingly relying on Global Navigation Satellite Systems (GNSSs) instead of ground-based infrastructure [3]. That also applies to approach procedures and has opened up a new range of procedures including *Required Navigation Performance Approaches* (RNP APCHs) and *Required Navigation Performance Authorization Required Approaches* (RNP AR APCHs). The main difference between both lies in higher performance requirements with RNP AR APCH that require the aircraft operator to show evidence of aircraft capability and sufficient crew training before obtaining authorization from the State regulatory authority to conduct such procedures. In return, RNP AR APCH offers greater flexibility in procedure design due to improved navigational accuracy, integrity and additional functionalities. [4, p. (vii)] The most relevant advantages over RNP APCH can be seen in smaller obstacle clearance areas, whose width depends on the required accuracy, and that curved legs may also be used in the final approach segment. For instance, RNP AR APCH allows lateral accuracies that are up to three times higher (0.1 NM 95 percent total system error (TSE)) than the highest possible accuracy with RNP APCH (0.3 NM 95 percent TSE) in all approach segments while RNP APCH only allows its (lower) maximum accuracy in the final approach. [4, pp. 1-4ff.] That increases the chance of being able to establish three-dimensional instrument approaches also where terrain, obstacle or airspace constraints prohibit more conventional procedures. The aim of this paper is to exploit the unique features of RNP AR APCH by designing such a procedure for runway (RWY) 15L at Isa Air Base (OBBS), a Bahraini airfield in the south of Bahrain Island near the coast along the Persian Gulf. As shown in Fig. 1, the air base currently has two issues: Its proximity to another air base and its lack of instrument approaches. It has only one runway, RWYs 15L/33R, for normal operations. While RWY 33R is equipped with ILS, there are not yet any instrument approaches available for RWY 15L so that the air base can only be approached from the north if weather permits a visual approach. [5, pp. AD 2-OBBS-1ff.] That might lead to Isa Air Base becoming effectively cut off if visibility is low, e.g. due to dust haze, and RWY 33R cannot be used for landings, e.g. due to tailwind. However, especially given its function as an air base, it should be accessible as independent of weather as possible. On the other hand, establishing an instrument approach on RWY 15L is complicated because another airfield, Sakhir Air Base (OBKH), is located just less than 8 NM to the north-west within the extension of the runway

centerline. As OBKH is protected by a control zone (CTR), a type of class D airspace, that ends less than 3.3 NM short of RWY 15L, every approach on this runway must be coordinated closely with air traffic control (ATC) at Sakhir Air Base to avoid interfering with arriving or departing traffic at that airfield. [5, pp. AD 2-OBKH-1ff.] Ideally, the new approach procedure would thus have to feature low minimums and enable aircraft to avoid entering the CTR while approaching RWY 15L. That would facilitate air traffic management (ATM) in the area and contribute to a more seamless traffic flow into and out of both airfields. We aim to show that RNP AR APCH fulfills both requirements by utilizing all the flexible design possibilities that are available with this approach procedure. Representative of many aerodromes in demanding environments, the application at Isa Air Base shall emphasize the potential of RNP AR APCH in improving airport access where other procedures fail. With more and more affected countries (like Austria and Portugal) having started to implement RNP AR approaches, this paper shall also lead through the different steps of procedure design to give an example of how such an approach can be constructed [6, 7].

RNP AR APCH and RNP APCH are strongly tied to the PBN concept. PBN itself encourages the use of area navigation, where aircraft are no longer bound to navigate solely by ground-based radio aids, which would only allow them to fly from station to station. Instead, navigation data from one or multiple input sources (mainly GNSS) is integrated in a navigation computer, allowing flights on any desired path within the navigation system capability. [8, pp. I-Att A-1…4] Under PBN, it is now suggested that area navigation procedures are no longer developed sensor-based, i.e. mandating specific navigation equipment on board, but should require a certain navigation performance to be met. This is expressed in navigation specifications, which are split up between RNAV and RNP specifications. They differ in that the latter include the requirement for on-board performance monitoring and alerting. Within PBN, RNP APCH and RNP AR APCH are the two main navigation specifications for approach operations. [8, pp. I-A-1-1…5]

Further explanation of PBN-related terms and implementation guidance is provided in the *PBN Manual* (ICAO document 9613) [8]. The construction of instrument approach procedures is laid out in the second volume of ICAO document 8168: *Procedures for Air Navigation Services – Aircraft Operations* (PANS-OPS) [9] with RNP AR APCH being separately covered in ICAO document 9905: *Required Navigation Performance Authorization Required (RNP AR) Procedure Design Manual* [4]. In Europe, the implementation of PBN is regulated by Commission Implementing Regulation (EU) No 1048/2018 [10] whereas the certification requirements are described in *Certification Specifications and Acceptable Means of Compliance for Airborne Communications, Navigation and Surveillance* (CS-ACNS) [11]. In Bahrain, the Civil Aviation Affairs (CAA) as the national civil aviation authority governs the operational approval of PBN applications in Civil Aviation Publication (CAP) 11, Volumes 1-3 [12-14].

Each approach procedure normally consists of four different segments: The initial, intermediate and final as well as the missed approach [8, p. I-A-2-4]. Under PBN, those segments consist of different waypoints that are connected using specified leg types, called path terminators (they will be presented in the next chapter) [9, p. III-5-1-5]. In this paper, the approach is built

bottom-up, i.e. starting at the landing threshold point (LTP) with the final approach segment (FAS) and ending at the initial approach fix (IAF) with the initial segment before adding the missed approach segment (MAS). Beforehand, we give an overview of the basics of RNP AR APCH and discuss the suitability of other than RNP AR approach procedures for Isa Air Base in the next two chapters. Thereafter, we build the approach in three steps as explained above and based on the theoretical framework given by Ref. [4]. All necessary calculations are performed with MATLAB (Release 2020a). MATLAB's geoplot3 function, which allows to map coordinates into a three-dimensional representation of the globe, is then used to perform a qualitative obstacle assessment in the subsequent chapter, which is necessary to release the procedure for validation. Last, the developed approach is tested in an Airbus A320 level D full flight simulator with the results being discussed in the final chapter. The implementation process beyond the simulator assessment is out of the scope of this paper.

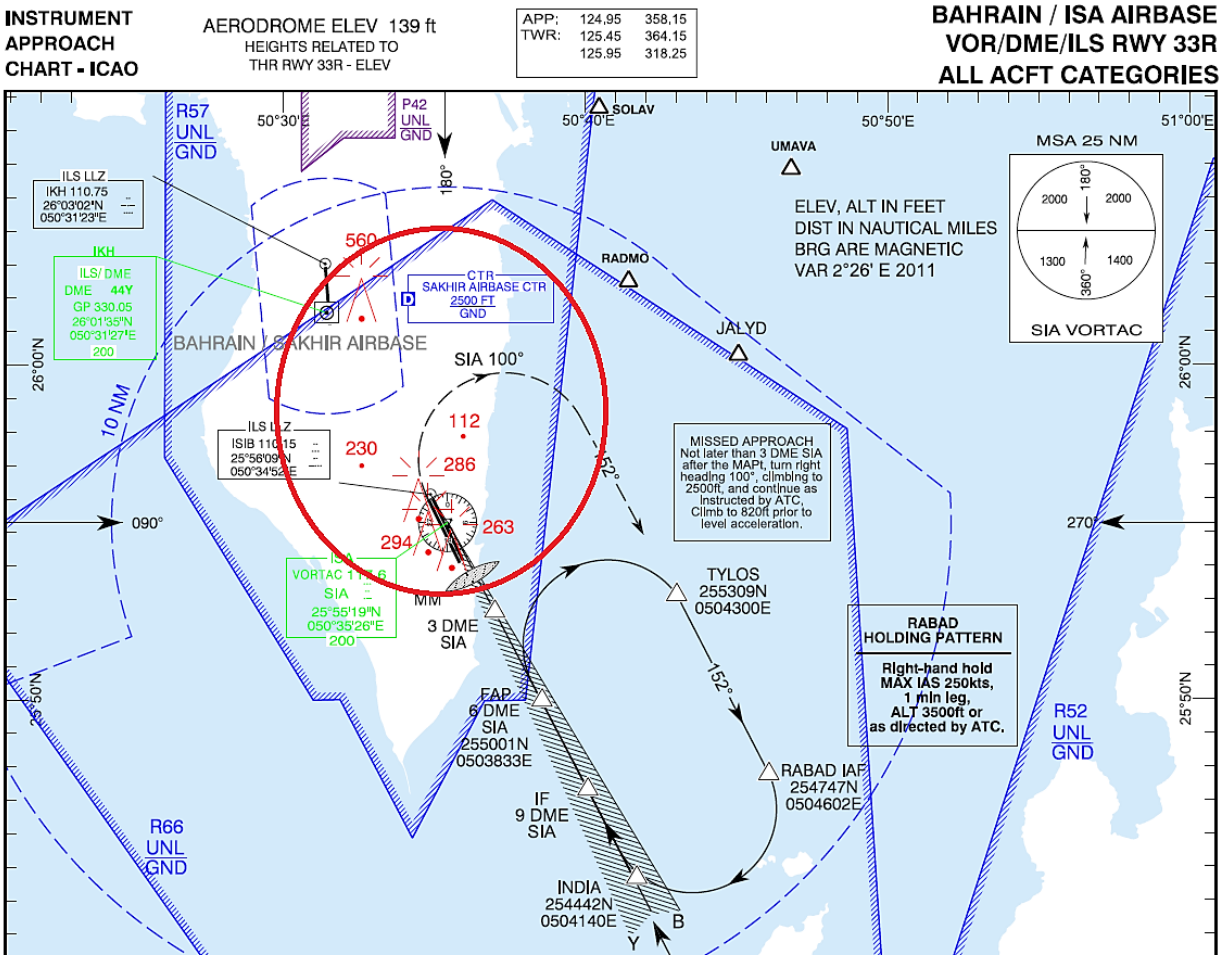

Fig. 1 Current approach situation at OBBS [5, p. AD 2-OBBS-14]

2. The basics of RNP AR APCH

The history of RNP AR APCH dates back to 1996, when Alaska Airlines conducted the first-ever RNP AR approach on RWY 08 at Juneau International Airport, Alaska. There, the airline had been frequently suffering from delays and disruptions due to bad weather before the new approach procedure enabled them to lower the minimums for landing and improve their operational performance. [15] At that time, RNP AR was not covered by Part 97 of the US Federal Aviation Regulations (FARs), under which all public instrument approach procedures in the US are developed. The US Federal Aviation Authority (FAA) instead approved it as a Special Airworthiness and Aircrew Authorization Required (SAAAR) procedure before officially recognizing the type later as *RNP SAAAR* procedures. [13, p. 68] Over the years, the regulatory basis for RNP SAAAR was expanded, e.g. in 2005 by providing airworthiness and operational approval guidance (advisory circular (AC) 90-101) [16] as well as procedure design rules (FAA order 8260.52) [17]. The term RNP itself has been around since 1990, when it was introduced by the ICAO Review of the General Concept of Separation Panel (RGCSP) as a "statement of the navigation performance necessary for operation within a defined airspace"[8, p. I-(x)]. However, the clear distinction between RNAV and RNP applications in terms of performance monitoring and alerting only came with the PBN concept, which was developed by the Required Navigation Performance and Special Operational Requirements Study Group (RNPSORSG) starting in 2003 [8, p. I-(xi)]. The publication of the PBN manual in 2008 finally harmonized the different perceptions of RNAV and RNP at ICAO level, which also heralded the change from RNP SAAAR to RNP AR [18, 19]. Yet, it probably does not help that until 30 November 2022, RNP AR APCH procedures may (according to ICAO) still be charted as "RNAV (RNP) RWY XX" [9, p. III-5-1-3]. That often leads to them being called "RNAV RNP approaches" or "RNP approaches" in contrast to "RNAV approaches" for RNP APCH procedures [18]. It should be clear that while RNP AR uses area navigation (RNAV, as it is done under all PBN navigation specifications), it essentially relies on performance monitoring and alerting functions and does so even more than RNP APCH, the other RNP specification for approaches [8, p. II-A-2-8]. In return, it offers greater operational safety and efficiency but only for those operators with an official approval, so as to ensure that they and their crews can cope with the higher demands and complexities of the approach procedure [4, p. (vii)]. That is reflected in "AR" (*authorization required*), the most notable difference at first sight.

In accordance with ICAO Annex 6, RNP AR APCH procedures are categorized as *approach procedures with vertical guidance* (APVs) [4, p. 1-1]. As RNP only applies to lateral performance under PBN, specifications like RNP AR APCH also contain requirements for vertical guidance that can be provided by systems using either barometric altitude or augmented GNSS [8, p. I-A-1-3]. The latter comes in the form of a space-based augmentation system (SBAS), which is currently not available in Bahrain [20]. Thus, we develop our procedure based on the use of a barometric vertical navigation (baro-VNAV) system.

Any PBN navigation specification consists of requirements in four domains [8, p. I-A-1-3]:

- navigational performance in terms of accuracy, integrity and continuity
- functionalities of the navigation system
- navigation sensors of the navigation system
- procedures (involving e.g. flight crew actions) necessary to meet the required performance

Lateral accuracy within PBN is generally defined by an accuracy value X as follows: RNAV X for RNAV specifications and RNP X for RNP specifications. X equals the total system error (TSE) in NM that must be achieved at least 95 percent of the flight time [8, p. I-A-1-4]. RNP AR APCH is unique in that it allows values as low as 0.1 for all approach segments, which will prove to be a major advantage during the implementation at Isa Air Base [4, p. 2-2]. Possible accuracy values for each segment are listed in table 1. The vertical accuracy is described by the vertical system error that (amongst others) depends on the aircraft height above the local altimetry reporting station and thus changes with the aircraft descending towards the runway. Its three-sigma value must not exceed a certain limit, which is calculated as described in the PBN manual and becomes smaller with decreasing aircraft height. Integrity is ensured using different monitoring and alerting systems as well as pilot procedures. In general, both undetected (integrity failure) and detected conditions must not lead to the aircraft exiting the obstacle clearance volume of the procedure with a probability greater than 10^{-7} per approach. [8, pp. II-C-6-7f.]

To allow the high performance, RNP AR APCH also requires a variety of functionalities. For instance, the flight crew must be enabled to distinguish the aircraft position relative to the defined path on the primary flight instruments so that they can determine whether the cross-track deviation exceeds the required lateral accuracy (1x accuracy value) and whether the vertical deviation exceeds a margin of 75 ft. Additionally, a numerical display of the lateral and vertical deviation with a high resolution must be provided. Further functionalities include one of the special features that RNP AR APCH is known for: The use of radius to fix (RF) legs, a path terminator describing curved paths based on a constant radius between two fixes. They may, unlike in other procedures, be employed in all approach segments including the final approach [8, p. II-C-App 1-1]. Moreover, the navigation system must be able to follow (at least) a geodesic line between two fixes (TF), a direct path to a fix (DF), a specified track to a fix that is defined by a course (CF) and a specified track to an altitude (FA). [8, pp. II-C-6-10…16] The sensor requirements with RNP AR APCH are based on GNSS as the primary navigation aid (NAVAID) infrastructure [8, p. II-C-6-1]. It is required that aircraft are equipped with a GNSS augmentation system based on GPS, such as an aircraft-based augmentation system (ABAS). Detailed sensor requisites are laid out in the PBN manual, e.g. that the sensor lateral accuracy for ABAS must be better than 36 m (95 percent probability). Other requirements address the use of Inertial Reference Units (IRUs), air data systems, flight management systems (FMSs) and the autopilot. [8, pp. II-C-6-8f.] Required flight crew procedures include the management of different navigation accuracies, monitoring the lateral and vertical track deviation and contingency procedures. Many more, also addressing ATC, the aircraft operator, the flight dispatcher etc. are listed in the PBN manual. [8, pp. II-C-6-16ff.]

Another important characteristic of instrument approaches is their protection against obstacles (including terrain), which is generally provided by two kinds of obstacle clearance areas called primary and secondary areas. Primary areas directly surround the nominal track and guarantee a constant minimum obstacle clearance (MOC) in the vertical direction across their width. Secondary areas are attached to the edges of the primary area and initially provide the same MOC (at the transition line), which then gradually decreases to zero towards their outer edges. [9, p. I-2-1-2] The lateral, vertical and longitudinal extent of the obstacle clearance areas creates an obstacle clearance volume that, as the name suggests, must be clear of obstacles. It can also be considered an expression of the navigation performance associated with a certain procedure: The smaller the volume, the higher must be the required accuracy to ensure that an aircraft does not leave the volume and run into obstacles. Therefore, primary and secondary areas are sometimes called containment areas because they must contain the aircraft position with a very high probability (RNP AR APCH: $1\text{-}10^{-7}$ or greater, see p. 3). [9, p. II-3-1-App B-1] RNP AR APCH does not use secondary areas. The primary area has a semi-width equal to 2x accuracy value of the respective approach segment. [4, p. 2-2] Hence, the total area width can vary from 0.4 NM with the highest navigation accuracy (RNP 0.1) to 4 NM with the lowest navigation accuracy (RNP 1). In most cases, different segments require different accuracies (with the final approach being the most sensitive), so that the surfaces become narrower towards the runway. The MOC changes with different approach segments as well: The initial approach requires 300 m, the intermediate approach 150 m whereas the final approach has a dynamic MOC that is based on the current vertical error performance of the baro-VNAV system [4, pp. 4-16ff.]. As the vertical accuracy improves with decreasing aircraft height, the MOC becomes smaller towards the runway. For the missed approach segment, the MOC may be as low as zero in certain cases [4, p. 4-44].

At Isa Air Base, small containment areas are material to avoid entering the CTR. The weather-related accessibility of the air base, though, is improved by achieving low values for the decision altitude/height (DA/H), at which the landing must be aborted if the required visual reference to continue the approach has not been established [4, p. (ix)]. With RNP AR APCH being categorized as APV, the lowest possible DH is 250 ft. However, approaches where the MAS is based on RNP 1 (standard value) only have the obstacle clearance altitude/height (OCA/H) published [4, p. 2-1]. That is the altitude/height until which obstacle clearance, which is always more and less limited by obstacles or terrain in the vicinity of the aerodrome, can be provided according to the respective obstacle clearance criteria [9, p. I-1-1-7]. Therefore, the minimum DA/H (the effective one can be further increased) must equal either 250 ft or the OCA/H, whichever is greater [9, p. I-4-5-12].

Segment	Minimum	Standard	Maximum
Initial Approach	0.1	1	1
Intermediate Approach	0.1	1	1

Final Approach	0.1	0.3	0.5
Missed Approach	0.1	1	1

Table 1 Possible navigation accuracies for different approach segments [4, p. 2-2]

3. RNP APCH and precision approach procedures at Isa Air Base

As described in the introduction, the main issue of Isa Air Base is its proximity to Sakhir Air Base and its CTR in the north-west. Following the centerline (= final approach track) of RWY 15L into OBBS, the CTR ends just less than 3.3 NM short of the runway threshold (THR) (see Fig. 1). It reaches from the surface up to 2500 ft – an altitude that would require approaching aircraft to descend on a glide path of at least 6.58 degrees towards the runway if they were to fly over the CTR. As most approaches are based on 3-degree glide paths, it becomes clear that the only way to avoid flying through the CTR is to fly by it [9, p. I-4-5-2].

While this paper deals with RNP AR APCH, that does not imply that no other procedures would be available. However, they might not be as suitable for the envisaged operations against the background of having to provide a short straight final, preceded by a sharp turn combined with a very high navigation accuracy to keep as much away from Sakhir Air Base and the CTR as possible. In general, instrument approach procedures are divided into non-precision approaches (NPAs), APVs and precision approaches (PAs). NPAs only provide two-dimensional guidance, whereas APVs and PAs provide three-dimensional guidance. In contrast to APVs, PAs also allow decision heights below 250 ft and have higher performance requirements. [21] Since RNP AR APCH procedures are already APVs, NPAs will not be considered as alternatives.

3.1. RNP APCH with LNAV/VNAV and LPV minima

RNP APCH is the other main PBN navigation specification for approach operations (advanced RNP (A-RNP) could also be used but is mainly based on RNP APCH [8, p. II-A-1-2]). It offers different performance standards for the final approach which are identified in different minima called LNAV, LP, LNAV/VNAV and LPV. Only the last two include vertical guidance. [8, pp. II-C-5-1ff.] The lateral navigation/vertical navigation (LNAV/VNAV) minimum is used when the RNP system VNAV capability relies on barometric altimetry or augmented GNSS. One significant difference to RNP AR APCH is the fixed and lower possible navigation accuracy of 0.3 NM in the final and 1 NM in all other approach segments (95 percent TSE) that results from lower aircraft and system requirements. [8, pp. II-C-5-4…9] The obstacle clearance areas are larger with semi-widths between 0.95 NM in the final and 2.5 NM in the initial and intermediate approach segments (RNP AR APCH: 0.2 NM with RNP 0.1 in all segments) [9, p. III-1-2-7]. In contrast to RNP AR APCH, the final segment must be straight and has a minimum length of 3 NM, while track changes at the final approach point (FAP), where the final segment begins, are limited to 15 degrees with fly-by turns and 45 degrees with RF legs [9, pp. III-3-2-3, III-3-3-1]. At Isa Air Base, that would cause the FAP to be located just 0.3 NM away from the beginning of the CTR so that it would be impossible to avoid entering the CTR during the preceding turn. Even though it would be possible to set the final approach track off by up to 15 degrees within a minimum distance from the threshold, the small offset angle and large containment areas would still lead to considerable

possible violations of the CTR. Besides, offset procedures are more complicated and likely to be degraded in availability with bad weather due to a higher minimum OCA/H. [9, p. III-3-4-9]

The localizer performance with vertical guidance (LPV) minimum applies to RNP systems using augmented GNSS mostly in the form of SBAS [8, p. II-C-5-17]. Although SBAS is not yet offered in Bahrain, it might be enabled by future projects such as the extension of the Indian GPS-aided GEO augmented navigation (GAGAN) system [22]. The main difference to LNAV/VNAV is the angular depiction of the deviations from the nominal track in the final approach, i.e. the required navigation performance (especially the flight-technical error (FTE)) becomes higher with the aircraft nearing the threshold. If certain signal-in-space requirements (improved vertical performance) are met, LPV procedures can even be flown as category (CAT) I precision approaches with a DH as low as 200 ft. [8, pp. II-C-5-17…25] However, these advantages mainly come into play shortly before landing. Compared to LNAV/VNAV, the minimum length of the straight final approach segment remains 3 NM while the preceding intermediate segment must be at least 2 NM long and aligned with the final segment, except when an RF leg with a track change of no more than 45 degrees is used [9, pp. III-3-2-3f.]. Accordingly, an LPV procedure would not be able prevent a violation of the CTR but the containment areas would be a bit smaller. For example, the minimum semi-area width corresponding to a 3-NM final segment equals 0.95 NM at the FAP compared to 1.45 NM with LNAV/VNAV. As LPV is intended to be used mainly with the final segment, though, improved containment cannot be achieved until 2 NM before the FAP. While the final approach track can generally be set off, the offset angle may not exceed 5 degrees compared to 15 degrees with LNAV/VNAV. [9, pp. III-3-5-2ff.] Therefore, LPV procedures would be preferred to LNAV/VNAV for normal operations due to their higher accuracy but probably abandoned for offset operations, where LNAV/VNAV allows greater flexibility.

3.2. ILS, GLS

Precision approaches are defined as three-dimensional instrument approach procedures based on ILS, a microwave landing system (MLS), a ground-based augmentation system (GBAS) landing system (GLS) or SBAS (CAT I) [21]. Since MLS has never been broadly used, only ILS and GLS are discussed. As opposed to APVs, both rely on ground-based infrastructure. For ILS, that is the localizer and glideslope emitting radio waves modulated with 90 Hz and 150 Hz signals to guide the user towards the runway. [2] GLS uses GBAS, the other common GNSS augmentation system besides SBAS, which requires GNSS reference receivers and a ground facility as well as a data link at the aerodrome to calculate and broadcast the correction signals [23]. The construction criteria for both procedures are very similar. As with SBAS, the precision guidance applies mainly to the final segment, while the initial approach is based on an RNAV or RNP specification with an accuracy of 1 NM or better. The Intermediate Fix (IF), marking the beginning of the intermediate segment, must be placed on the final approach (GLS)/localizer (ILS) course at least 3 NM ahead of the FAP (assuming an intercept angle of up to 90 degrees). The then following precision segment must also be at least 3 NM long, i.e. the minimum length of the runway-aligned straight segment equals 6 NM. Consequently, ILS and GLS procedures would cause the most extensive violation of

the CTR, even though the effectively flown straight distance would be a bit smaller due to the fly-by turn at the IF. Obstacle clearance at the FAP is assessed with ILS obstacle assessment surfaces that are smaller than those of LNAV/VNAV and similar to those of LPV. However, they might be overlapped by the RNAV- or RNP-based protection areas of the IF turn if the turn angle is big enough. Thus, PAs should only be considered for Isa Air Base if it was necessary to achieve minimums below 250 ft without being able to use SBAS. The procedure design criteria are too conservative and inflexible for the application in restricted airspace. [GLS: 9, pp. III-3-6-1ff.; ILS: 9, pp. II-1-1-1ff.]

All in all, none of the alternative approach procedures would allow to avoid flying through OBKH CTR while approaching RWY 15L. That is due to the requirement of a straight final segment and bigger containment areas related to degraded accuracy towards the FAP. Only RNP AR APCH does not have those limits - it is the only approach procedure allowing curved segments in and providing a high accuracy beyond the final approach. Therefore, it is obviously the best-fitting option for Isa Air Base.

4. Procedure Construction

4.1. Basic Considerations

4.1.1. Reference Frame

The procedure can only be constructed in a suitable reference frame. For RNP AR APCH, that must be "a conventional x, y, z coordinate system with its origin at LTP and parallel to the world geodetic system (WGS) WGS-84 ellipsoid […] The x-axis is parallel to the final approach track: positive x is the distance before threshold and negative x is the distance after threshold. The y-axis is at right angles to the x-axis. The z-axis is vertical, heights above threshold being positive" [4, p. 4-2]. Assuming that the last part of the final approach is aligned with the runway centerline, we need at least two points to define the frame - the threshold positions of RWYs 15L and 33R. They are given in the aeronautical information publication (AIP) for the Bahrain flight information region (FIR), which also covers Isa Air Base, in the latitude, longitude and height (LLH) format [5, p. AD 2-OBBS-3]. The required frame, however, is based on a rotated east north up (ENU) frame. ENU frames are local and tangent as their origin can be freely chosen with the x-axis pointing east, the y-axis pointing north and the z-axis pointing up opposite to the gravity vector at the origin. [24, p. 1] If such a frame is placed at the LTP (= THR RWY 15L) and rotated until the x-axis lies on the (extended) centerline, pointing in the direction of RWY 33R, all requirements for the reference frame are fulfilled. To do so, we first convert both threshold positions from LLH into ENU with the LTP as origin. The conversion process is explained in Drake [24], Table 2 contains the new threshold coordinates in ENU (not yet rotated). The frame must then be rotated in the X-Y plane counterclockwise through the angle between local east (x-axis) and the true bearing of RWY 33R (new x-axis). The exact bearing is determined using trigonometric functions as shown in Fig. A1. With true bearings of 153.8194° (RWY 15L) and 333.8194° (RWY 33R), the ENU frame must be rotated by 116.1806° (90° + φ, see Fig. A1). Any position in the "old" ENU frame is expressed in the rotated frame by multiplying its position vector by a rotation matrix as in Eq. (1) [25]. Table 2 also contains the rotated threshold positions.

$$\begin{bmatrix} x \\ y \\ z \end{bmatrix}_{ENU,rotated} = \begin{bmatrix} \cos(\alpha) & \sin(\alpha) & 0 \\ -\sin(\alpha) & \cos(\alpha) & 0 \\ 0 & 0 & 1 \end{bmatrix} * \begin{bmatrix} x \\ y \\ z \end{bmatrix}_{ENU,old} ; \alpha = 116.1806° \quad (1)$$

Position	LLH	ENU [m]	ENU (rotated) [m]
THR RWY 15L	(255601.55N, 0503456.12E, 136 ft)	(0, 0, 0)	(0, 0, 0)
THR RWY 33R	(255410.69N, 0503556.38E, 29 ft)	(1677.2, -3411.5, -33.75)	(-3801.5, 0, -33.75)

Table 2 RWY 15L/33R THR positions in different coordinate systems (rounded)

The rotated x-coordinate of THR RWY 33R should now equal the runway length (3800 m according to the AIP [5, p. AD 2-OBBS-3], probably rounded), which is the case. The y-coordinate is zero, proving that the x-axis of the rotated frame is fully aligned with the runway centerline.

From here on, all calculations are performed inside the rotated frame. Once the procedure design is completed, positions of e.g. waypoints must be converted back into LLH for coding and publication. To do so, the ENU frame must first be rotated back by $-\alpha$ before the positions (then in standard ENU) can be further converted (see Ref. [26]).

4.1.2. General Approach Shape

Before any approach segment can be constructed, we must decide on the general shape of the approach so that the first segment (final approach) can be designed accordingly. The top priority is to avoid entering OBKH CTR. As explained in chapter III, that requires approaching aircraft to fly by it in a turn as flyovers are not possible. The chart for the ILS approach on RWY 33R (see Fig. 1) provides an example of how that could look like: The ILS missed approach procedure includes a sharp right turn immediately behind the threshold of RWY 15L so that the CTR is not violated. If it were possible to fly that procedure backwards, i.e. turning left towards the runway as late and as sharply as possible, we could avoid entering the CTR if the containment areas were small enough. However, that requires the permissibility of turns so close to the runway and that the required turn radius is flyable. The feasibility of that model, which primarily concerns the final segment, is examined in part B. The possibility of approaching Isa Air Base from the West (in a right turn) is not considered because the probability of entering the CTR would obviously be higher then (see Fig. 1).

4.1.3. Speed Category

Every approach is designed for a certain aircraft performance, which significantly depends on speed. It influences the construction of e.g. turns and the glide path. In order to provide a standardized basis for the comparison of different aircraft, they are classified into five different speed categories (A – E) according to their speed at threshold. The procedure herein is developed for aircraft of category D or lower, i.e. the indicated air speed (IAS) at threshold must not exceed 165 kt. [4, p. 3-1]

4.2. Final Approach Segment

Even though RNP AR APCH allows curved segments in the form of RF legs in the final approach, the turn must not end directly at the runway. Instead, a straight segment between the exit point of the RF leg, called final approach roll-out point (FROP), and the LTP is mandated whose minimum length is defined by the greater of two requirements: [4, p. 4-22]

a) The FROP must be located at least 150 m above the LTP. That yields a minimum length D_{150} (see Eq. (2)).

b) The FROP must be located so that it is reached at least 15 s before the aircraft reaches the OCA/H if the missed approach is based on RNP 1, or 50 s if the missed approach is based on a higher navigation accuracy or RNP APCH. That yields a minimum length $D_{15s/50s}$ (see Eq. (3)).

$$\boldsymbol{D_{150} = \frac{150 - RDH}{\tan(VPA)}} \tag{2}$$

$$\boldsymbol{D_{15s/50s} = \frac{OCH - RDH}{\tan(VPA)} + (V_{TAS} + 27.78) * 4.167 \left[* 3\frac{1}{3}\ for\ D_{50s}\right]} \tag{3}$$

Since the turn cannot end at the runway, it should at least end as close to the runway as possible. Therefore, we need to minimize the length of the straight segment by minimizing D_{150} and $D_{15s/50s}$. The greater of both values sets the position of the FROP, from which we then construct the turn and examine whether it is still possible to avoid entering the CTR.

4.2.1. Minimizing D_{150}

D_{150} depends on the reference datum height (RDH) and the vertical path angle (VPA). The RDH is the height of the glide path above threshold and the VPA is the angle of the glide path [4, p. 4-2]. Steep VPAs and large RDHs minimize D_{150}. With RNP AR APCH, the recommended RDH for CAT D is 50 ft plus or minus 5 ft, thus we choose 55 ft (*RDH = 55 ft*) [4, p. 4-26]. Table B1 contains the standard and maximum VPA values for the different approach segments, the final approach may have VPAs between 3 (standard) and 3.1 degrees. While choosing the latter value would make sense in terms of a minimizing D_{150}, we must also consider that the maximum permitted VPA can be limited further by temperature. That is due to the use of a baro-VNAV system which is calibrated according to the International Standard Atmosphere (ISA) model. Any temperature deviations from ISA cause errors in the pressure altimeter readings that grow with the deviation. Temperatures above ISA cause the output of lower altitudes than real, leading the effectively flown VPA to be higher (compared to the design value). Conversely, temperatures below ISA cause lower effective VPAs. If temperatures are very hot, that effect might lead to exceeding the maximum permitted effective VPA which equals 1.13 times the maximum design VPA, i.e. 3.503 degrees for the final approach. Choosing higher design VPAs increases that risk and with the air base lying in the Gulf Region where temperatures are very high during summer, we assume that even the standard VPA could turn into a critical effective VPA during the hottest days of the year. Therefore, once we have built the final approach, it must be checked that the effective VPA does not exceed its lower and upper limit for the lowest and highest expectable temperature, respectively. That check requires the position of the FAP, though, which is yet unknown. [4, pp. 4-26…30] For this reason, we set the VPA at 3 degrees first (*VPA = 3°*). The procedure should be available all year long, thus it is essential that the maximum effective VPA is not exceeded because the design VPA is too high. If the chosen VPA proves to be uncritical, it can still be increased.

Taken together, the RDH and the VPA lead to a required minimum FROP distance of D_{150} = *2541.6 m*.

4.2.2. Minimizing $D_{15s/50s}$ and initial obstacle assessment

Besides the RDH and the VPA, $D_{15s/50s}$ also depends on the OCH, the true airspeed (TAS) and the missed approach RNP. We choose the latter at 1 so that we can implement the 15-second requirement ($RNP_{missed\ approach}$ = *1*). The TAS is the speed of the aircraft relative to the surrounding airmass and is based on the IAS corrected for instrument and position installation errors, compressibility effects as well as temperature and pressure altitude [27]. For RNP AR APCH, it is calculated according to Eq. (4) (non-SI units) [4, pp. 3-2f.]:

$$\boldsymbol{TAS = \frac{IAS * 171233 * [(288 + VAR) - 0.00198 * H]^{0.5}}{(288 - 0.00198 * H)^{2.628}}} \quad (4)$$

VAR equals the temperature deviation from ISA, H equals the aircraft altitude. For D_{15s}, the TAS must be based on a flight at aerodrome elevation (139 ft, [5, p. AD 2-OBBS-1]) and with 15 degrees Celsius above ISA (ISA+15). The IAS must be chosen according to the fastest applicable aircraft category (CAT D). Table B2 lists the standard and minimum speeds for CAT D aircraft within the different approach segments. Since lower speeds minimize D_{15s}, we choose the minimum possible IAS of 165 kt for the final approach which yields a TAS of approximately 169.6 kt.

The last variable is the OCH, which can only be obtained from an obstacle assessment for the final and the missed approach. It is determined with obstacle assessment surfaces (OASs) that must be established around the existing approach track. As we have not yet constructed any of the required segments, we cannot determine the OCH although we need it to build the approach since it could define the FROP position (via D_{15s}) and with that the position and shape of the final approach turn. Consequently, the interdependence between obstacle assessment and procedure design forces us to develop the approach iteratively: At first, we can only estimate the OCH and use that value to build a test version of the final approach, which is used to build the rest of the approach. It is then possible to construct the OASs so that we must carry out a full obstacle assessment to examine whether the estimated OCH equals the true one, can be lowered or must be further increased. The latter case would lead to an increase in D_{15s}, i.e. the FROP and the preceding trajectory would have to be pushed further away from the threshold. Then again – with the new approach trajectory, it would have to be verified that obstacle clearance is still achieved with the updated OCH *and* the shifted surfaces. [4, pp. 4-43f.] The next step will thus be to find an estimate for the OCH to calculate D_{15s} and determine the FROP position. It should be as accurate as possible to avoid having to revise the approach later.

With RNP AR APCH, the OCH is determined using three OASs: The final approach OAS, the missed approach/Z surface and a horizontal surface in between. It equals the sum of the height of the highest real or equivalent approach obstacle, whichever is greater, and a height loss margin

(161 ft for CAT D). In terms of obstacle assessment, obstacles are those objects that penetrate an OAS. Obstacles penetrating the final approach or the horizontal surface are called approach obstacles, obstacles penetrating the Z surface are called missed approach obstacles. The height of real approach obstacles refers to the physical height of approach obstacles while the height of equivalent approach obstacles refers to calculated imaginary heights (equivalent heights) of missed approach obstacles. Equivalent heights are used for comparison between both obstacle types as missed approach obstacles are located in an area of the MAS where aircraft are assumed to be climbing again, i.e. the greatest physical obstacle height does not necessarily lead to the largest OAS penetration [4, pp. 4-39…46]. The construction of the different OASs is described in appendix C. Even though we cannot yet determine the exact coordinates of each OAS, it is possible to determine the start of climb (SOC), i.e. the beginning of the Z surface, with the variables that we have already set. Its threshold distance is calculated according to Eq. (5) as the horizontal distance to the point where the applicable height loss margin is reached on the glide path (here: 161 ft as fictitious OCH') less the transition distance (TrD). The TrD, in turn, is calculated as in Eq. (6) and can also be determined (see appendix C for explanation). [4, p. 4-39]

$$X_{SOC} = \frac{OCH' - RDH}{\tan(VPA)} - TrD = \frac{161\,ft - 55\,ft}{\tan(3°)} - 4466.5\,m \approx -3850\,m \tag{5}$$

$$TrD = \frac{15\,s * GS}{3600} + \frac{4}{3} * \sqrt{(1.225 * RNP)^2 + (18.3\,m)^2 + (\frac{22.9}{\tan(VPA)}\,m)^2} = [\dots] \approx 4466.5\,m \tag{6}$$

It is based on a 15-second transition from the final approach RNP to the missed approach RNP and consists of the horizontal distance flown with the maximum final approach speed (has been restricted to 165 kt IAS) during that time and a four-standard deviation value for the along-track error components. The error value consists of the 99.7 percent along-track error (first bracket, 1.225 NM), the 99.7 percent waypoint resolution error (second bracket, 18.3 m fixed) and the 99.7 percent flight technical error (third bracket, 436.958 m).

According to Eq. (5), the Z surface begins approximately 3850 m down the runway, even behind the threshold of RWY 33R. Knowing that the final approach OAS must end before the threshold of RWY 15L, the entire runway and also significant parts of the air base must hence be covered by the horizontal surface (depending on whether they lie within the missed approach splay or not). To find an estimate for the OCH, we therefore consider any obstacles at the aerodrome first as many of them can be assumed to penetrate that surface. The AIP specifies no obstacles in approach and take-off areas as well as only three aerodrome obstacles for Isa Air Base whose coordinates are converted from LLH into the reference format [5, p. AD 2-OBBS-3]. They are also marked on the approach chart for RWY 33R (see Fig. 1). Table 3 contains their

positions, the lateral and longitudinal offsets are related to the LTP and equal the y- and x-coordinates, respectively, of the obstacles in the reference frame. The height above threshold equals the z-coordinate. The north antenna is the tallest obstacle and would cause an OCH of 318 ft (157 ft + 161 ft) if it is located within the missed approach splay. The splay also depends on the navigation accuracy for the final approach, which determines its initial width. With the top priority of avoiding entering OBKH CTR by keeping the containment areas as small as possible, we choose the highest navigation accuracy with RNP 0.1 ($RNP_{final\ approach} = 0.1$). Thus, the lateral OAS bounds splay from 0.2 NM at the OCA/H point[1] to 2 NM semi-width, which happens over 6.7 NM. The splay to 0.52 NM semi-width, which would be sufficient to include the north antenna, is completed after 1.19 NM. An OCH of 318 ft would place the OCA/H point more than 0.82 NM before the threshold (see Fig. A2) so that a semi-width of 0.52 NM would already be reached 0.37 NM behind the threshold. Since the north antenna lies 0.96 NM behind the threshold, it is definitely covered by and penetrates the horizontal surface.

Neither the approach chart for RWY 33R nor satellite images show any indication of even higher obstacles in the vicinity of the air base. For that reason, we set the OCH at 318 ft based on the north antenna (*OCH = 318 ft*).

Designator	Elevation, ft	Height above THR, ft	Lateral offset, NM	Longitudinal offset, NM
Water Tower	285	148.68	0.6	0.085
North Antenna	294	156.95	0.52	-0.96
South Antenna	263	124.72	0.52	-1.52

Table 3 Aerodrome obstacles

For the 15-second requirement, that yields a minimum FROP distance of $D_{15s} = 2954\ m$ from the threshold. As D_{15s} is larger than D_{150} (see p. 8), the FROP is placed at 2954 m before the threshold ($x_{FROP} = 2954$) on the final approach track ($y = 0$), where the glide path has a height of 563 ft ($z = 171.6\ [m]$) above threshold. Its position relative to the runway and the CTR is illustrated in Fig. A3.

4.2.3. Final approach turn construction

With the FROP given, it is now possible to construct the turn segment. The turn must be as sharp as possible, therefore we need to minimize the radius, which is calculated according to Eq. (7). The radius depends on a flown TAS, a tailwind component (TWC) and a turn rate (R) (see Eq. (8)), which also depends on the flown bank angle (α): [4, p. 3-4]

[1] Our abbreviation for the point where the respective OCA/H is reached on the glide path.

$$r = \frac{TAS + TWC}{20 * \pi * R} \tag{7}$$

$$R = \frac{3431 * \tan(\alpha)}{\pi * (TAS + TWC)} \tag{8}$$

Greater turn rates lead to smaller radii, which can be achieved with higher bank angles and lower speeds. We set the bank angle at 20 degrees, the maximum possible value for RNP AR APCH ($\alpha = 20°$) [4, p. 3-6]. The tailwind and the TAS both depend on altitude, the TAS additionally requires the flown IAS and the outside temperature (see Eq. (4)). The IAS for the final approach was already set for the straight segment with the lowest possible value of 165 kt. Higher temperatures increase the TAS, which is counterproductive in terms of smaller radii. However, we must ensure that the procedure is safe to fly even on the hottest days of the year. That is why the turn construction is based on the highest expectable temperature, which is determined as explained in appendix D and equals 45.01 degrees Celsius. In July 2020 though, temperatures in Bahrain even rose above 47 degrees Celsius [28]. We therefore choose a temperature deviation of ISA+35 that covers temperatures up to 50 degrees Celsius, providing a margin in case temperatures should rise further in future. Higher altitudes equally cause greater radii because they lead to a higher TAS and usually more tailwind. The construction must be based on the highest altitude in the turn, which is reached at the entry point as the straight segment VPA is extended into the turn. For a fixed altitude, the corresponding TWC can either be derived from local wind data or interpolated from the tables given in the procedure design manual (see table B3), which we use herein (our values are based on linear interpolation). [4, pp. 3-3f.] The turn altitude is the last missing variable. With a constant VPA within the turn, the height difference between the entry and the exit point grows with the turn length. Knowing that higher altitudes lead to larger radii, we thus need to find a compromise between the track change achieved with the length of the turn and the resulting radius. The turn must ensure to lead approaching aircraft past Sakhir Air Base, providing as much distance between the approach track and OBKH CTR as possible. Assuming that entering the CTR can indeed be avoided, the most critical point within the turn is where the distance to the CTR becomes minimal. Fig. 2 shows that the turn and the CTR boundary first converge until the south-eastern endpoint of the CTR (hereafter called "SE point") with the straight CTR boundary segment running south-southeast while the turn – a left turn coming from the east – converges. Behind the SE point, though, the CTR boundary suddenly changes into a right turn running west while the approach track continues as a left turn running south, i.e. both tracks diverge. Due to that convergent-divergent configuration, the minimum distance to the CTR will be reached at a point near the SE point. Consequently, the turn should not begin behind that point (hereafter called "critical point").

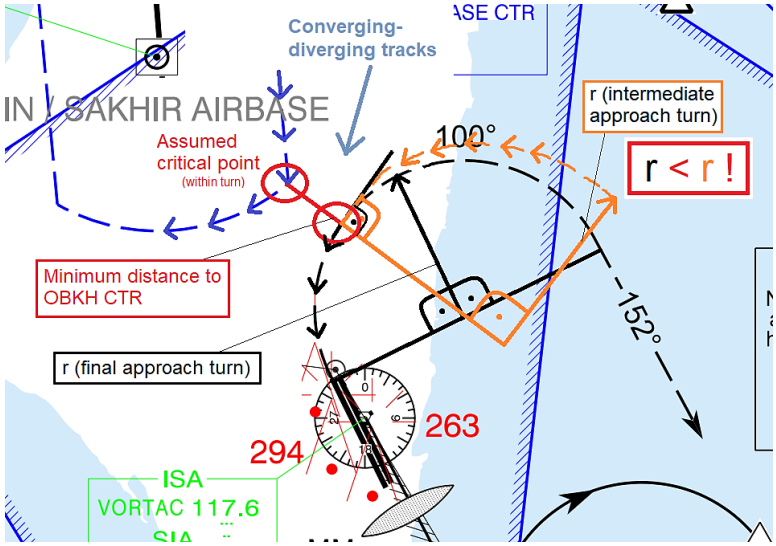

Fig. 2 Converging-diverging configuration of the approach and CTR boundary tracks [5, p. AD-2-OBBS-14]

However, there are no arguments against starting the turn at or just before the critical point. That would keep the entry altitude as low as possible, hence minimize the radius and increase the minimum distance to the CTR. A larger total track change (e.g. 180 degrees as in Fig. 2) can still be achieved by employing another RF leg beforehand that we would use as intermediate approach segment. Since RF legs are tangent to their in- and outbound tracks at the entry and exit points, respectively, and since the previous turn would follow the same turn direction, its larger radius would not influence the minimum distance to the CTR [4, p. 4-10]. That is also due to the converging-diverging track configuration. If anything, the larger radius might cause the aircraft to fly a bit closer to the CTR before the critical point than if the final turn was extended before the CTR. However, that is acceptable as long as the minimum distance, which is the only relevant one, can be increased in return. To determine the optimal turn radius, it is necessary to find the altitude that is reached at the desired entry point – at or just before the critical point – within the turn when used for the turn construction (see Eqs. (4), (7), (8)). If it is reached later (behind the critical point), the aircraft would enter the turn at a higher altitude that might cause a larger radius, so that the turn would no longer be flyable. If it is reached earlier (well before the critical point), the aircraft would pass the critical point at a lower altitude, thus the calculated radius would be larger than necessary, shortening the distance to the CTR. Since the shape of the turn and hence the position of the critical point change with different "construction altitudes", we need an iterative approach to find the optimal radius: First, we choose an initial construction altitude based on trial and error and calculate the resulting turn. The turn, including its lateral containment areas (the VEB is irrelevant in relation to the CTR), is then plotted in MATLAB together with the CTR boundary, which enables us to visually assess whether the CTR is violated or not. Next, we calculate the minimum distance between the outer turn area boundary, i.e. the outer boundary of the containment area as it is closest to the CTR, and the CTR boundary. That gives us the position of the critical point within the turn, including its altitude. If that altitude is higher than the initial value, the construction altitude is increased; if it is lower, also the construction altitude is

lowered. Those steps should technically be repeated until the current construction altitude matches the current critical point altitude. However, since the turn entry point also serves as FAP, which is (along with other relevant fixes) only established at round altitudes in 100-ft increments, we can stop iterating for the round altitude that is reached closest to, but still before the critical point [4, p. 4-18]. The limited step size also keeps the number of required iterations relatively small. The results are summarized in table 4. The following sections deal with the implementation of the single steps of an iteration.

Construction altitude (CA) ->	**Radius ->**	**Penetration of OBKH CTR? ->**	**Minimum distance to OBKH CTR ->**	**…reached at ->**	**Consequence**
1500 ft	2.0342 NM	NIL	≈ 11 m	1311 ft	Lower CA
1400 ft	**1.9863 NM**	**NIL**	**≈ 47.6 m**	**1307 ft**	**Lower CA**
1300 ft	1.9389 NM	NIL	≈ 84.6 m	1304 ft	Higher CA -> 1400 ft

Table 4 Final approach turn iterations

Step 1 consists of the turn construction. With the given altitude (e.g. 1500 ft), we first calculate the TAS according to the other chosen parameters and interpolate the TWC before determining the turn rate and the radius (see p. 10). We describe every turn in cylindrical coordinates where any position within the turn is defined by the turn radius, an angle from a reference direction, the position of the turn center and a height above the origin of the reference frame. Since the outbound track of the final approach turn (from the FROP towards the RWY) follows the x-axis, we locate the turn center as the position of the FROP shifted by -r (r = radius) lengths along the y-axis (see Fig. 3). The height z of any point within the turn, specified by an angle φ to a reference direction, equals the arc length to a reference point which is multiplied by the tangent of the VPA and added to the height of the reference point. With the FROP as reference, that yields (φ in rad):

$$z(\varphi) = d_{arc}(\varphi) * \tan(VPA) + z_{ref} = (r * |\varphi_{FROP} - \varphi|) * \tan(3°) + z_{FROP} \quad (9)$$

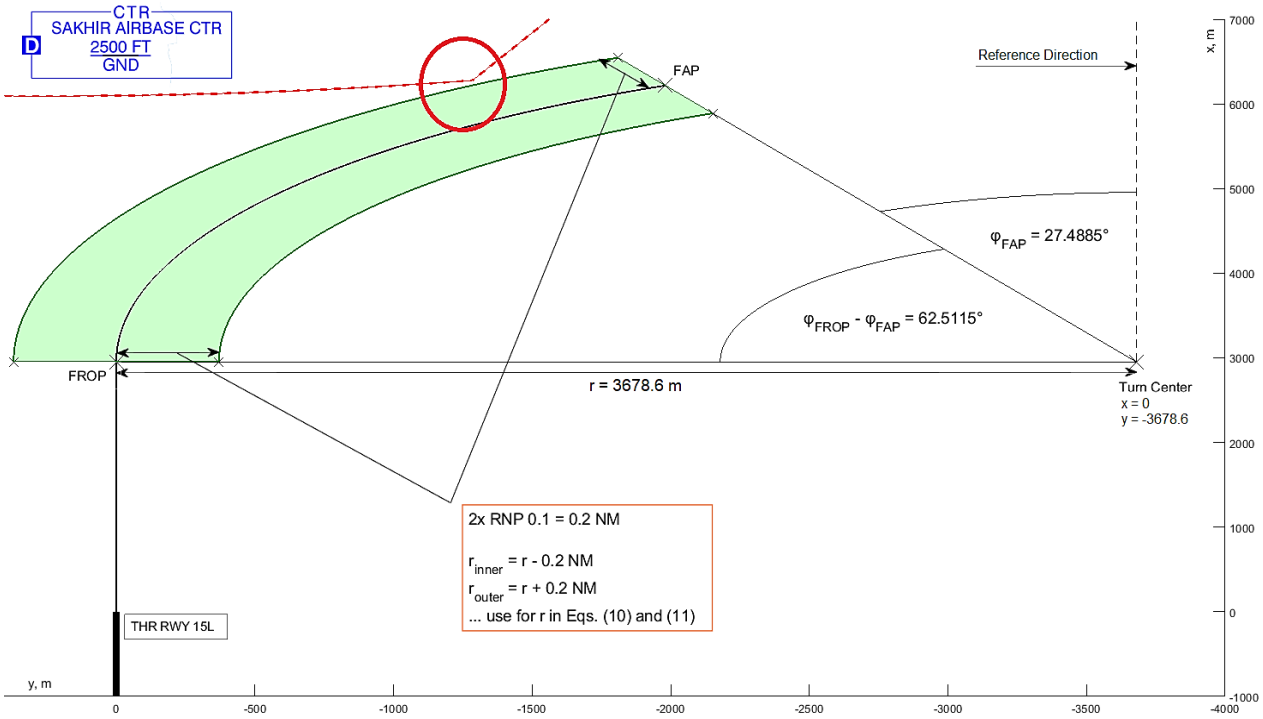

Fig. 3 Final approach turn construction (final version with FAP at 1400 ft, containment areas in green).

The position of the entry point is yet unknown because we do not know its angular position φ. However, we can use its altitude (e.g. 1500 ft) to solve Eq. (9) for φ, which is needed to describe the turn in the horizontal plane as with Eqs. (10) and (11). It is important to note that "altitude" refers to height above mean sea level and does not equal the z-coordinate in our reference frame, which is the height above THR RWY 15L. Consequently, all altitudes must be converted accordingly before they can be used as z-coordinates. The interval for φ in Eqs. (10) and (11) is adapted to the reference direction we chose for the final turn (positive x from the turn center, constant y) and based on the FAP altitude of 1400 ft, as illustrated in Fig. 3. In this case, the turn ends at 27.4885 degrees left off the turn center, where 1400 ft are reached on the 3-degree glide path.

$$\boldsymbol{x(\varphi) = r * \cos(\varphi) + x_{turn\ center};\ \varphi \in [27.4885°, 90°]} \tag{10}$$

$$\boldsymbol{y(\varphi) = r * \sin(\varphi) + y_{turn\ center};\ \varphi \in [27.4885°, 90°]} \tag{11}$$

Besides the nominal track, we must also construct the lateral containment areas for the turn. For RF legs, that is the area between the outer and inner turn area boundaries, which are themselves RF legs. They cover the same angular sector as the nominal turn, though with radii being increased or decreased, respectively, by 2x navigation accuracy (here: RNP 0.1). Their height equals the height of the nominal track on the same radius (constant φ) and is determined by

inserting any φ from the defined interval back into Eq. (9). [4, p. 4-10] That yields the vertical profile shown in Fig. 4.

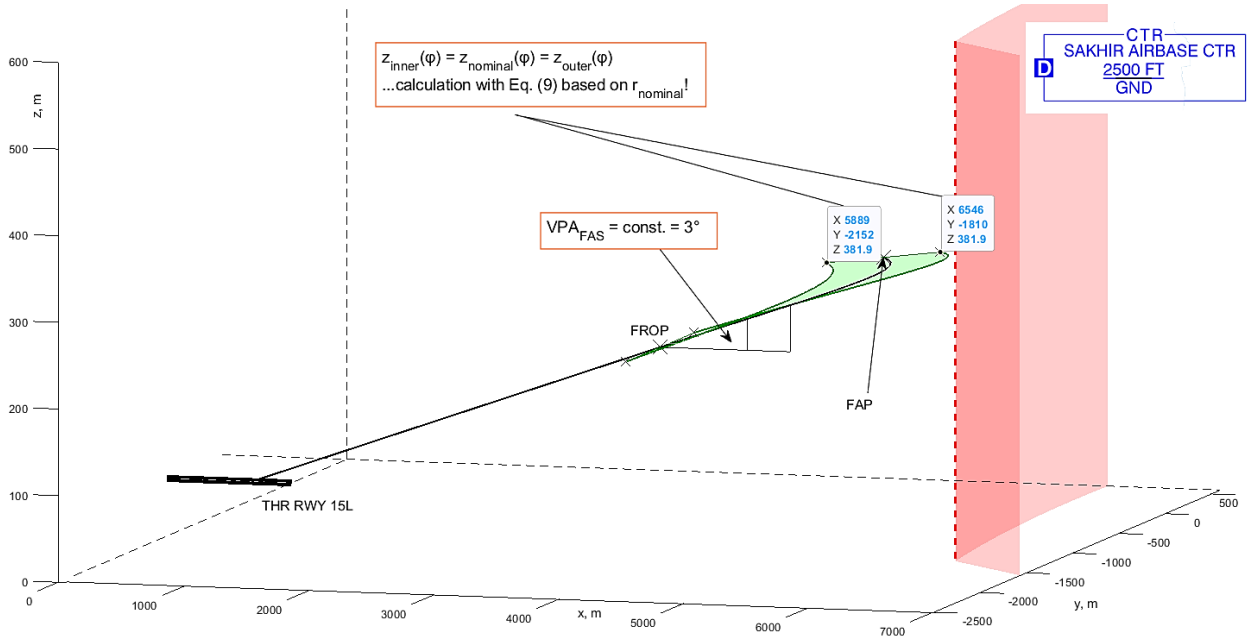

Fig. 4 3-D profile of the final approach turn (FAP at 1400 ft, containment areas in green)

Step 2 consists of assessing possible violations of the CTR by plotting the turn and its containment area together with CTR boundary. That requires a mathematical description of the CTR that can be implemented along with Eqs. (9)-(11), resulting in imagery such as Figs. 3 and 4. The implementation is described in detail in appendix E, part A.

Step 3 is the last step and consists of determining the minimum distance to the CTR and locating the critical point. Due to the convergent-divergent configuration of the outer turn area and the CTR boundary (see Fig. 3), it is safe to assume that the minimum distance occurs between the south-eastern endpoint of the CTR (hereafter called "SE point") and the nearest point on the outer turn area boundary. We therefore only need to consider the section of both boundaries within that region. The idea is to define and discretize those sections and calculate the 2-D (X-Y) Euclidean distances between each of the outer turn area and each of the CTR boundary positions. The minimum of those distances is considered the minimum distance to the CTR, which thus is numerically determined. The implementation of this concept is described in appendix E, part B. As shown in table 4, we carried out three iterations whose results are summarized in Fig. 5. We discovered that the initially chosen construction altitude of 1500 ft does not lead to a CTR violation and is reached before the critical point so that we could lower the construction altitude to the next possible value (1400 ft). This also meant that we could exclude any CTR violations for the remaining iterations as the final construction altitude (FAP altitude) would not become greater than the initial value. The determination of the critical points proved that the minimum distance to the CTR always occurs

towards the SE point (as expected) on the radial line from the turn center to the SE point. That is not surprising as the shortest distance theorem states that the minimum distance between a point (SE) and a line (outer turn area boundary) is always described by the perpendicular line between both. As the third iteration revealed that a FAP at 1300 ft would be located behind the critical point, we choose the FAP altitude with 1400 ft which yields a turn radius of 3678.6 m (see Figs. 3-4) and a minimum distance of just 47.6 m to the CTR.

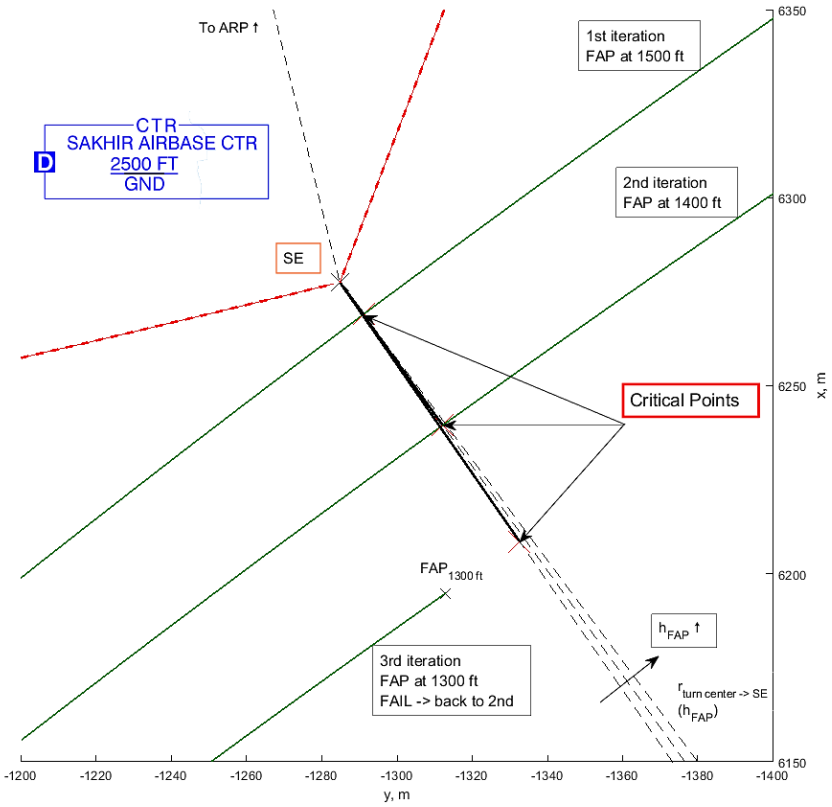

Fig. 5 Outer turn area boundaries for different construction altitudes near OBKH CTR

Before finishing the final approach segment and as mentioned during the selection of the VPA (see p. 8), it must still be checked whether the effective VPA, caused by the temperature-related pressure altimeter errors of uncompensated baro-VNAV systems, does not deviate too significantly from the design VPA. Its lower limit is 2.5 degrees for the average coldest temperature (11.33° C), its upper limit is 3.503 degrees for the average hottest temperature (45.01° C). In both cases, it is assumed that any temperature deviation from ISA leads to an altimeter error that grows with the height difference between the FAP and the LTP as follows (non-SI units): [4, pp. 4-28…30]

$$\Delta z_{error} = \Delta T * \left(\mathbf{0.19} + \left(\mathbf{0.0038} * (z_{FAP} - z_{LTP})\right)\right) + \left(\mathbf{0.032} * (z_{FAP} - z_{LTP})\right) + \mathbf{4.9} \quad (12)$$

ΔT is the temperature difference to the ISA temperature at aerodrome elevation (139 ft, 14.7248° C). The altimeter error (Δz_{error}) equals the vertical displacement of the aircraft at the FAP, i.e. the FAP is overflown at an "effective" height that equals its nominal height minus ($\Delta T < 0$) or plus ($\Delta T > 0$) the altimeter error. The effective VPA is then calculated between the origin of the glide path at threshold level and the effective FAP height (the horizontal distance between the FAP and the runway remains unchanged). [4, pp. 4-28…30]

Due to the mild winter in Bahrain, the minimum effective VPA barely differs from the design value (3 degrees) with approximately 2.93 degrees. In contrast, the upper effective VPA limit is reached at ISA+33.5, which equals 48.5 degrees Celsius at sea level. Since that is hotter than the average hottest temperature, the chosen VPA is proven safe to fly all year long. If we had chosen a steeper VPA of 3.1 degrees at the beginning, the maximum allowable temperature would have sunk to 38.9 degrees Celsius, a temperature that is regularly exceeded in Bahrain during the summer months. Consequently, our initial decision to use a 3-degree VPA is confirmed and the final approach segment, as depicted in Figs. 3 and 4, can remain unchanged.

4.3. Intermediate Approach Segment and Initial Approach Segment

The intermediate approach segment "is the segment in which aircraft configuration, speed and positioning adjustments are made for entry into the FAS" [4, p. 4-16]. We develop it together with the initial segment so that we need to define the starting point of the approach first. In general, approaches begin at the IAF and continue on the initial segment until the intermediate fix (IF), where the intermediate segment to the FAP begins [9, pp. I-1-1-4f.].

We choose the IAF to be an already existing waypoint in the vicinity of the aerodrome to facilitate the transition from en-route navigation structures (waypoints and airways) to local approach structures. The en-route navigation can then be exited at a waypoint that also serves as the beginning of the approach with no additional segment required in between [9, p. I-4-2-1]. The ILS approach chart for RWY 33R (see Fig. 1) shows six waypoints around Isa Air Base. Two of them, TYLOS and RABAD, are also used for the ILS approach. While starting the approach out of RADMO or JALYD would mitigate the magnitude of the required turn towards the runway, TYLOS and RABAD have the operational advantage that they could be used as IAFs for both runways. That would provide greater flexibility in ATM because approaching aircraft only need to be dispatched to one waypoint[2] irrespective of the approach direction, which is why we choose TYLOS as IAF (RABAD is located further away from the threshold).

To reach the FAP out of TYLOS, the approach must first lead straight ahead down to a point where a left turn towards the FAP is initiated. With any turn making the procedure more complex, we choose to follow the track from RABAD to TYLOS also out of TYLOS down to the point where it intersects with the turn from the FAP. That way, the approach could also be started out of RABAD (e.g. after a go-around) without having to fly another turn at TYLOS. With only two

[2] According to the approach chart, RABAD is used as IAF for RWY 33R, however the approach could also be started out of TYLOS since it includes a procedure to fly from TYLOS to RABAD.

segments between the IAF and the FAP, the straight segment will form the initial approach while the intermediate approach will consist of the turn to the FAP. That turn is, like all turns for this approach are, constructed as an RF leg. We prefer them to fly-by turns due to their higher precision (smaller containment areas), especially with large track changes, which facilitates the obstacle assessment and narrows the noise affected area on the ground [4, pp. 4-9, 11].

As RF legs are tangent to their in- and outbound tracks at their entry and exit points, respectively, there is only one possible geometry allowing a turn that is aligned with both the final approach track at the FAP and the RABAD-TYLOS-track at a yet unknown IF. That geometry is defined by the turn center and the turn radius, which are determined as follows: First, the intersection of the in- and outbound tracks must be found. Both span a certain angle at the intersection. The turn center is then located on the bisector through that intersection at the point where the bisector intersects with the line perpendicular to the outbound track at the FAP. The radius equals the length of the perpendicular. This geometric method is illustrated in Fig. 6 that shows the finished RF leg - the result of implementing the method, which is described in the following section.

The in- and outbound tracks, despite being straight segments, can still be defined in cylindrical coordinates where the radius is variable and the radial (angular position φ) is fixed. Since the problem is two-dimensional (at least in our reference frame), we do not have to use the z-coordinate so that the cylindrical coordinates become polar coordinates. The inbound track starts out of TYLOS on the same radial as the track to TYLOS does at RABAD. TYLOS lies at 0.9777 degrees left off RABAD (in relation to positive x), thus the track is not exactly parallel to the runway centerline but the two converge towards north. Consequently, any position on the inbound track at a distance r from TYLOS is calculated as follows (see Fig. A4 for illustration):

$$\boldsymbol{x_{inb} = \cos(0.9777°) * r_{inb} + x_{TYLOS}} \tag{13}$$

$$\boldsymbol{y_{inb} = \sin(0.9777°) * r_{inb} + y_{TYLOS}} \tag{14}$$

The outbound track is tangent to the final approach turn at the FAP, which lies at 27.4885 degrees left off the final approach turn center (in relation to positive x). Any position on the outbound track at a distance r from the FAP is thus calculated as follows (see Fig. A4 for illustration):

$$\boldsymbol{x_{outb} = x_{FAP} + \sin(27.4885°) * r_{outb}} \tag{15}$$

$$\boldsymbol{y_{outb} = y_{FAP} - \cos(27.4885°) * r_{outb}} \tag{16}$$

To find the common intersection, we follow the same procedure as for determining the minimum distance to the CTR (see Appendix E). Therefore, Eqs. (13)-(16) are discretized with radius

values, which yields vectors with the x- and y-coordinates of the discrete in- and outbound track positions. Next, we calculate the Euclidean distances between all possible position pairs and search for the minimum distance together with the associated radii. The minimum distance must be zero at the intersection, hence the discrete radii are adjusted in range and step size until that is achieved. We then obtain the position of the intersection by inserting one of the two associated radii (in- or outbound track) back into Eqs. (13)-(14) or (15)-(16), as appropriate. Together with the angle of intersection and as illustrated in Fig. A5, we can determine that the bisector lies at 59.2331 degrees left off the intersection in relation to positive y. Consequently, any position on the bisector at a distance r from the intersection is calculated as follows:

$$\boldsymbol{x_{bi} = x_{intersection} - \sin(59.2331°) * r_{bi}} \tag{17}$$

$$\boldsymbol{y_{bi} = y_{intersection} + \cos(59.2331°) * r_{bi}} \tag{18}$$

The perpendicular to the FAP is calculated based on the outbound track rotated by 90 degrees, i.e. it lies at 27.4885 degrees right off the FAP in relation to negative x (see Fig. A6):

$$\boldsymbol{x_{perp} = x_{FAP} - \cos(27.4885°) * r_{perp}} \tag{19}$$

$$\boldsymbol{y_{perp} = y_{FAP} - \sin(27.4885°) * r_{perp}} \tag{20}$$

The intersection of the bisector and the perpendicular is determined as explained above. It equals the turn center of the intermediate approach turn and lies at a distance of 5171 m from the FAP (= turn radius). The angular positions of the IF and the FAP, which define the central angle over which the turn extends, are given by the in- and outbound tracks, respectively. Thus, the intermediate approach is fully defined in the X-Y plane and can be described by Eqs. (21) and (22). As the reference direction has changed compared to the final approach, the FAP now lies at 117.4885 degrees left off the turn center (namely in relation to negative y). The entire segment is shown in Fig. 6.

$$\boldsymbol{x_{int} = x_{int\ turn\ center} + \sin(\varphi) * 5171\ m;\ \varphi \in [0.9777°, 117.4885°]} \tag{21}$$

$$\boldsymbol{y_{int} = y_{int\ turn\ center} - \cos(\varphi) * 5171\ m;\ \varphi \in [0.9777°, 117.4885°]} \tag{22}$$

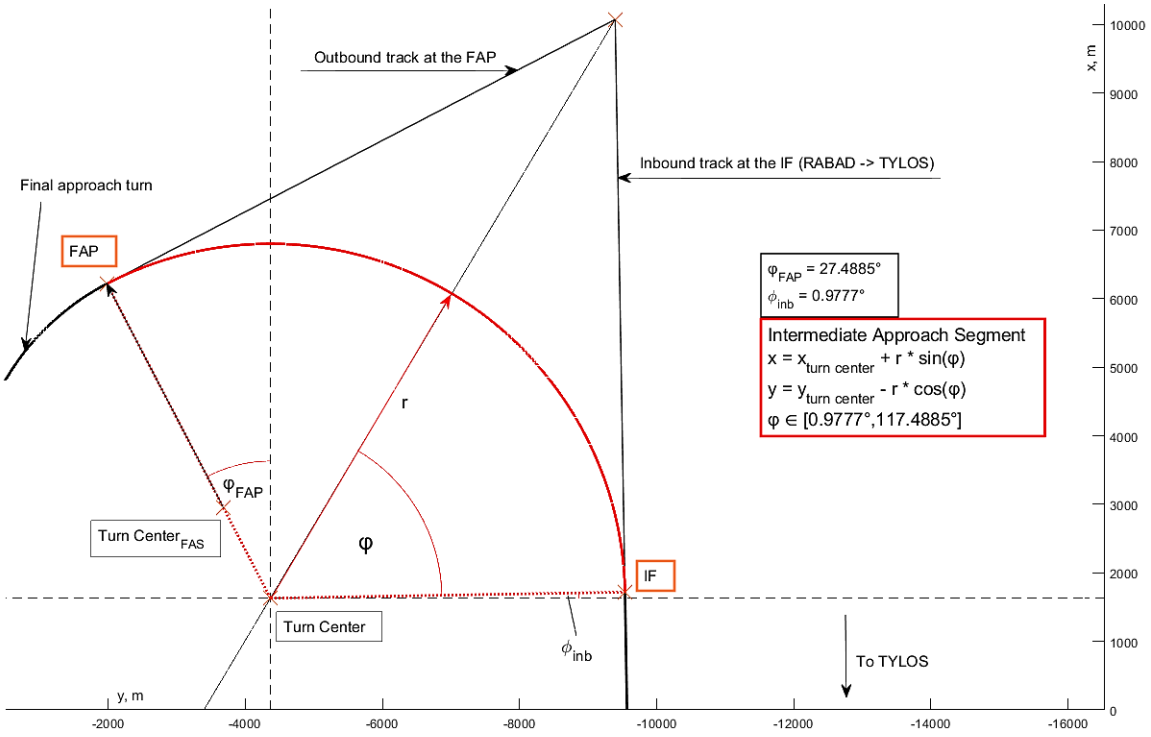

Fig. 6 Intermediate approach RF leg construction and definition

The heights within the turn depend on the VPA, which has a standard value of 1.4 degrees or lower for the intermediate approach (see table B1). Like the FAP, also the IF and the IAF must be established at round altitudes (multiple of 100 ft) [4, pp. 4-16, 18]. In contrast to the construction of the final approach, the (X-Y) position of the turn entry point is fixed this time so that we need to adjust the VPA to achieve that. The height of any intermediate approach position is calculated with Eq. (9), though with the FAP as reference point and not the FROP. For a VPA of 1.4 degrees, that yields an IF altitude of 2256 ft. In order not to exceed the standard VPA, we select the next lower altitude of 2200 ft for the IF which leads to a VPA of 1.3066 degrees (promulgated as 1.3 degrees). For the final approach turn, the radius was determined based on certain values for aircraft and wind speed, altitude, temperature and the bank angle, whereas the intermediate turn has been constructed on a geometric basis as a required ground track. Therefore, it must be checked whether the radius is at all flyable within the allowed limits [4, p. 4-10]. To do so, we choose initial values for the IAS, the bank angle and the temperature deviation and calculate the resulting radius with the chosen IF altitude and the corresponding wind values based on Eqs. (8) and (9). Table 5 shows the results for different configurations.

Altitude (fixed)	TWC (fixed)	IAS (variable)	Bank Angle	Temperature Deviation (variable)	Radius
2200 ft	50 kt	180	18°	ISA+35	5070.6 m < 5171 m
2200 ft	50 kt	185	18°	ISA+35	5297.8 m > 5171 m
2200 ft	50 kt	185	19°	ISA+35	4999.2 m < 5171 m

Table 5 Resulting turn radii for different speeds and bank angles (intermediate approach)

Consequently, the intermediate approach is safe to fly even in the most unfavorable conditions (high temperatures, strong tailwind), though only if the highest possible speed restriction (180 kt IAS, see table B2) or a higher than standard bank angle is used.

The initial approach consists of the straight segment from TYLOS to the IF. It has a horizontal length of more than 6.7 NM, which would allow to descend over 1700 ft on the standard initial approach VPA of 2.4 degrees (see table B1). That would place the IAF at approximately 3900 ft. Generally, there are barely any requirements for a specific IAF altitude, however "the initial segment procedure altitude/height should be established to allow the aircraft to intercept the FAS descent gradient/angle from within the intermediate segment" [4, p. 4-16]. We therefore place the IAF at 3000 ft, especially considering the tight speed restrictions of the intermediate and the final approach that become increasingly hard to manage with greater descent rates.

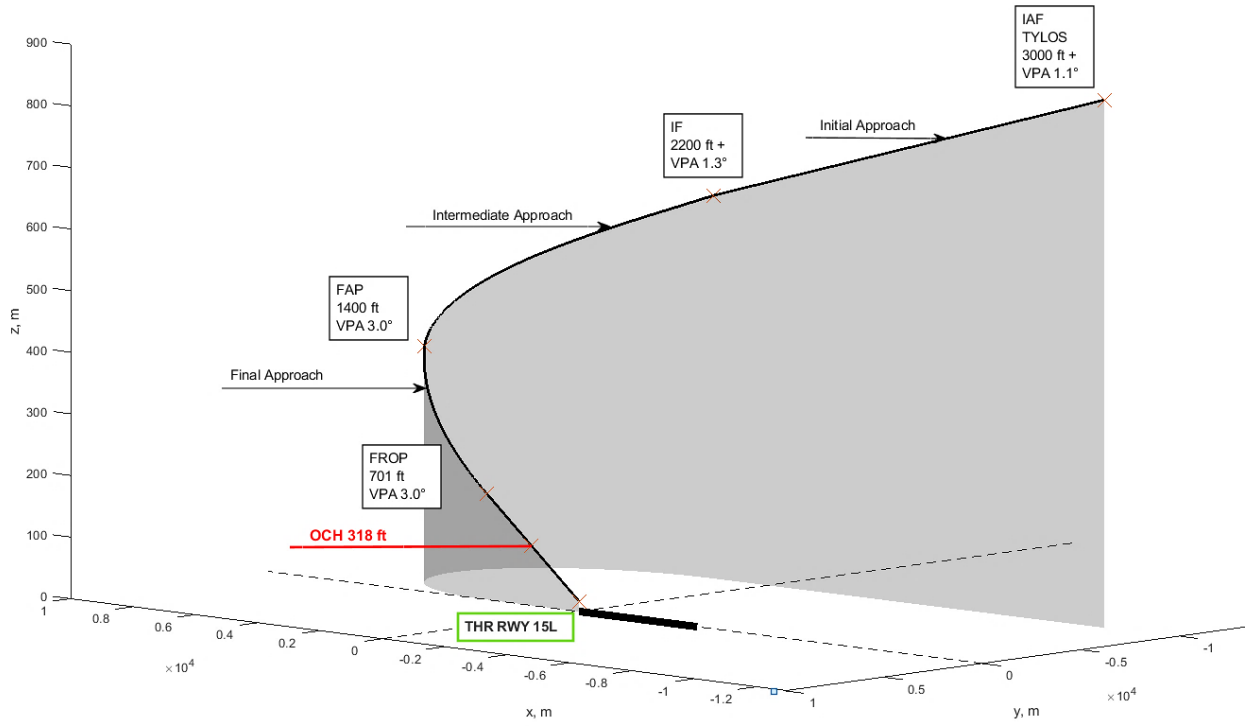

a) Vertical profile

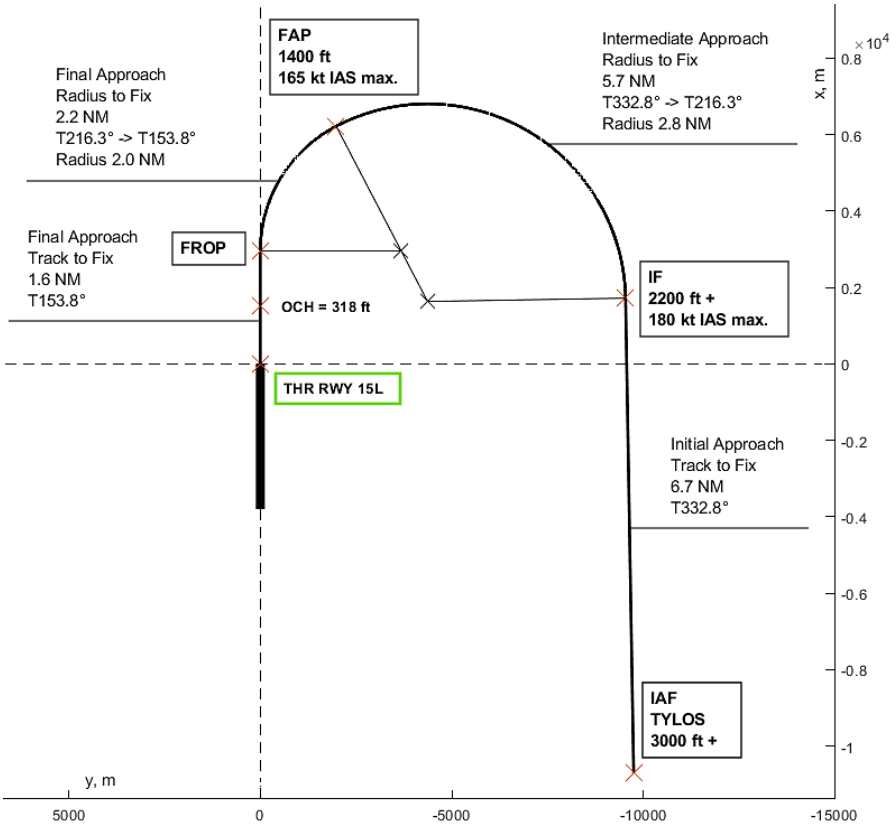

b) Horizontal profile

Fig. 7 Approach trajectory (without MAS)

Smaller VPAs facilitate slowing down the aircraft, thus placing the IAF at a lower altitude facilitates the configuration of the aircraft for landing. Moreover, we issue an altitude constraint to designate 3000 ft as the minimum altitude so that the IAF may also be passed higher if the aircraft can cope with the steeper descent (coded as 'A3000+', i.e. 3000 ft or above, see Ref. [9, pp. III-5-1-5, 6] for details). The resulting (minimum) VPA equals 1.08 degrees. A similar altitude constraint (coded as 'A2200+') is issued for the intermediate approach as its VPA is a bit smaller than the standard value, too. The entire approach trajectory from the IAF down to the runway is depicted in Fig. 7, including both the horizontal and the vertical profile. At this point, the only missing segment is the missed approach.

4.4. Missed Approach Segment

The MAS starts at the OCA/H point and ends at the point where a new approach, holding or return to en-route flight is initiated [4, p. 4-32]. Its construction is strongly tied to obstacle assessment, which was already discussed for the final approach (see pp. 9f.). As explained in appendix C, a go-around at the OCA/H point is modeled in three phases that also have an influence on the construction of the MAS. The three phases do not reflect any real go-around trajectory, they are rather used to build a procedure that allows for the occurrence of e.g. along-track errors during

the transition to the missed approach RNP (horizontal segment) and engine failures (2.5 percent climb gradient).

Our aim for the missed approach is to bring the aircraft back to either TYLOS or RABAD, where it can enter a holding or proceed with a new approach. As approaches are started out of at least 3000 ft at TYLOS, that should also be the minimum altitude reached at the end of the missed approach. With a gradient of only 2.5 percent, the climb to 3000 ft requires a horizontal distance of more than 17.8 NM between the SOC' and the termination fix. The approach chart for RWY 33R (see Fig. 1) suggests that this might be too long for a TYLOS-bound procedure (e.g. maintaining the runway track until joining an RF leg inbound TYLOS), which is why we choose RABAD as the termination fix. To keep the procedure as simple as possible, the number of legs and especially turns should be minimized. We thus implement the necessary left turn towards RABAD as an RF leg reaching from RABAD onto the final approach track which can be connected to the OCA/H point by only one further, straight segment. The construction process consists of two main steps: First, the construction of the RF leg and the verification whether the radius is flyable within the speed and bank angle limits. Secondly, the construction of the straight segment and the verification whether the position of the SOC' and the climb profile permit 3000 ft as the initial climb altitude.

As starting a new approach out of RABAD requires flying to TYLOS, the RF leg shall end on the RABAD-TYLOS-track. We therefore need to find the RF leg tangent to that track at RABAD and tangent to the x-axis (final approach track) at a yet unknown missed approach turning fix (MATF). As for the intermediate approach, the turn is geometrically constructed. Here, we need to find the intersection of the RABAD-TYLOS-track and the x-axis first. From there, the bisector is drawn until it intersects with the line perpendicular to the RABAD-TYLOS-track at RABAD. That intersection is the turn center and its distance from RABAD is the turn radius. The result is shown in Fig. 8, which also illustrates Eqs. (23) and (24) for the description of the turn in the X-Y plane. With φ being expressed relative to positive y, RABAD lies at 179.0223 degrees left off (i.e. almost but not directly behind) the turn center, which is due to the RABAD-TYLOS-track deviating from the final approach track by 0.9777 degrees (see Eqs. (13)-(14)). The radius equals 4970.1 m.

$$\boldsymbol{x_{MAS\ turn} = x_{MAS\ turn\ center} + \sin(\varphi) * 4970.1\ m;\ \varphi \in [179.0223°, 360°]} \tag{23}$$

$$\boldsymbol{y_{MAS\ turn} = y_{MAS\ turn\ center} + \cos(\varphi) * 4970.1\ m;\ \varphi \in [179.0223°, 360°]} \tag{24}$$

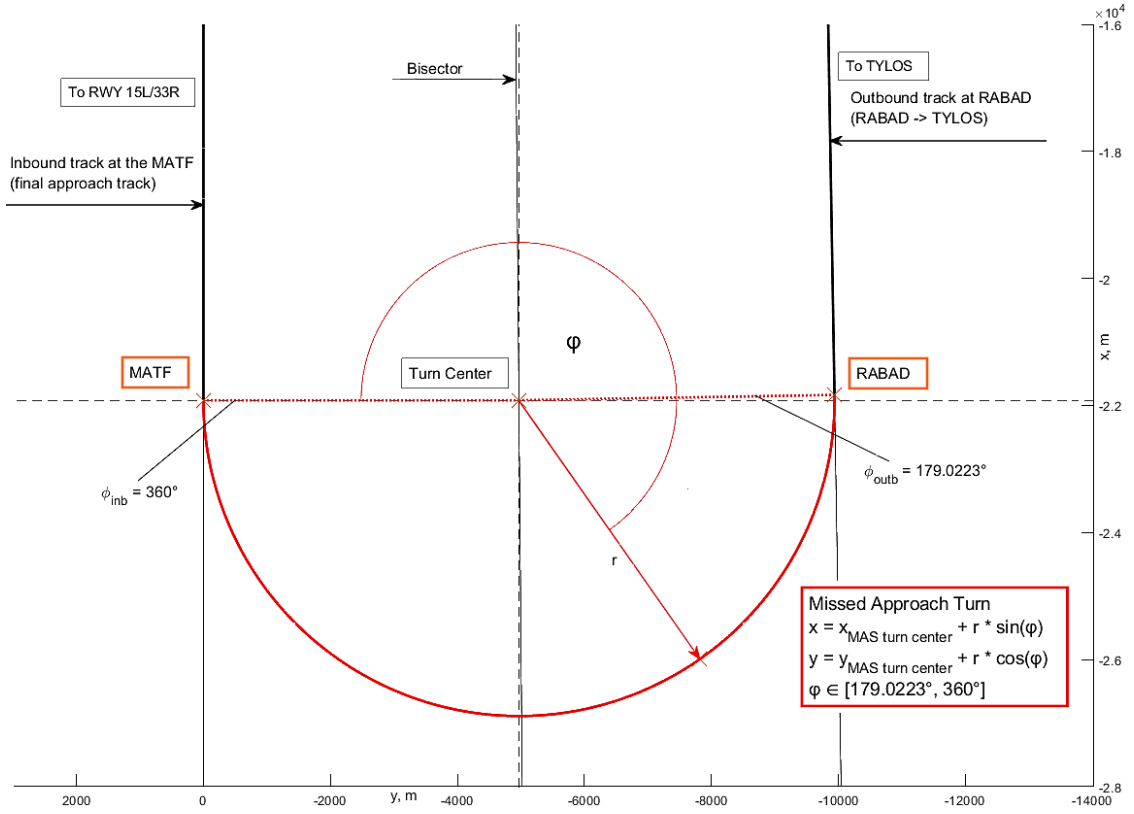

Fig. 8 Construction and definition of the missed approach RF leg

The flyability assessment also works as described for the intermediate segment (see p. 17) and reveals that the radius can only be flown with the minimum possible speed restriction (185 kt IAS, see table B2) and the maximum possible bank angle (20 degrees) for ISA+35 if the TWC equals 50 kt, as mandated. The radius margin is less than 150 m, emphasizing the need for such assessments if the turn radius is established on a geometric basis.

The straight segment begins at the OCA/H point and ends at the MATF, which is located more than 11.8 NM away from the threshold. It consists of the descent, horizontal and climb segments with the last one beginning after the transition distance to the OCA/H point at the SOC'. As depicted in Fig. 9, the entire straight segment lies on the x-axis of the reference frame so that the position of the SOC' can be determined by subtracting the threshold distance of the OCA/H point (x-coordinate) from the transition distance that was already calculated for the final approach with Eq. (6) and equals 4466.5 m. The OCH is reached 1529.6 m before the threshold, thus the SOC' is located 2936.9 m behind the threshold, still above the runway. It must now be checked whether the remaining distance from the SOC' to RABAD is sufficient to climb to 3000 ft on the 2.5 percent gradient. Equation (25) is used to calculate the height of any point on the straight segment during the climb phase. For the MATF (x_{MATF} = -21918 m/-11.835 NM), that yields a height of 1713.9 ft above threshold and an altitude (LLH) of 1973.9 ft.

$$z_{MAS\ straight}(x) = 0.3048 * 157\ ft + (-x + x_{SOC'}) * 0.025;\ x \in [x_{MATF}, x_{SOC'}] \quad (25)$$

The height within the RF leg, assuming a constant gradient, is calculated with Eq. (26). For RABAD ($\varphi_{RABAD} \approx 3.1245$ rad), that yields a height of 3001.5 ft above threshold and an altitude (LLH) of 3285.5 ft.

$$z_{MAS\,curved}(x) = z_{MATF} + (r_{MAS} * |\varphi_{MATF} - \varphi|) * \mathbf{0.025};\ \varphi \in [\mathbf{179.0223}° * \frac{\pi}{\mathbf{180}}, \mathbf{2}\pi] \tag{26}$$

Consequently, the missed approach is long enough to enable the climb to at least 3000 ft. Furthermore, due to the small climb gradient, 3000 ft are not reached until the remaining track distance to RABAD is approximately 2.1 NM, which confirms the decision to lead the missed approach to RABAD instead of TYLOS. For aircraft that have demonstrated the required climb performance, though, it would be possible to increase the gradient with the approval of the appropriate authority. This option could be used in the future to design an alternative missed approach procedure. Finally, it should be mentioned that the use of turns in the missed approach is subject to some restrictions. Any turn must not occur before the missed approach splay is complete or until the aircraft has reached a height greater than 150 m/492 ft on the 2.5 percent gradient out of the SOC', whichever is later [4, pp. 4-33, 47]. Here, the splay extends over 6.7 NM (see p. 10) and is thus completed less than 5.9 NM behind the threshold, while the 150-m height is reached 2 NM earlier. With the MATF lying more than 11.8 NM from the threshold, both requirements are fulfilled and the turn does not have to be moved.

Fig. 9 shows the entire missed approach segment including the vertical profile, which includes the initial height loss of 161 ft that puts the aircraft at 157 ft above threshold – the height of the north antenna as the tallest obstacle.

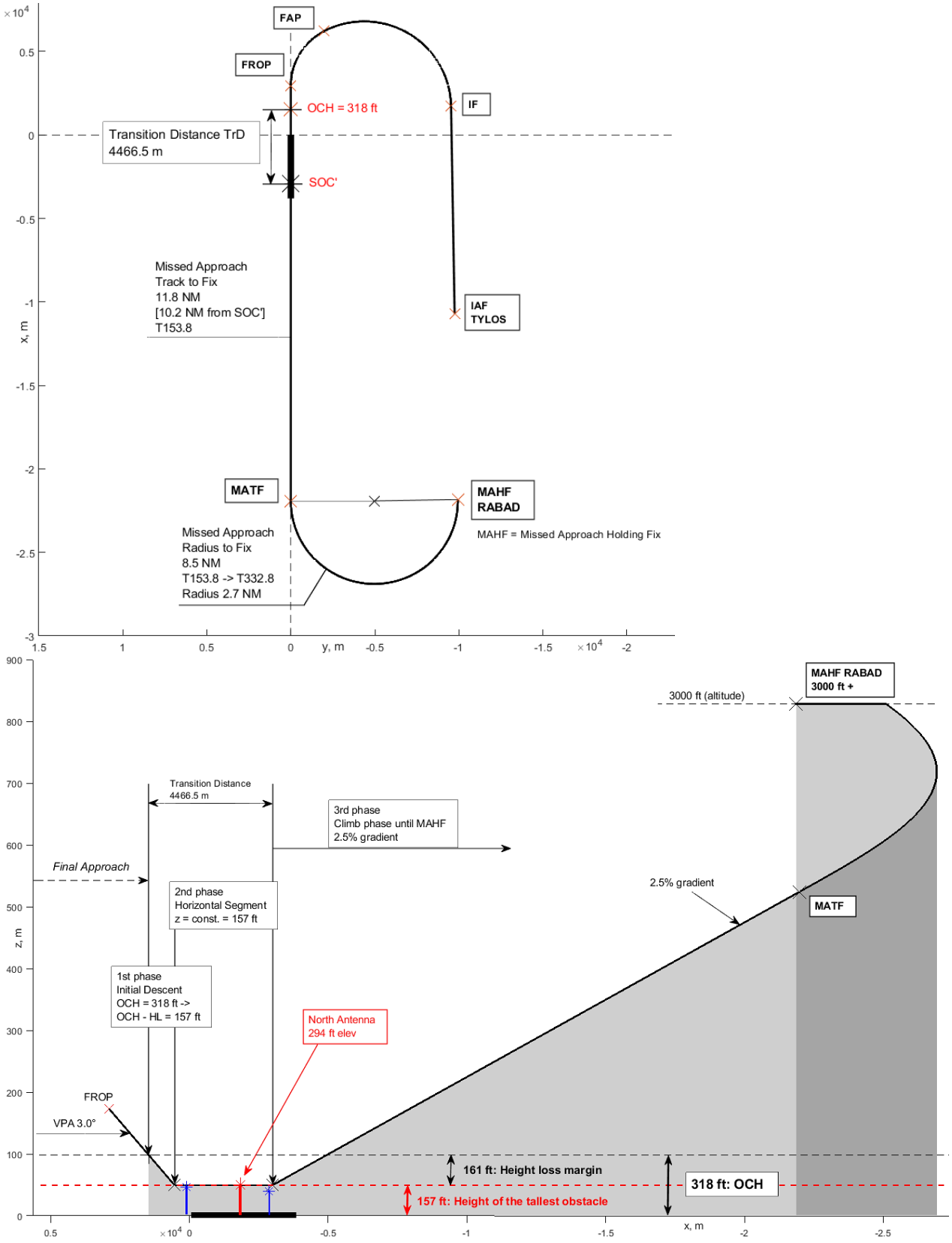

Fig. 9 Missed approach trajectory

4.5. Obstacle assessment and visualization with MATLAB's geoplot3 function

Each newly designed approach procedure must be followed by an obstacle assessment to determine whether the procedure is safe to fly or not. While obstacle clearance within RNP AR APCH is generally based on primary areas and a certain MOC as outlined in chapter II, obstacle clearance in the final and missed approach segments can only be provided down to the OCH that is determined with three OASs as explained in appendix C [4, p. 2-3]. Consequently, our assessment must ensure that the obstacle clearance volume of the initial and the intermediate approach is not penetrated while penetrations of the OASs in the final and the missed approach are tolerable as long as they do not cause a higher OCH than the estimated one that was used for the final approach construction (see p. 10). If the (true) OCH was higher, we would be forced to revise certain parts of the approach (first and foremost the straight final segment), which would be unfavorable. We do not have all the tools available to perform a full obstacle assessment, though we can perform a qualitative one with the geoplot3 function of MATLAB. This function enables us to plot the approach trajectory and the obstacle assessment surfaces in a freely accessible geographic globe. The globe model includes high-resolution satellite imagery by Esri and terrain data so that we cannot only perform a visual assessment of whether any surface is penetrated but also visualize the approach trajectory within the approach environment. [29] The terrain data are based on the GMTED2010 model by the U.S. Geological Survey (USGS) and National Geospatial-Intelligence Agency (NGA). [30] geoplot3 requires that the positions to be plotted are handed over in the LLH format, thus we need to convert them from the reference frame into LLH first, which is also needed for the database coding later. For the obstacle assessment, we must convert both the waypoint coordinates and the discrete turn positions (see appendix E for examples) because the function can only draw straight lines between two points. Fig. F1 consists of an example shot of the entire approach trajectory and a zoom on RWY 15L. Obviously, both our calculations and the plotting mechanism seem to be very accurate with the final approach track lying almost on the centerline and the LTP (white circle) being indeed plotted at the threshold. The surfaces are best defined in the reference frame before they are converted into LLH for plotting, which is also required by the procedure design manual. Each surface has a lateral and a vertical extent and ranges over a certain length, thus we need at least eight points to describe its boundaries. With their width depending on the accuracy value, we will also set the navigation accuracy for the initial and the intermediate segment (the FAS and MAS values have already been set). The curved surfaces for the RF legs must equally be discretized.

The initial approach, depicted in Fig. F2, is the least critical segment as it only leads over water. We therefore set the RNP at the least critical value of 1 ($RNP_{initial\ approach} = 1$) which results in a primary area of 2 NM semi-width across the initial segment, ranging 300 m (= MOC) below the track. The intermediate segment requires a more stringent RNP value due to its proximity to the CTR, which leads to an RNP change at the IF. In general, RNP changes (at fixes) require the area within ± 1x accuracy value of the fix to be

evaluated for both segments so that we must extend the initial approach surfaces until 1 NM after the IF [4, p. 4-7]. Nevertheless and as shown by Fig. F2, the entire obstacle clearance volume still ends off the coast and is obviously not penetrated. The intermediate segment ends close to the CTR. Entering the CTR during the final approach can be avoided due to the use of RNP 0.1 and the optimum placement of the FAP. If the navigation accuracy for the intermediate segment was chosen higher (e.g. RNP 0.2), the obstacle clearance areas would have to be extended over 0.2 NM beyond the FAP due to the RNP change. Fig. F3(a) shows that this would lead to a violation of the CTR, thus we must set the RNP value for the intermediate approach at 0.1 as well ($RNP_{intermediate\ approach} = 0.1$). The segment has a constant MOC of 150 m and is depicted in Fig. F3(b) including its obstacle clearance volume. After crossing the coastline just north of the village of Jaww, it only leads over a relatively flat and barren desert area. Neither tall buildings nor terrain infringe on the surfaces; the highest point in Bahrain is the Mountain of Smoke at 440 ft MSL which lies just 1.2 NM north-west of the FAP but still more than 460 ft lower than the lowest point of the obstacle clearance volume [31].

The final approach is examined from the FAP to the OCA/H point, where it technically ends. It is protected by the VEB surface, where the MOC is based on the vertical error performance of the baro-VNAV system (see appendix C for details). Fig. F4 shows the entire segment from different angles. The semi-width of the OAS remains constant with 0.2 NM while the calculation of the variable VEB-defined MOC yields a maximum of 77 m at the FAP and a minimum of approximately 54 m at the OCA/H point, which translates into a surface gradient of 4.93 percent ($VPA_{VEB} \approx 2.82$ degrees). However, the VEB MOC may not be applied immediately after the FAP because of its difference to the intermediate segment MOC (150 m vs. 77 m) so that any large discontinuities in the vertical profile are avoided. Instead, vertical protection is provided by extending the intermediate approach MOC (horizontally) into the final approach until it intersects the VEB surface (see Fig. F4(b)). [4, p. 4-19] Furthermore, it should be noted that the VEB MOC is slightly higher for RF legs due to changed relation between the navigation reference point on the aircraft and the wheels (called body geometry error). The higher value must also be applied within 1x accuracy value (0.1 NM) of the turn entry and exit points, which leads to a small bump in the vertical profile near the FROP. [4, p. 4-31] Until the OCA/H point, the approach continues to lead over flat and undeveloped desert land with no sign of a surface penetration. Therefore, we also consider the final approach to be clear of obstacles.

The beginning of the missed approach is characterized by the incipient 15-degree lateral OAS splay as depicted in Fig. F5(a), which shows the transition area between the OCA/H point and the beginning of the Z surface. The first part is still protected by the VEB surface and ends with that surface reaching the threshold level approximately 663 m before the runway. It is replaced by the horizontal surface whose beginning is delineated by an interrupted horizontal line (see Fig. F5(b)). That is due to the geoplot3 function not plotting any position that lies below the terrain level (at that position). With the horizontal surface lying at threshold level, which is 3 ft lower that the published aerodrome elevation, slight terrain-related penetrations like this one must be expected and are tolerable since their magnitude is negligible compared to the

obstacle-related penetrations. Apart from that, Fig. F5(b) shows that the VEB surface is not penetrated so that the VEB-protected area of the missed approach is considered uncritical for the obstacle assessment. The figure also shows a white and much narrower surface along the approach track prior to landing, the visual segment surface (VSS). The purpose of the VSS is to protect the visual approach segment against, therefore it must normally be clear of obstacles for all IAPs, including RNP AR APCHs operations. Here, it originates 60 m prior to the threshold at threshold level with a semi-width of 70 m according to the ICAO Annex 14 aerodrome reference code of Isa Air Base (4F) [32]. Its slope is 1.12 degrees less than the final approach design VPA and extends until the surface height equals the OCH. [9, p. I-4-5-7] The entire VSS is depicted in Fig. F5(c) and is obviously clear of obstacles as required.

Fig. F5(a) also shows the next part of the missed approach, which is protected by the horizontal surface, including the three aerodrome obstacles from the AIP. As predicted, the surface is penetrated by the north antenna that is the most relevant obstacle due to its height. Given the lack of 3-D representations of buildings and the aerodrome infrastructure, the figure does not allow to assess whether there are even higher obstacles leading to a penetration of the OAS. However, we rely on the AIP that does not list any other than the three mentioned obstacles. If no other penetration greater than that of the northern antenna is discovered during the rest of the missed approach, the initial OCH of 318 ft can thus be verified.

The last part of the missed approach is protected by the Z surface, which is depicted in Fig. F5(d). The beginning of the Z surface was determined during the final approach construction and lies 3850 m behind the threshold at the end of RWY 15L (see Eq. (5)). Thereafter, the missed approach leads straight out towards the sea with the coastline being reached shortly behind the aerodrome site. While the eastern half of the lateral splay is uncritical because it mainly leads over water, the western half covers another bit of flat of mostly undeveloped land before it reaches Durrat Al Bahrain, a resort island city that is currently under construction (see Fig. F5(e)) [33]. The reference missed approach track that was calculated in the previous chapter has reached an altitude of more than 980 ft when the splay is complete. Thus, a future skyscraper at that position would have to be taller than 980 ft (required MOC = 0 m) to cause a penetration of the Z surface that yields a greater equivalent approach obstacle height than the current value (157ft, north antenna). For comparison, the currently tallest building in Bahrain is the Four Seasons Hotel Bahrain Bay with 890 ft [34]. While such a penetration cannot be completely excluded for the future, we base our assessment on the present conditions and since the satellite images do not indicate any tall buildings and suggest that the construction is still in the early stages, we do not assume any penetrations in that area. In case the Z surface should be penetrated someday, its gradient could still be adjusted as mentioned during the missed approach construction (see p. 21). The rest of the surface leads over water except for small parts in the south-east, which lead over flat and mostly undeveloped areas on the Hawar Islands at greater heights (see Fig. F5(f)).

Consequently, it is safe to assume that neither terrain nor obstacles cause a more relevant penetration of any OAS than the one caused by the north antenna. The initially chosen OCH has been verified and offers sufficient obstacle clearance in the final and missed approach

segments. The initial and intermediate segments are protected by their obstacle clearance areas, which have been examined with no penetrations found. In summary, we expect that no obstacle-related adjustments of the approach trajectory are necessary anymore.

5. Implementation

The next step after the approach building is the procedure implementation, which is complex and not the subject of this paper. However, we carried out a simulator assessment of the procedure as part of the necessary ground validation, which will be discussed in this chapter. The entire implementation process is detailed in the PBN manual. For instance, it includes a safety assessment such as a FOSA (flight operations safety assessment), where a variety of factors (e.g. aircraft and navigation systems, ATC and flight crew procedures, hazards and the operational environment) are analyzed to ensure operational safety [8, p. II-C-6-28]. The implementation also requires a procedure validation that is split up in ground and flight validation. Its purpose is to verify all obstacle and navigation data, the data used for the procedure construction as well as the information on the approach chart and to assess the flyability of the procedure. For RNP AR APCH, ground validation should always involve a simulator assessment. [8, p. II-C-6-2]

5.1. Charting and Coding

The procedure can only be flown after it has been coded and stored in the navigation database of the FMS in the simulator or onboard the aircraft that is used for flight validation. Each database can be updated every 28 days once a new *Aeronautical Information Regulation and Control* (AIRAC) cycle is released [35]. The procedure details needed for the coding include waypoint information (identifier, coordinates, type, path terminator etc.), track lengths, altitude and speed constraints, VPAs, RNP values and RF leg-specific data (turn center, radius) [9, pp. III-5-1-5ff.]. We put that information together in a chart (see table B4) and sent it to Lufthansa Systems, where the procedure was coded. After receiving the updated database, we used it for the simulator tests described in the next chapter.

5.2. Simulator assessment

The simulator assessment took place on FT76, an Airbus A320-214 full-flight simulator (level D) in Essen, in December 2020 with two pilots (Captain: ATPL, First Officer: CPL, both with A320 type rating) [36]. We performed a total of eight approaches followed by either a go-around shortly before reaching the OCA/H (which equals the DA/H in our case) or a touch-and-go landing. In particular, the assessment involved different wind and weather conditions. Below, we will discuss six of the flown approaches whose conditions are summarized in table 6.

Scenario	A/C Gross Weight	Weather: Phenomena and Visibility	Wind [°/kt] // Temperature	End of Scenario	Remarks
1	60 t	CAVOK	NIL // ISA	Go-Around without MAS	Managed Speed

2	As #1	CAVOK	NIL // ISA	Go-Around without MAS	Selected Speed
3	As #1	CAVOK	4200 ft: 050/50, GND: 060/20 || Effectively: IF: 058/36, FAP: 060/31 // ISA	Go-Around without MAS	Selected Speed; medium conditions (wind/temperature)
4	As #1	CAVOK	4200 ft: 050/80, GND: 060/20 || Effectively: IF: 057/53, FAP: 060/42 // ISA+35	Go-Around with MAS	Selected Speed; heavy conditions
5	As #1	OVC008, 3000	4200 ft: 050/80, GND: 060/20 || Effectively: IF: 057/56, FAP: 060/40 // ISA+35	Touch and Go	Selected Speed; heavy conditions
6	As #1	CAVOK	GND: 110/15 // ISA	Touch and Go	Selected Speed; manual flight with F/D

Table 6 Approach conditions within the different scenarios

Every approach was started out of a predetermined position south-west of TYLOS with an aircraft gross weight of 60 t, 5 t below the maximum landing weight as recommended by the pilots. During the approach, we recorded a variety of flight parameters such as true aircraft position (LLH), calibrated airspeed (CAS) and roll angle in 0.5-second steps that we use to evaluate the aircraft trajectory. The main assessment is based on the determination whether the actual navigation accuracy, given by cross-track error (CTE) and the vertical error, met the required one, i.e. whether the nominal approach track could be safely maintained. Both errors are determined by converting the LLH positions into the reference frame used for the procedure construction. The CTE is then given by the shortest distance to the respective approach leg in the X-Y plane, the vertical error equals the height difference between the actual position and the associated position on the respective approach leg (-> CTE). Besides, we will focus on the RF legs of the intermediate and the final approach to prove their flyability under the conditions used for the turn construction: heavy tailwind and high temperatures which cause a larger (flown) radius if the roll angle is not increased. Here, we will verify that the maximum bank angle (as per procedure design) is not exceeded. The discussion below is based on the error plots that we have created for each scenario and that can be found in appendix G. Each figure consists of separate parts for the CTE and the vertical error with the CTE plots also containing the recorded CAS and the roll angle values.

5.2.1. Scenarios 1 and 2: Smooth conditions as control scenarios

Scenarios 1 and 2 (see Fig. G1 and G2 for plots) serve as control scenarios without any wind and clouds but with good visibility (CAVOK = Clouds And Visibility OK, more in [37]). Both scenarios differ in the speed management (Airbus-specific): If flying with *managed speed*, the speed is controlled by two Flight Management Guidance Computers (FMGCs) that set a target speed according to the entries in the FMS, the Flight Control Unit (FCU, control panel for autopilot and autothrust), the current aircraft configuration and the current flight condition [38]. During the approach, the target speed mainly depends on the flap setting determined by the pilots which cannot be varied as it is operationally required. In our case, the intermediate approach was entered with flaps 2 (of 4), the gear was selected down after passing the IF. Flaps 3 and then flaps full were selected shortly thereafter. Flaps 2 already commands the so-called F speed, which equals the stall speed in that configuration times a factor between 1.38 and 1.47. [39] That speed was around 140 kt IAS, which means that the intermediate and final approach RF legs were flown slower than for what they had been constructed (180 and 165 kt IAS, respectively). However, we also wanted to assess the flyability of the approach for CAT D aircraft on whose performance (higher approach speeds) the approach is based. With the A320 being a CAT C aircraft [40], we increased the approach speed by *selecting* the speed directly at the FCU using the procedure design values, i.e. 180 kt shortly before passing the IF, 165 kt shortly before passing the FAP and the actual approach speed shortly before leaving the final turn. Consequently, the roll angle grew from between 6 and 8 degrees with managed speed to between 10 and 12 degrees with selected speed. The CTE was slightly larger with higher speeds as well, although the values are still very small compared to the RNP 0.1 TSE of 182.5 m. With managed speed, the CTE varied from +15 m (+ equals to the right of the track) near the IF to -24 m (- equals to the left of the track) during the final approach whereas it grew to -36 m near the FAP with selected speed. In general, we recognize a distinctive trend in the CTE pattern that affects all scenarios: While the intermediate approach is always started a bit too far to the right, the aircraft crosses the nominal approach track sooner or later after the IF und continues to fly too far to the left with the biggest deviation most often reached within the final approach turn. This effect grows with higher speeds. The vertical error is mainly considered within the final approach, as the initial and intermediate segments just have minimum altitudes published (see table B4). In the plots, the vertical error is depicted along with a limit of ±22 m (in red), which is the maximum tolerable deviation within the FAS as monitored by the pilots. If that value is exceeded below the glide path, a go-around must be performed (as it is the case if the lateral deviation exceeds 1x RNP). [8, p. II-C-6-18] In both scenarios, the vertical error was well within the 22-meter limit. Nevertheless, the lower deviations (between 3 and 4 meters) were again achieved with managed speeds while flying with selected speed caused a maximum deviation of +15 m within the final RF leg, though only for a short time until the nominal path was recovered.

5.2.2. Scenarios 3 and 4: Flying in advanced and challenging conditions

Scenario 3 (see Fig. G3 for plots) is based on scenario 2 with (tail-)wind. Our aim was to simulate the maximum allowed tailwind at the IF and the FAP since we knew that up to two wind values (along with the surface wind) could be specified at the instructor station. We had therefore calculated the required wind directions and speeds, however we only discovered during the assessment that no wind could be specified below 4200 ft (2000 ft above the IF) so that we were not able to directly simulate the calculated wind. Instead, with the simulator interpolating between the surface and the upper-level values, we tried to approximate the desired IF and FAP values by choosing a fitting wind for 4200 ft. Even though we would have preferred to establish the maximum tailwind at the FAP (1400 ft: 038/44) due to the smaller radius of the final RF leg, the north-east wind would have caused a significant TWC near the threshold as well, which would have made landing difficult. Instead, we chose the surface wind as crosswind from 060 degrees and an upper-level wind from 050 degrees so that the simulated wind blew parallel to the track a bit ahead of the FAP, still within the intermediate approach. Therefore, the effective wind speeds at the FAP from table 6 do not equal the TWC but are a bit higher as the wind is hitting the aircraft slightly from the left. In scenario 3, the FAP TWC equals more than half of the maximum allowed value whereas it is just a few knots below the maximum in scenario 4 (see Fig. G4 for plots). Moreover, we used ISA temperatures in scenario 3 but increased it to ISA+35 in scenario 4. Consequently, both scenarios represent different severities in terms of approach conditions: While scenario 3 features medium conditions with significant tailwind but moderate temperatures, scenario 4 features heavy conditions close to the worst-case scenario that we used for the turn construction. That difference is also reflected in the recorded roll angles which increased from 12 (#3) to between 16 and 17 degrees (#4) within the intermediate approach and from 15 (#3) to partially 19 degrees (#4) within the final approach. Thus, the maximum allowed roll angle (20 degrees) was not reached even in very challenging conditions. We expect that the turn construction values (18 and 20 degrees, respectively) could only be reached in the real worst case, where the aircraft experiences maximum tailwind throughout the turn, though this scenario is neither likely to occur nor could be reproduced in the simulator. Scenario 4 also included flying the entire missed approach. Given that tailwind in the first two RF legs turns into headwind within the missed approach RF leg, it is not surprising that the roll angles there were smaller than modeled (between 6 and 13 instead of 20 degrees). The growing tailwind and temperatures also caused larger lateral deviations over scenarios 2 to 4: After +27 m at the IF, the maximum CTE within scenario 3 was reached with -46 m at the FROP; the nominal track was not recovered until the go-around. The fourth scenario caused CTEs of +36 m at the IF and up to -63 m before the FROP, thereafter the aircraft kept flying approximately 40 m to the left of the track until the go-around. The maximum CTE within the MAS equaled -70 m and occurred during the climb along the straight segment. Within the RF leg, the aircraft crossed the nominal track from left to right and reached RABAD with a CTE of +50 m. As those values are all well within 1x RNP, the lateral accuracy is considered sufficient. The

vertical error needs to be treated differently. The error behavior in scenario 3 can be compared well to scenario 2 and features a slightly larger deviation below the glide path at the FAP (-12 m), followed by an overshoot of up to 14 m before the aircraft returns to a position slightly below the glide path without ever infringing on the 22-meter limit. Those bumps in the error profile (see Fig. G3(b)) can likely be explained with slight accelerations to keep the selected speed at the same time, causing a nose-up pitching moment. The vertical error in scenario 4 is significantly larger. At the FAP, the aircraft flies 38 m higher than planned, i.e. the FAP is overflown at more than 1520 ft instead of 1400 ft. After a short time however, the error becomes continuously smaller and the nominal glide path is captured shortly before reaching the OCH. Besides the 22-meter limit in red, we also plotted the required 99.7 percent vertical accuracy from the PBN manual in magenta (see Fig. G4(b)), which equals approximately 30 m for the final approach but is only valid with ISA temperatures [8, p. II-C-6-7]. As the recorded altitude is true altitude and not indicated altitude, we can conclude that the FMS in the simulator did not include a temperature correction model so that the increased outside temperature caused a pressure altimeter error putting the aircraft at higher (true) altitudes, leading to a higher effective VPA. The highest deviation was reached six seconds after passing the FAP with almost +40 m, which translates into an effective VPA of 3.362 degrees. As that is well below the maximum effective one of 3.503 degrees (see p. 14) and with the glide path being captured in time, we do not assume a degraded vertical accuracy. Rather, the error profile seems normal in the context of temperature-related pressure altimeter errors and since this effect has been included in the procedure design, we do not consider the flyability of the approach to be impaired. Fig. G4(c) shows the vertical profile of the missed approach trajectory. It can be recognized that the climb gradient during normal operations is much higher than the 2.5 percent gradient used for the procedure design.

5.2.3. Scenario 5: Flying in challenging and low visibility conditions

Scenario 5 (see Fig. G5 for plots) equals scenario 4 with degraded visibility. We set the ceiling to 800 ft (OVC = overcast) and the visibility on the ground to 3000 m. With this setting, the first visual clues do not become available until the aircraft leaves the final approach turn. As the scenario should include a touch-and-go landing, we could not lower the ceiling and the visibility further because Lufthansa Aviation Training, who had added the runway to their database beforehand, did not place it in the right spot but shifted the runway position a few hundred meters to the west. That forced the pilots to deviate to the right after leaving the turn to be able to land, for which we wanted to provide sufficient time and which also explains the transition from negative to positive values in the CTE profile after the FROP. In general, the lateral deviations are not as significant as in scenario 4 despite the same wind and temperature conditions (+34 m at the IF, -45 m within the final approach turn), which might be due to the lower flown airspeed in the final approach in preparation for landing. This also caused slightly smaller roll angles (17 instead of 19 degrees). The vertical error profile is similar to that of scenario 4, the glide path is again captured in time.

5.2.4. Scenario 6: Flying manually

The sixth and last scenario (see Fig. G6 for plots) involved good weather with a light wind from the left upon landing, no clouds, good visibility and ISA temperatures. It differed from the others in that the captain flew the approach manually with assistance by the coupled flight director (and autothrust). Despite the manual flying, the accuracy was absolutely within the limits: It reached from +23 m at the IF to -67 m within the final approach turn in the lateral direction and varied between +10 and -10 m in the vertical direction. Like scenario 5, also this scenario involved a touch-and-go landing which explains the rapid transition in the CTE profile after the FROP. The small deviations prove that an RNP AR APCH does not necessarily have to be flown by the autopilot to obtain the required accuracy, a skilled pilot can achieve sufficiently small FTEs as well.

5.2.5. Summary

We evaluate the outcome of the simulator test positively. We were able to show that the approach is safe to fly not only in ideal but also in very critical conditions (as far as mandated by the procedure design). Especially the intermediate and final approach RF legs, which are more challenging to fly due to their small radius and low altitude, were accurately flown also at higher aircraft and wind speeds without exceeding the maximum allowed roll angle. The lateral deviations in all approach segments were significantly smaller than RNP 0.1, the vertical deviations varied within the limits for ISA temperatures and grew with temperatures above ISA due to the pressure altimeter error, though without the resulting effective VPA exceeding its limit. We assume that the approach can cope well with the conditions in Bahrain and can also be flown safely with larger aircraft, as the tests with higher approach speeds show. Nevertheless, it is important that the pilots are well prepared and aware of the special characteristics of this approach, e.g. that there is not much time to stabilize the aircraft on the final approach track once they have left the RF leg or that a different than usual configuration management might be necessary. Not for nothing did both pilots describe the approach as rather challenging.

6. Conclusion

The aim of this paper was the development of an RNP AR APCH procedure on RWY 15L of Isa Air Base in Bahrain. The approach was supposed to enable approaching aircraft to avoid entering the CTR of the neighboring air base and feature sufficiently low minimums to permit operations also in bad weather. Our developed approach is able to fulfill both requirements due to the combination of two unique design characteristics that are only available with RNP AR APCH: The application of curved segments in the final approach, which enables track changes and hence flying by the CTR even shortly before landing, and the availability of very high navigation accuracies (RNP 0.1) in all approach segments, which keeps the containment areas small enough to not violate the CTR while the OCH becomes potentially smaller. Even with the highest performance requirements however, the minimum distance between the containment areas and the CTR becomes less than 50 m, emphasizing how tight constraints in the application environment of RNP AR APCH can be. It is a procedure type that does not require any ground-based infrastructure and despite it not offering the same accuracy as precision approaches near the threshold, it is unmatched in its flexible approach design and precision where precision approaches are not an option. We consider it the perfect alternative for aerodromes that must cope with airspace constraints, terrain- or obstacle-rich environments or a combination of all. The application at Isa Air Base is an extreme example where we exploited the potential and found the limits of RNP AR APCH procedure design but were yet successful in establishing an approach within the given constraints. This would have been impossible with any other approach procedure and we suspect that there are many other airports where this is no different.

Register of illustrations

List of tables

Formula directory

Appendix A

Figures

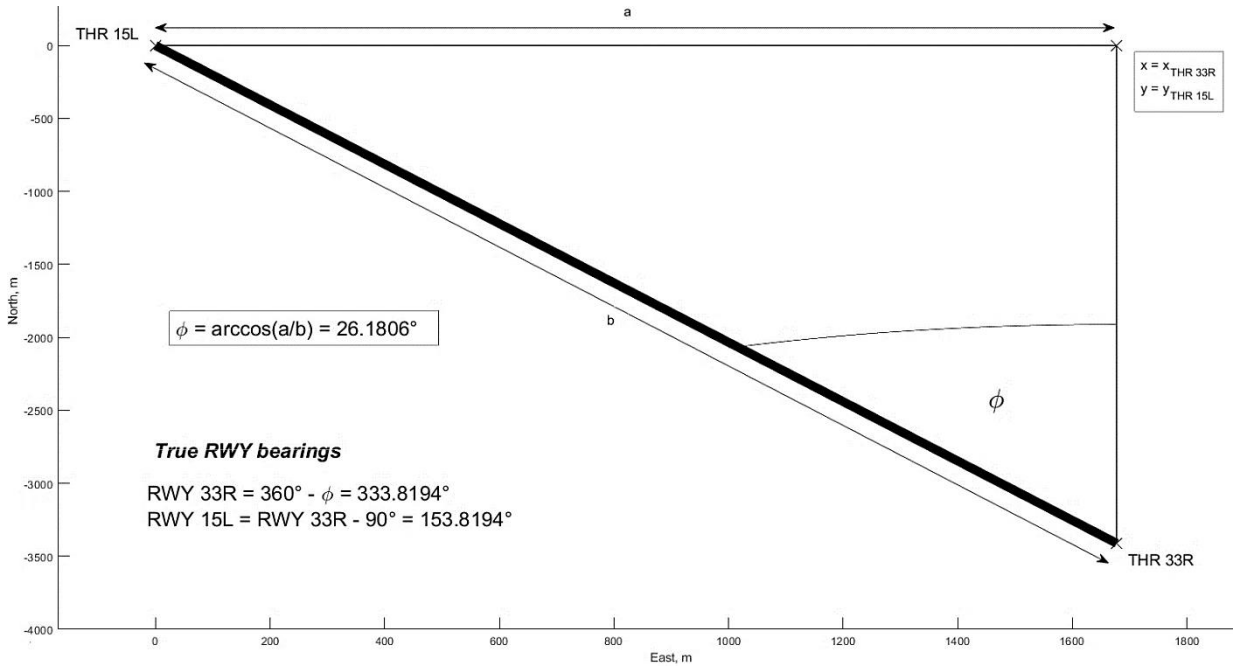

Fig. A1 Determination of the true runway bearings

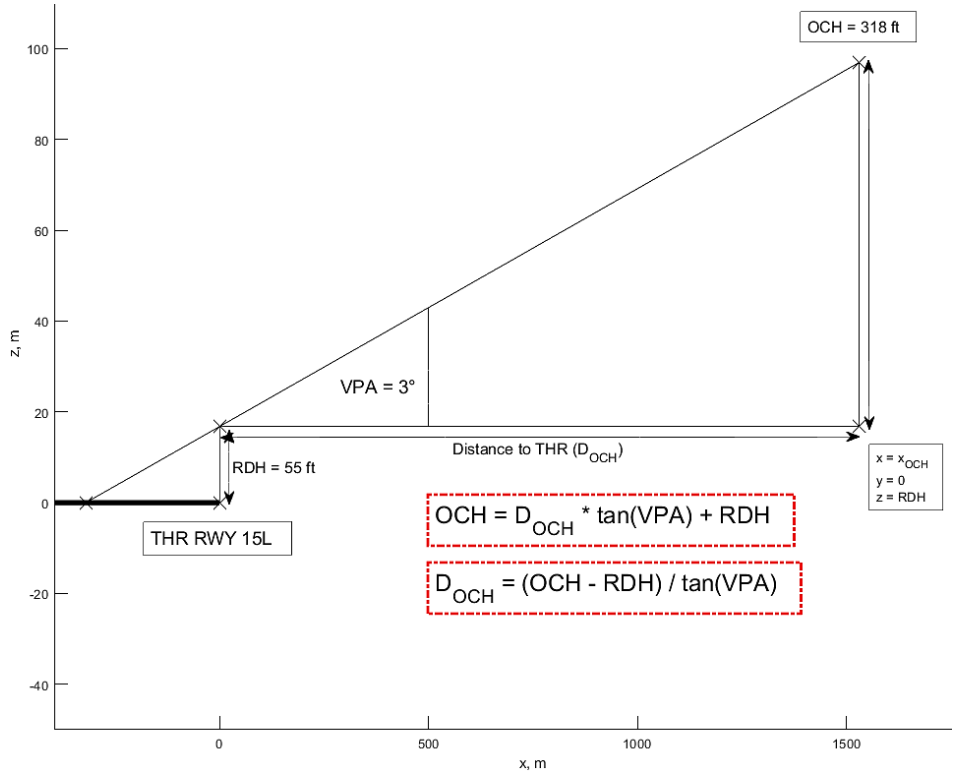

Fig. A2 Determination of any point (here: OCH) located on the straight final approach segment

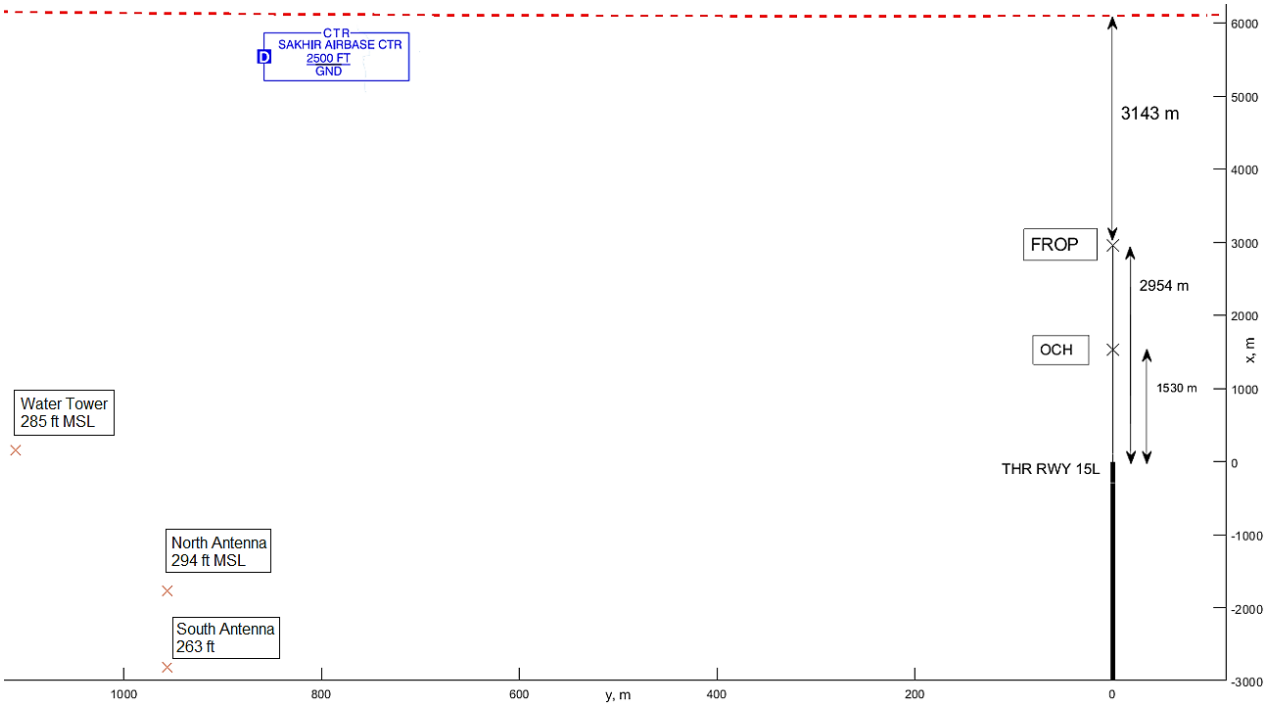

a) X-Y plane

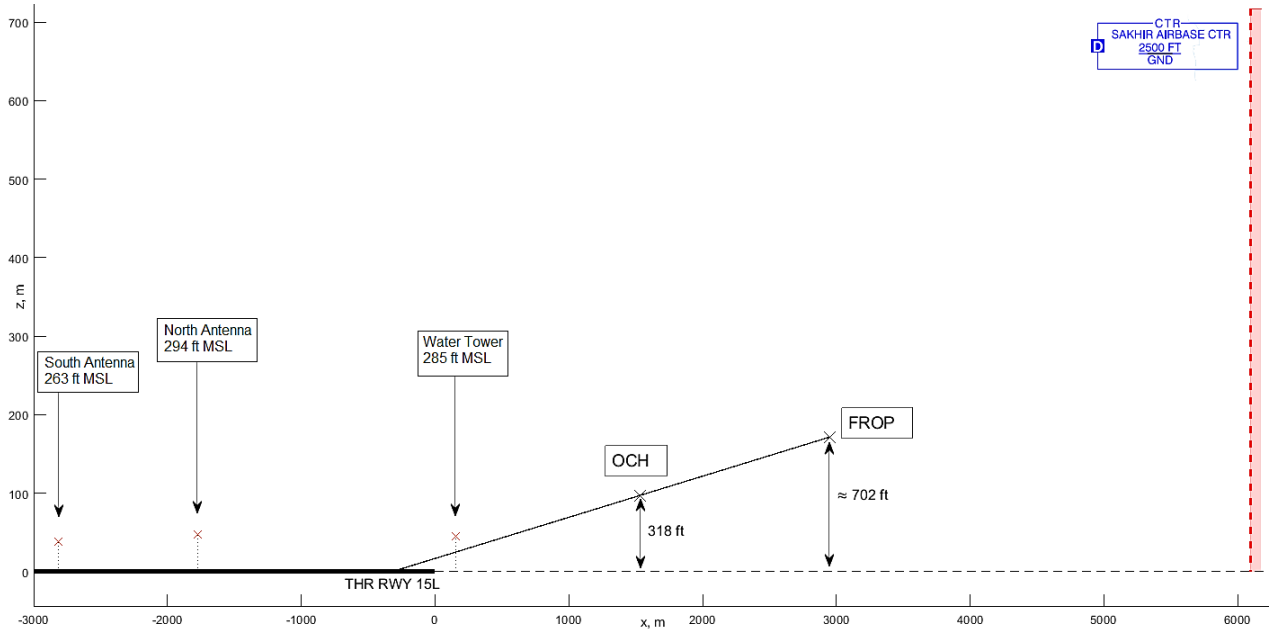

b) X-Z plane

Fig. A3 FROP position between RWY 15L and OBKH CTR

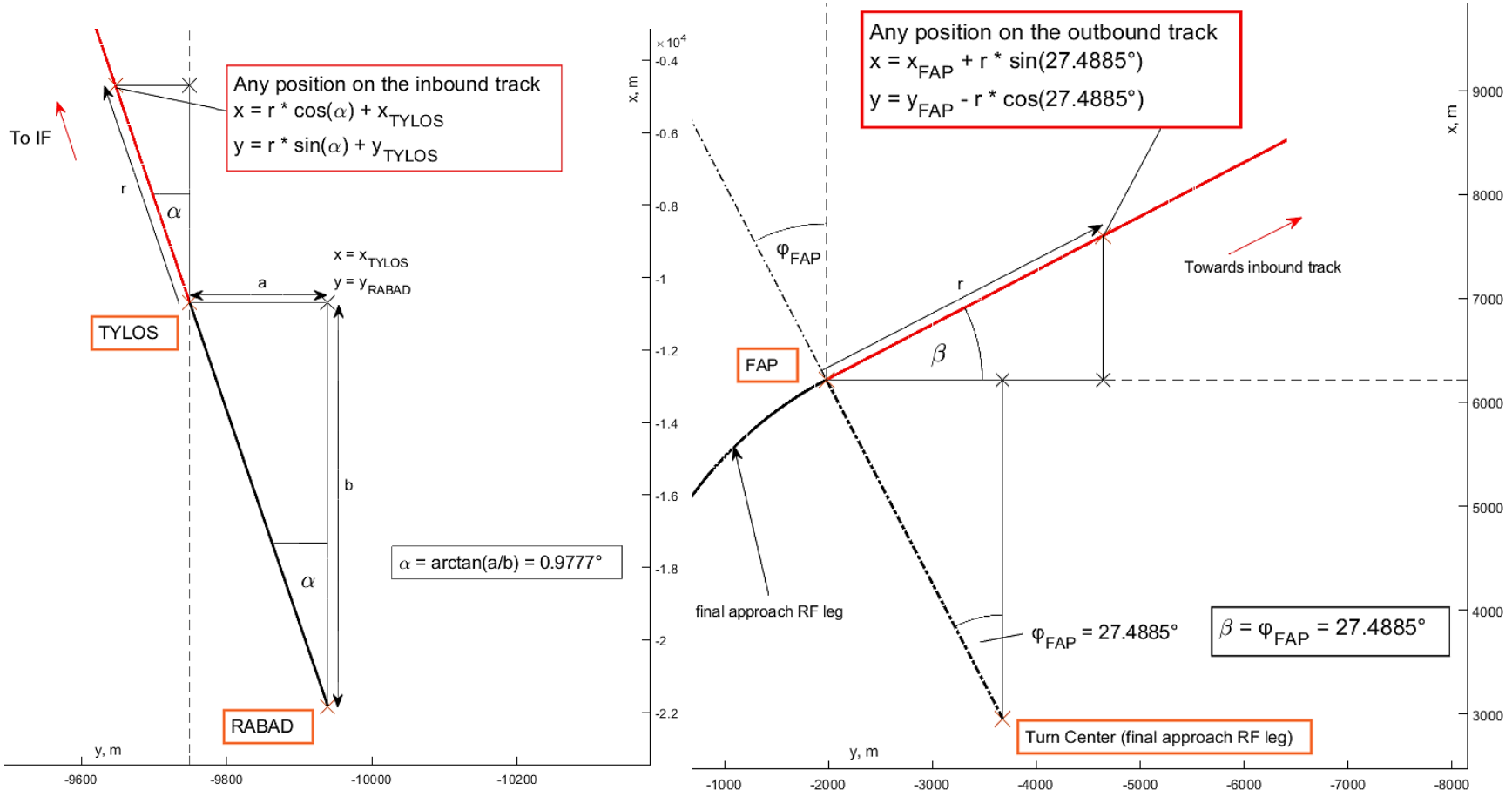

Fig. A4 Calculation of the intermediate approach inbound (left) and outbound (right) track

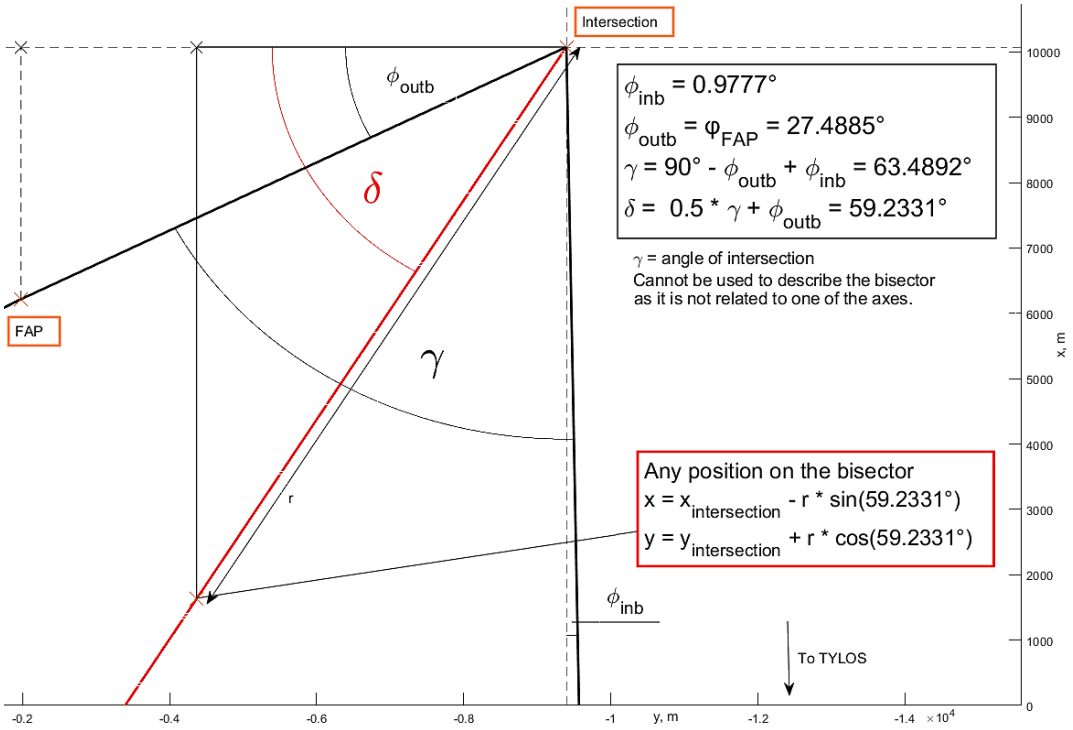

Fig. A5 Calculation of the bisector

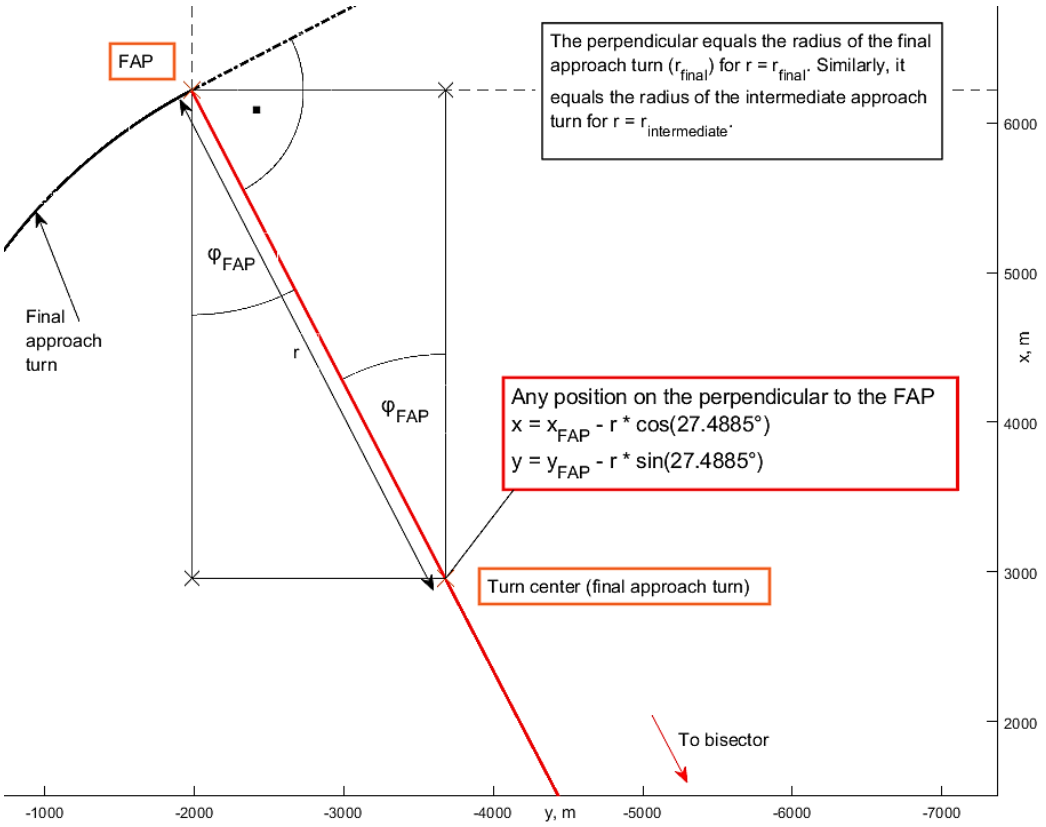

Fig. A6 Calculation of the perpendicular to the FAP.

Appendix B

Tables

Segment	**VPA**	
	Standard	*Maximum*
Initial	2.4°	4.7°
Intermediate	≤1.4°	3.1° (CAT D)
Final	3°	3.1° (CAT D)

Table B1 Standard and maximum VPAs for different approach segments [4, pp. 4-16f.]

Segment	**IAS, kt**	
	Standard	*Minimum*
Initial	250	210
Intermediate	250	180
Final	185	165
Missed Approach	265	185

Table B2 Standard and minimum IASs for different approach segments (CAT D) [4, p. 3-2]

TWC (kt) for turn calculations	
Turn height above aerodrome (ft)	*Standard tailwind component (kt)*
500	25
1 000	38
1 500	50
2 000	50
2 500	50
3 000	50
3 500	55
4 000	60
4 500	65
5 000	70
5 500	75
6 000	80
6 500	85
7 000	90
7 500	95
8 000	100
8 500	105
9 000	110
9 500	115
10 000	120
10 500	125
≥11 000	130

Table B3 TWCs for fixed altitudes [4, p. 3-5].

OBBS ISA AIR BASE RNP Y RWY 15 (AR)

PATH TERMINATOR	WAYPOINT				Course/Track ° MAG (VAR 2020) (° True)	DIST NM	Turn Direction	ARC Centre Waypoint		ARC Radius NM
	Identifier	Type	Flyover	Coordinates				Identifier	Coord.	
IF	TYLOS	IAF	no	N255309.00 E0504300.00						
TF	BS112	IF	no	N255908.30 E0503936.56	N/A (332.8417°)	6.7083				
RF	BS221	FAP	no	N255931.23 E0503421.40		5.6777	left	BS555	N255751.68 E0503651.15	2.7921
RF	BS332	(FROP)	no	N255727.69 E0503409.27		2.1671	left	BS666	N255820.42 E0503607.94	1.9863
TF	RW15		yes	N255601.55 E0503456.12	N/A (153.8194°)	1.5950				
TF	BS444	MATF	no	N254522.32 E0504043.10	N/A 153.8194°	11.8350				
RF	RABAD	MAHF	yes	N254747.00 E0504602.00		8.4768	left	BS777	N254633.46 E0504323.21	2.6837

Waypoint		Constraints		RNP Value NM	VPA [°]	Center Fix	
Identifier	Path Terminator	Altitude	Speed			Name	Radius
TYLOS	IF	A3000+		1.0			
BS112	TF	A2200+	K180-	0.1	1.083		
BS221	RF	A1400	K165-	0.1	1.307	BS555	2.7921
BS332	RF			0.1	3	BS666	1.9863
RW15	TF			0.1	3		
BS444	TF		K185-	1.0			
RABAD	RF	A3000+		1.0		BS777	2.6837

Table B4 Approach chart used for coding

Appendix C

OAS construction for RNP AR APCH procedures

As mentioned in chapter IV, section B, RNP AR APCH uses a total of three OASs to determine the OCH: The final approach surface (also called VEB surface), the horizontal surface and the Z surface. They are depicted in Fig. C1:

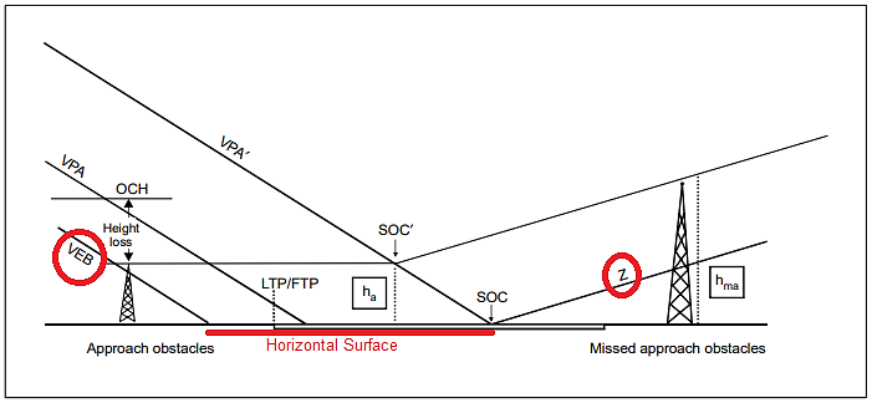

Fig. C1 Relationship between the OASs [4, p. 4-40].

The final approach surface starts at the FAP and ends at a specific point at threshold level between the point where the OCA/H is reached on the glide path (hereafter called "OCA/H point") and the LTP. Assuming that the same navigation accuracy is required for the intermediate and the final segment, the surface is laterally bound by 2x that accuracy (e.g. RNP 0.1) abeam the nominal track between the FAP and the OCA/H point [4, pp. 2-2f.]. Thereafter, during the transition to missed approach RNP 1, it splays to a width of ±2 NM at 15 degrees relative to the course centerline [4, p. 4-33]. The splay also defines the lateral bounds for the horizontal and the Z surface and is shown in Fig. C2. The final approach OAS is vertically bound by the error performance of the baro-VNAV system, called the vertical error budget (VEB). With the VEB, the MOC is based on a four-standard deviation vertical error value that is added to bias errors. Due to the improving error performance with decreasing aircraft height, the MOC reaches its maximum at the FAP and decreases continuously thereafter until the surface reaches the threshold level, i.e. the MOC equals the aircraft height above threshold. That is the "specific point" where the surface ends at a distance D_{VEB} from the threshold. The calculation details and formulae are provided in appendices 1 and 2 to Ref. [4]. Obviously, the final approach OAS is defined similarly to the containment areas we explained in chapter II (see p. 5). That is because the OCH is established based on the navigation performance of the aircraft, too. With the performance being expressed in the shape of the containment areas, it makes sense to adopt a similar shape for the OASs.

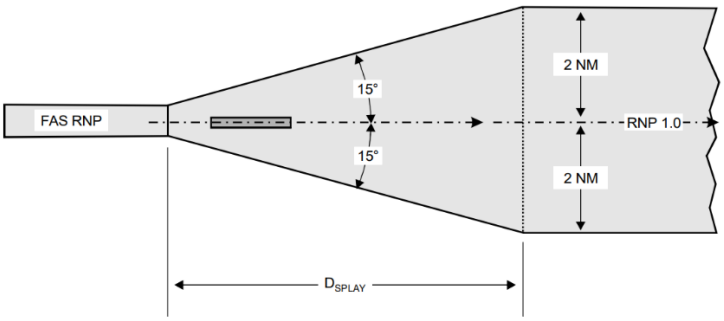

Fig. C2 Lateral OAS splay during the transition to missed approach RNP 1 [4, p. 4-38].

The horizontal surface lies at threshold level, begins at D_{VEB} and extends until the start of climb (SOC), where the Z surface begins. The Z surface, in turn, extends from the SOC until the end of the missed approach. It has a gradient of 2.5 percent and is laterally bound by a semi-width of 2 NM after the missed approach splay is complete. [4, pp. 4-39…43] The term 'SOC', though, is sometimes used ambiguously in Ref. [4] as visible in Fig. C1. It shows a point *SOC* as the origin of the Z surface and a displaced point *SOC'*, where an aircraft is expected to start its climb - also on a 2.5 percent gradient - having gone around at the OCA/H. Both are the result of how go-arounds are modeled for obstacle assessment purposes within RNP AR APCH: Each go-around consists of three phases. The first phase comprises the initial height loss, i.e. the descent from the OCA/H point to the point on the glide path that lies 161 ft below the OCA/H (CAT D). That is followed by a horizontal segment at the height of the tallest real or equivalent approach obstacle until the point (SOC') where the climb (third phase) starts. The horizontal segment always has the same length for a given VPA, no matter how large the OCA/H is, i.e. the SOC' is always located within the same distance from the respective OCA/H point. That distance is called transition distance (TrD) and is intended to allow for the occurrence of possible along-track errors during the transition to the missed approach RNP (see Eq. (6)). Thus, it can be excluded that an aircraft is not able to fly over a missed approach obstacle because it started climbing later than expected. The small climb gradient considers possible failures (e.g. one engine inoperative) that limit the climb performance of the aircraft. If the OCH is increased, the SOC's move accordingly. [4, pp. 4-39…41] The position of the Z surface, however, remains constant so that it is not pulled into the final approach segment for very high OCHs. Therefore, its origin (SOC) is modeled as the SOC' for a go-around at a fixed OCH, which must equal the applicable height loss margin if the climb/Z surface shall, as required, be started from threshold level. The SOC position can hence be determined at a distance TrD from the point where e.g. 161 ft are reached on the glide path (see Eq. (5)). Fig. C3 illustrates the concept.

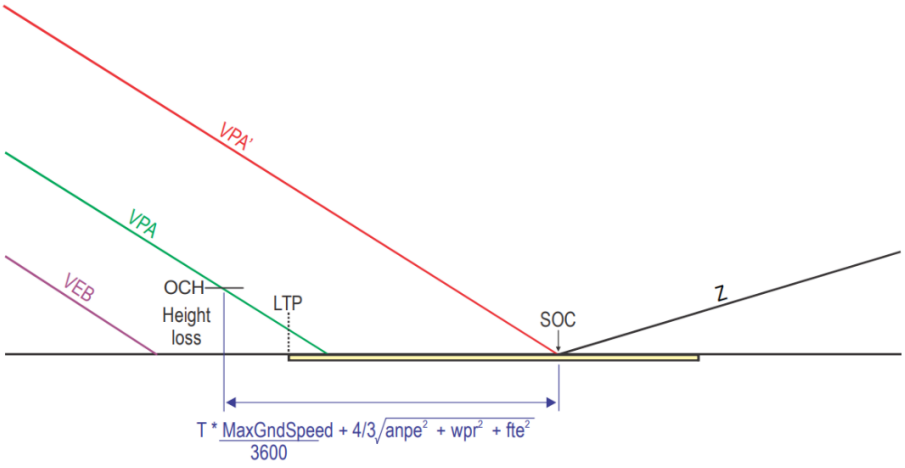

Fig. C3 Definition of the Z surface [4, p. 4-43].

Appendix D

Establishing lower and higher temperature limits for an airport

The RNP AR APCH procedure design manual includes the following method to establish a lower and a higher temperature limit from a five-year history: First, determine the month with the lowest/highest average temperature for each year. Then, take the lowest/highest measured temperature within each of those months. The average of those five values constitutes the lower/higher temperature limit and is referred to as the average coldest/hottest temperature. [4, p. 4-27] Extensive surface meteorologic data from weather stations around the world is available as part of the integrated surface dataset (ISD) from the United States National Centers for Environmental Information (see Ref. [41]). We use ISD data from Bahrain International Airport from 2015 to 2019 and apply the described method, which yield limits of 11.33° C and 45.01° C, respectively.

Appendix E

Modeling and plotting the final approach turn and the CTR boundary in MATLAB & Determining the minimum distance to the CTR and the critical point

A. Modeling and plotting the final approach turn and the CTR boundary

In MATLAB, curved segments must be discretized before they can be plotted. To do that, we define φ as a vector of linearly spaced, discrete angles in small steps (e.g. 27.4885° - 90° in 0.001° increments) before applying it to Eqs. (9)-(11). That yields vectors of the same size as φ, each containing the x-, y- or z-coordinates, respectively, of the discrete positions. The plot3 function combines each triple (e.g. x(1), y(1), z(1)) into one position, plots it and connects adjacent positions with a line [42]. Generally, the step size should be as small as possible to minimize the discretization error. Before OBKH CTR can be plotted, its boundaries must be described in the reference frame. The shape that we must reproduce is shown in Fig. 1 and defined in the AIP as follows:

OBKH AD 2.17 ATS AIRSPACE

1	Designation and lateral limits	SAKHIR AIRBASE CTR; centered at ARP (260205N 0503128E) and orientated parallel to RWY (353 / 173 degrees magnetic) extending 7.0 NM in length and 4 NM wide defined by Coordinates 255901N 0502932E - 260446N 0503128E0502857E following an arc of radius 3.5 NM centered on 260205N 0503128E (ARP) to 260508N 0503323E - 255923N 0503358E following an arc of 3.5 NM radius centered on 260205N 0503128E (ARP) to Origin.
2	Vertical limits	SFC - 2500 FT
3	Airspace classification	D

Fig. E1 OBKH CTR limits from the Bahrain FIR AIP [5, p. AD 2-OBKH-5]

To do so, we first convert the coordinates of the aerodrome reference point (ARP) and the four endpoints from LLH into the reference frame and plot them, which is equally possible with plot3. The two straight segments do not need to be discretized as plot3 can connect two points (the western and eastern endpoints, respectively) with a straight line. The arc segments are constructed as RF legs with the ARP as turn center. For the southern arc, the exact radius is determined as the norm of the 2-D (X-Y) vector from the ARP to the south-eastern endpoint (r_{SE}). It is slightly larger than the rounded 3.5 NM from the AIP with 3.5103 NM. The angular positions of the two endpoints define the central angle of the arc and are determined using trigonometric

functions (see Fig. E2). The arc can now be described by Eqs. (E1) and (E2), which must be discretized as described above before it can be plotted. Fig. E2 shows the result.

$$\boldsymbol{x_{arc}(\varphi) = r_{SE} * \cos(\varphi) + x_{ARP};\ \varphi \in [124.12°, 193.72°]} \quad \text{(E1)}$$

$$\boldsymbol{y_{arc}(\varphi) = r_{SE} * \sin(\varphi) + y_{ARP};\ \varphi \in [124.12°, 193.72°]} \quad \text{(E2)}$$

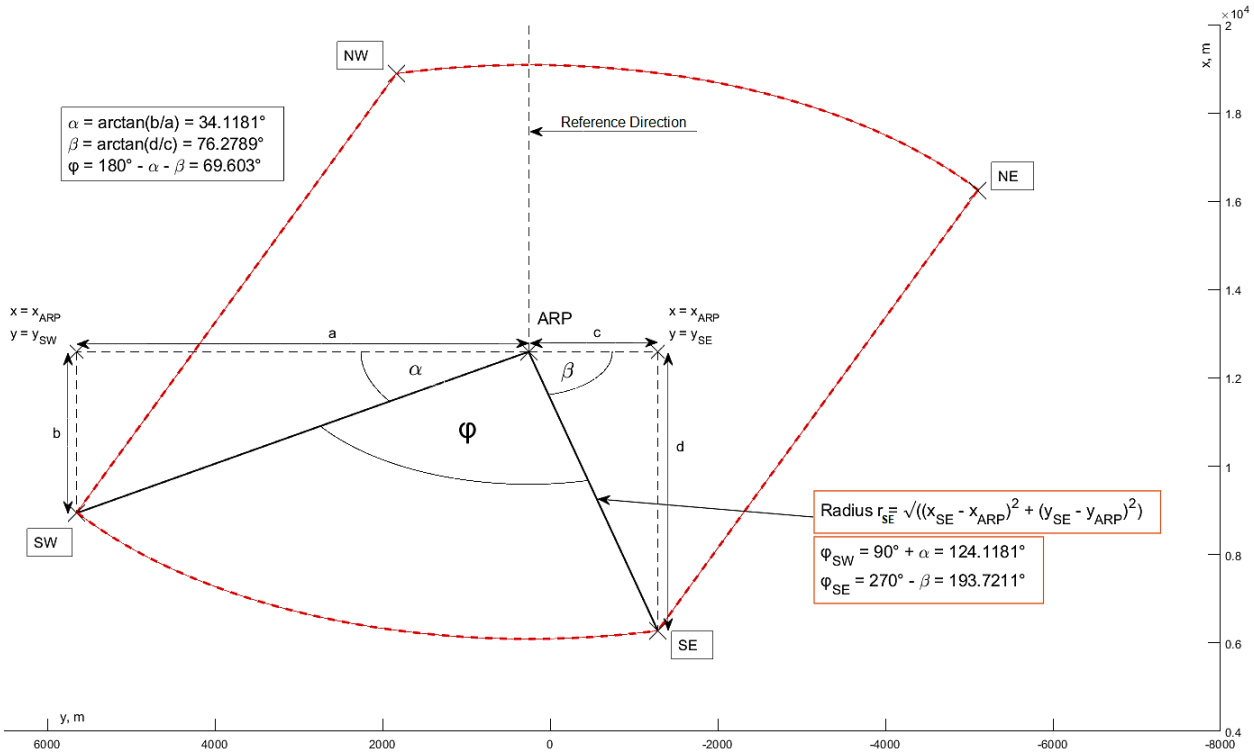

Fig. E2 OBKH CTR construction in MATLAB

B. Determining the minimum distance to the CTR and the critical point

Assuming that the minimum distance occurs between the south-eastern endpoint of the CTR (referred to as "SE") and the nearest point on the outer turn area boundary, we discretize only a small section of the CTR boundary within 50 m from the SE in 1-m steps for verification. That is translated into a discrete angle interval by means of Eq. (E3) for the arc length:

$$\boldsymbol{d_{arc}(\varphi) = r_{arc} * \varphi;\ \varphi = central\ angle\ [rad]} \quad \text{(E3)}$$

Consequently, Eqs. (E1) and (E2) must be discretized for φ (defined as in Fig. E2) between φ_{SE} and $(\varphi_{SE} - \frac{50}{r_{SE}})$ in steps of $\frac{1}{r_{SE}}$. For the outer turn area boundary, we discretize the section within ±50 m from the point that lies on the radial line from the turn center to the SE (see Fig. E3),

also in 1-m steps. Accordingly, Eqs. (10) and (11) must be discretized for φ (defined as in Fig. 3) between $(\varphi_{SE} - \frac{50}{r_{outer}})$ and $(\varphi_{SE} + \frac{50}{r_{outer}})$ in steps of $\frac{1}{r_{outer}}$.

The discretization in MATLAB yields the vectors containing the x- and y-coordinates of the discrete boundary positions. To find the minimum distance, we use a nested loop to iterate through a total of m outer turn area boundary positions (outer loop) and calculate, for each of those positions, the 2-D (X-Y) Euclidean distances to all n CTR boundary positions (inner loop). The results are put into a matrix whose dimension mxn (or nxm) corresponds to the number of discrete positions. Hence, the minimum of the matrix can be related to a specific outer turn area and a specific CTR boundary position by its two indices. The former is considered the critical point, which is defined by its angle $\varphi_{critical}$ from the chosen reference direction (see Fig. E3). The height of the critical point is determined by applying $\varphi_{critical}$ to Eq. (9) but must then be converted into altitude before it is compared to the current construction altitude. Fig. E3 illustrates the process.

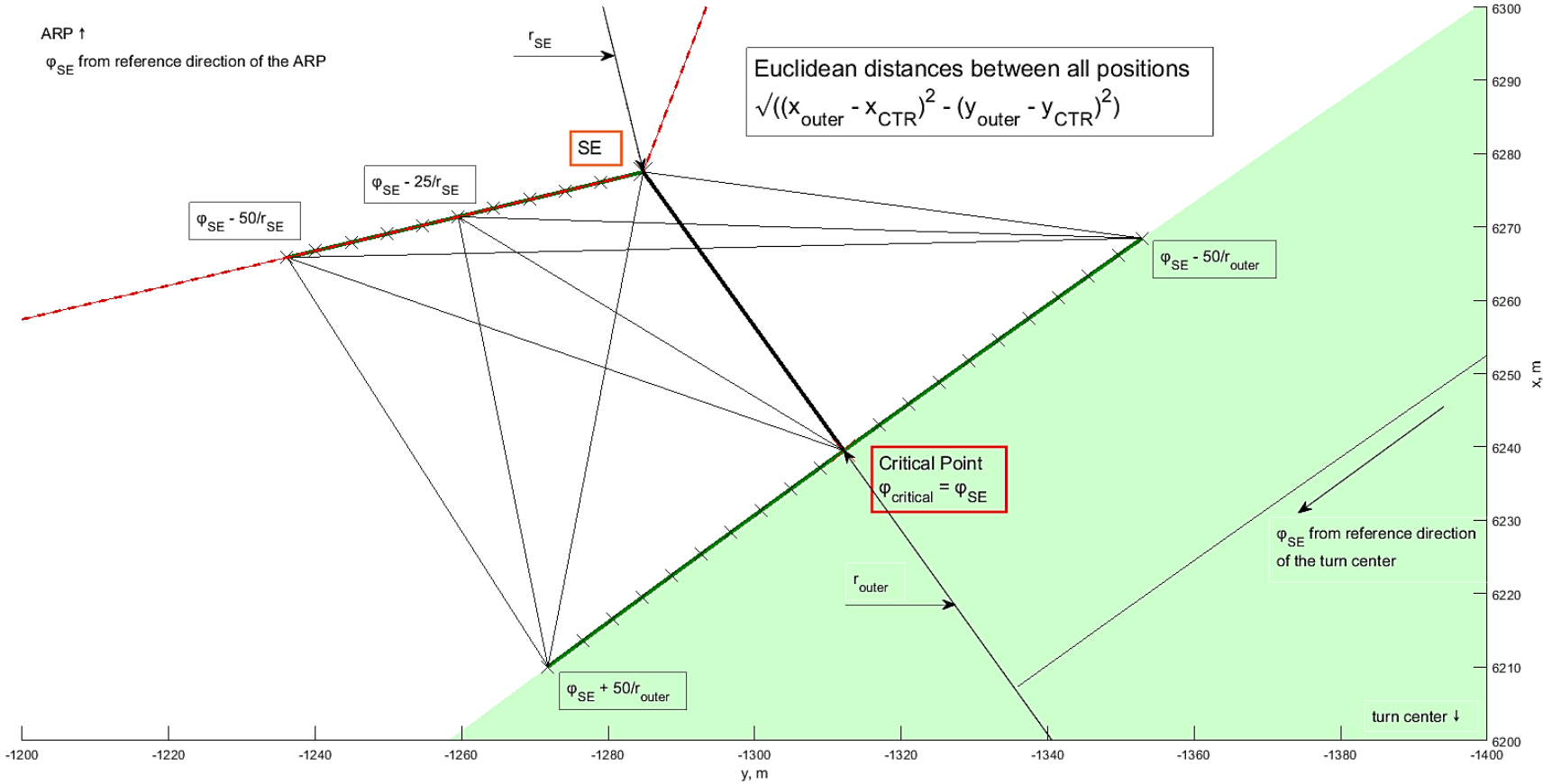

Fig. E3 Determination of the minimum distance (in bold) by discretization

Appendix F

Obstacle assessment and visualization with geoplot3 (MATLAB)

a) Horizontal view of the entire approach

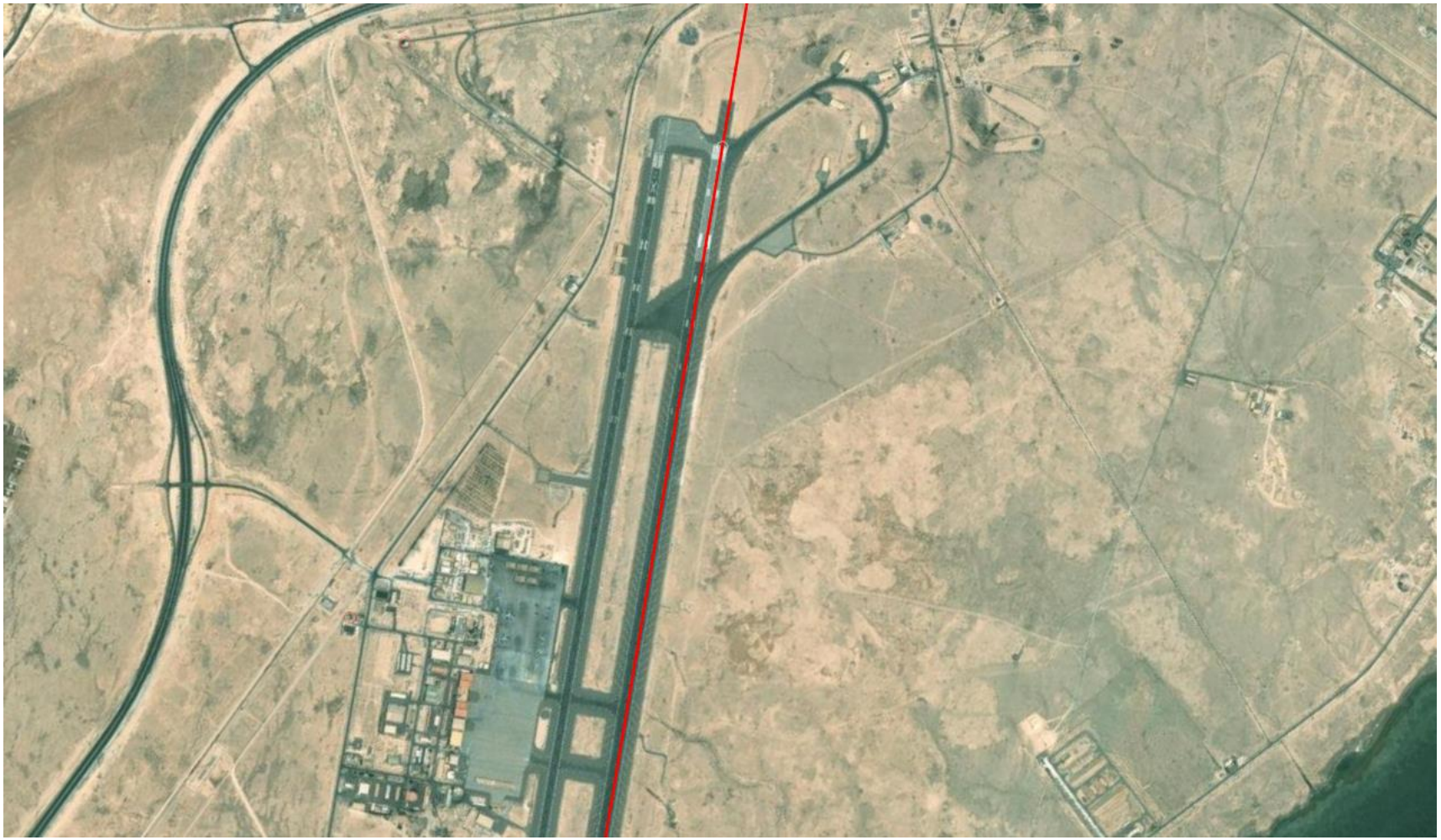

b) Zoom on THR RWY 15L / Isa Air Base

Fig. F1 Approach trajectory (red) without obstacle assessment surfaces

Fig. F2 Initial approach track (red) including the obstacle clearance volume (green)

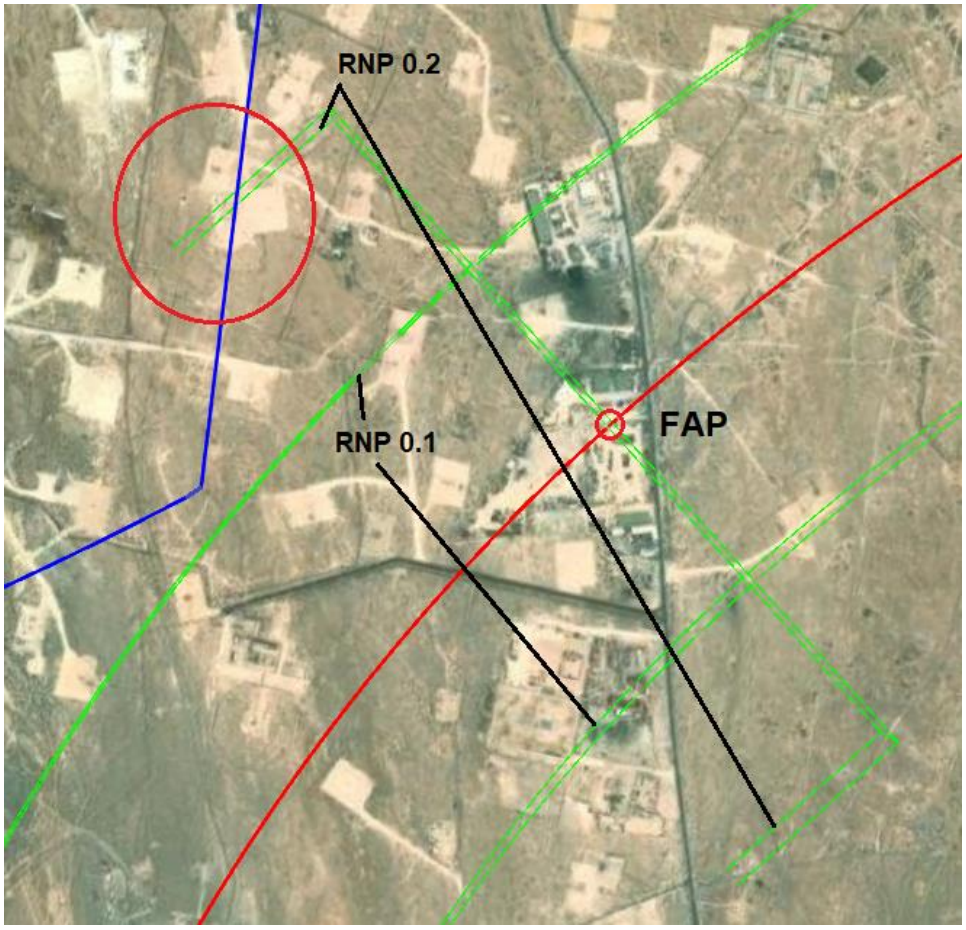

a) Penetration of OBKH CTR due to RNP change at the FAP

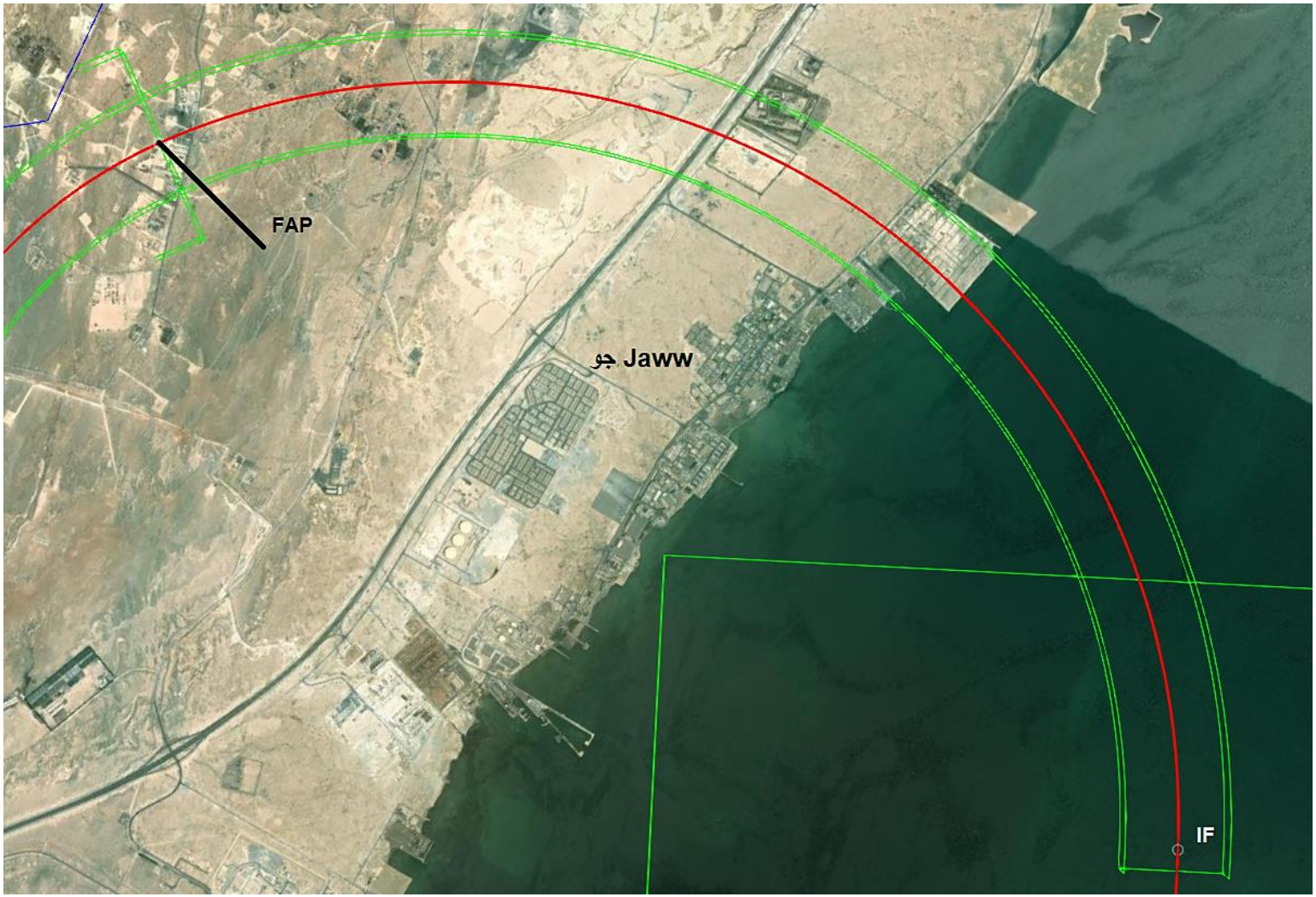

b) Approach track (red) including the obstacle clearance volume (green)

Fig. F3 Intermediate approach segment

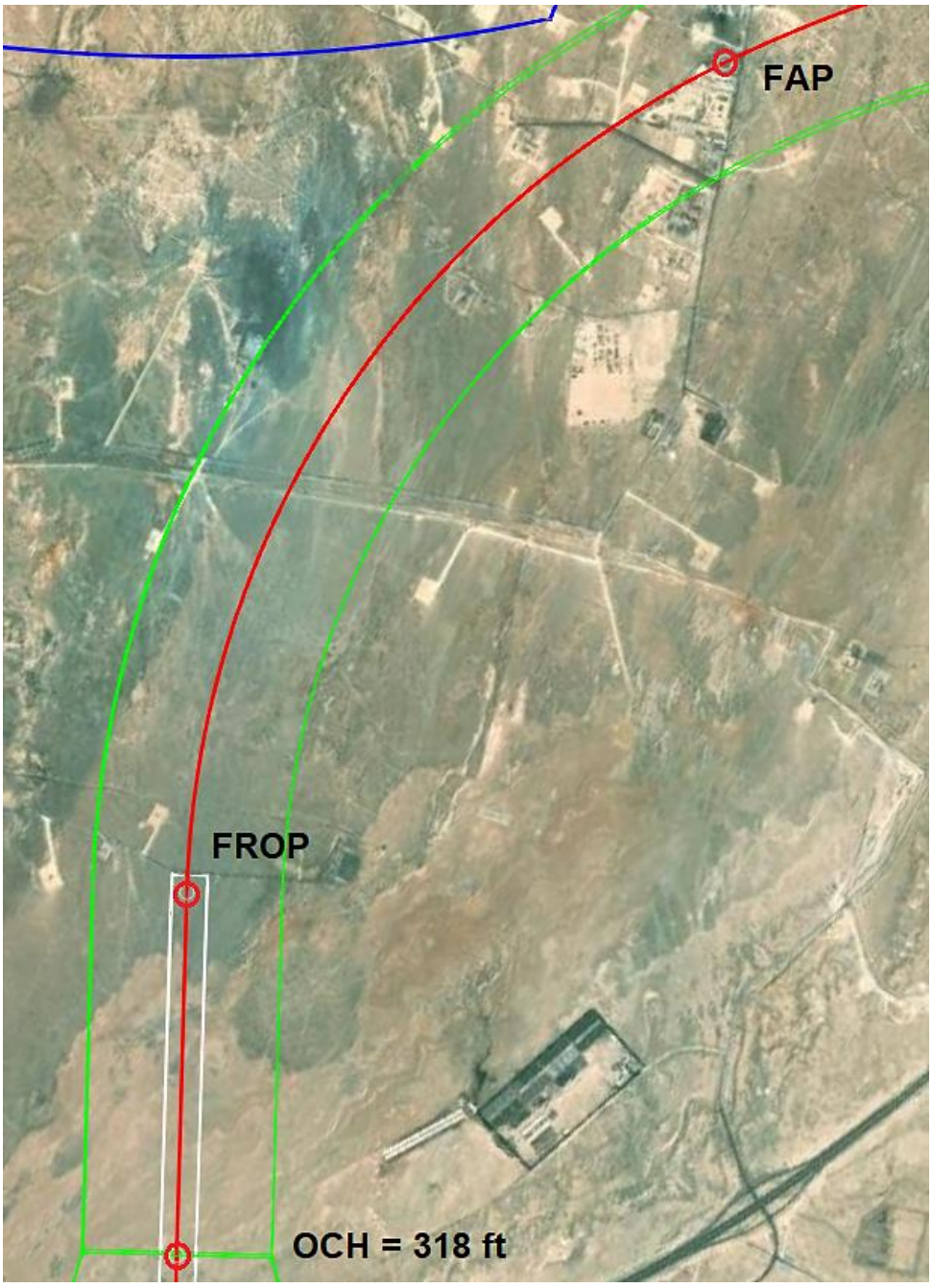

a) Horizontal view

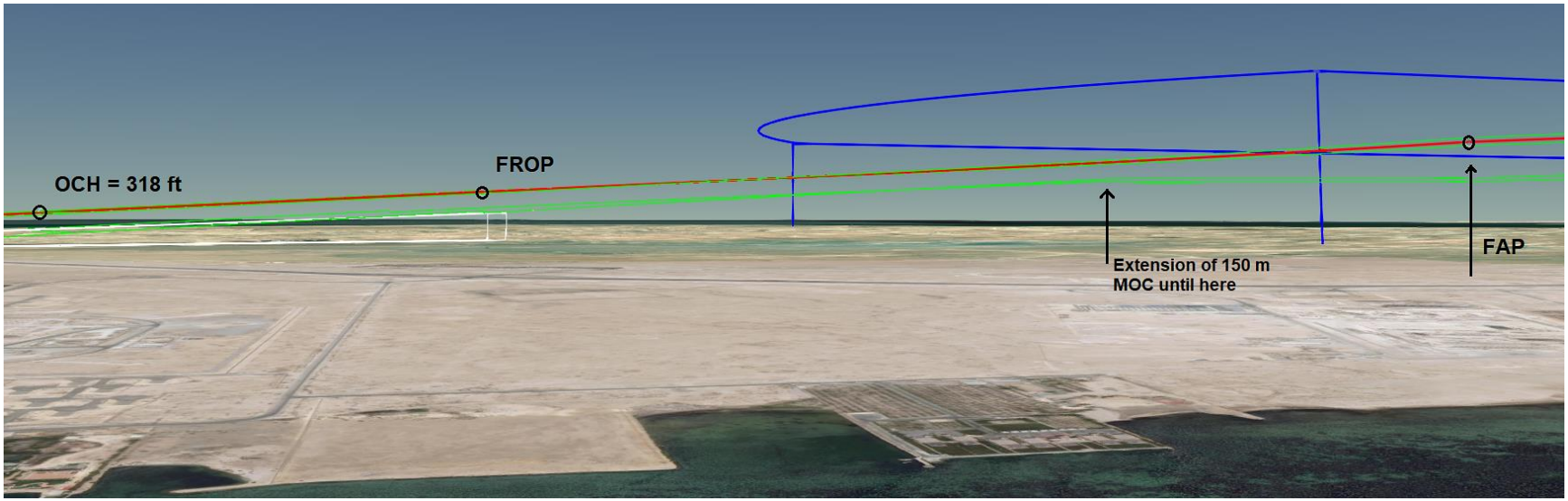

b) Vertical profile

Fig. F4 Final approach segment

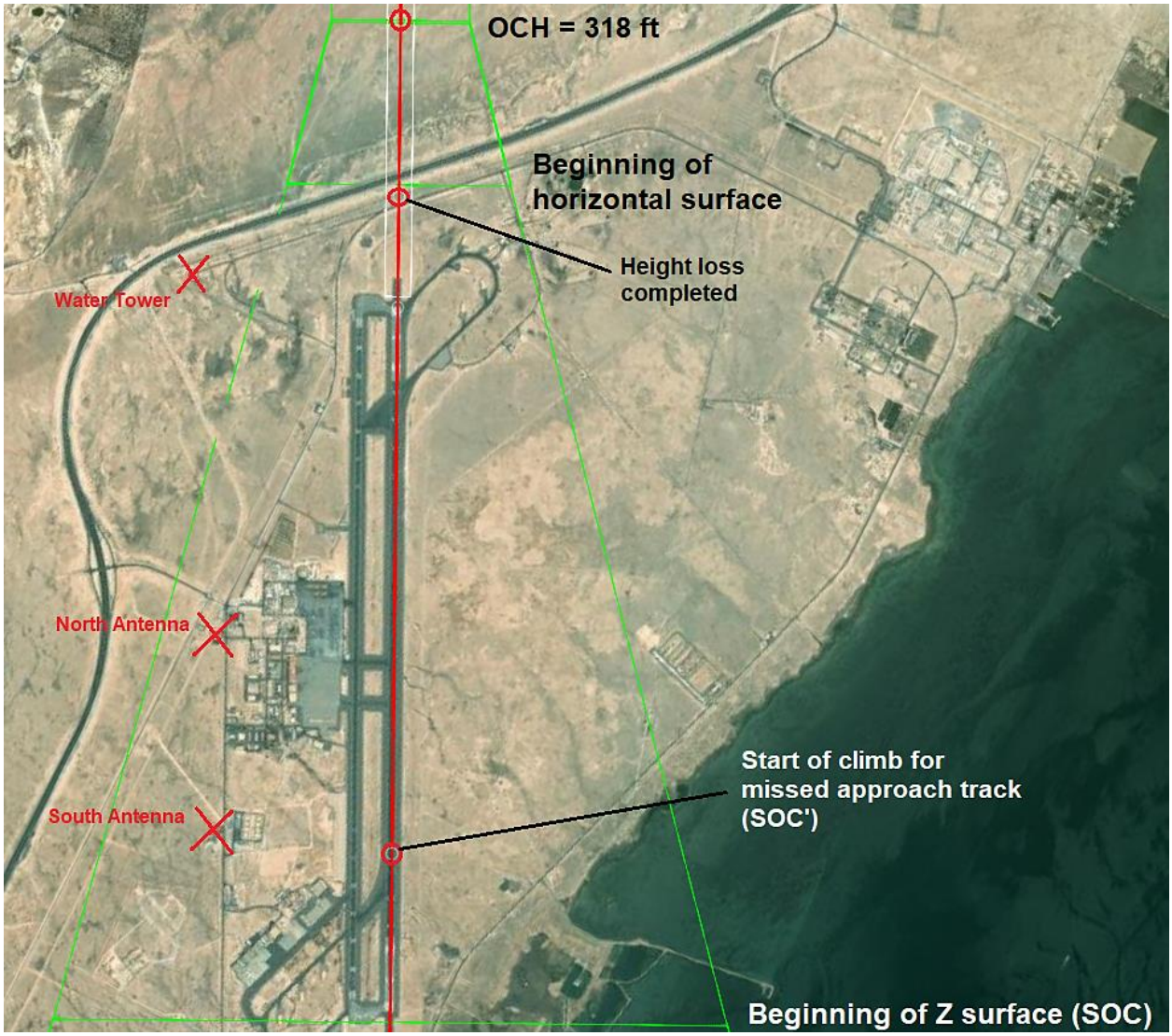

a) VEB and horizontal surface in the missed approach segment

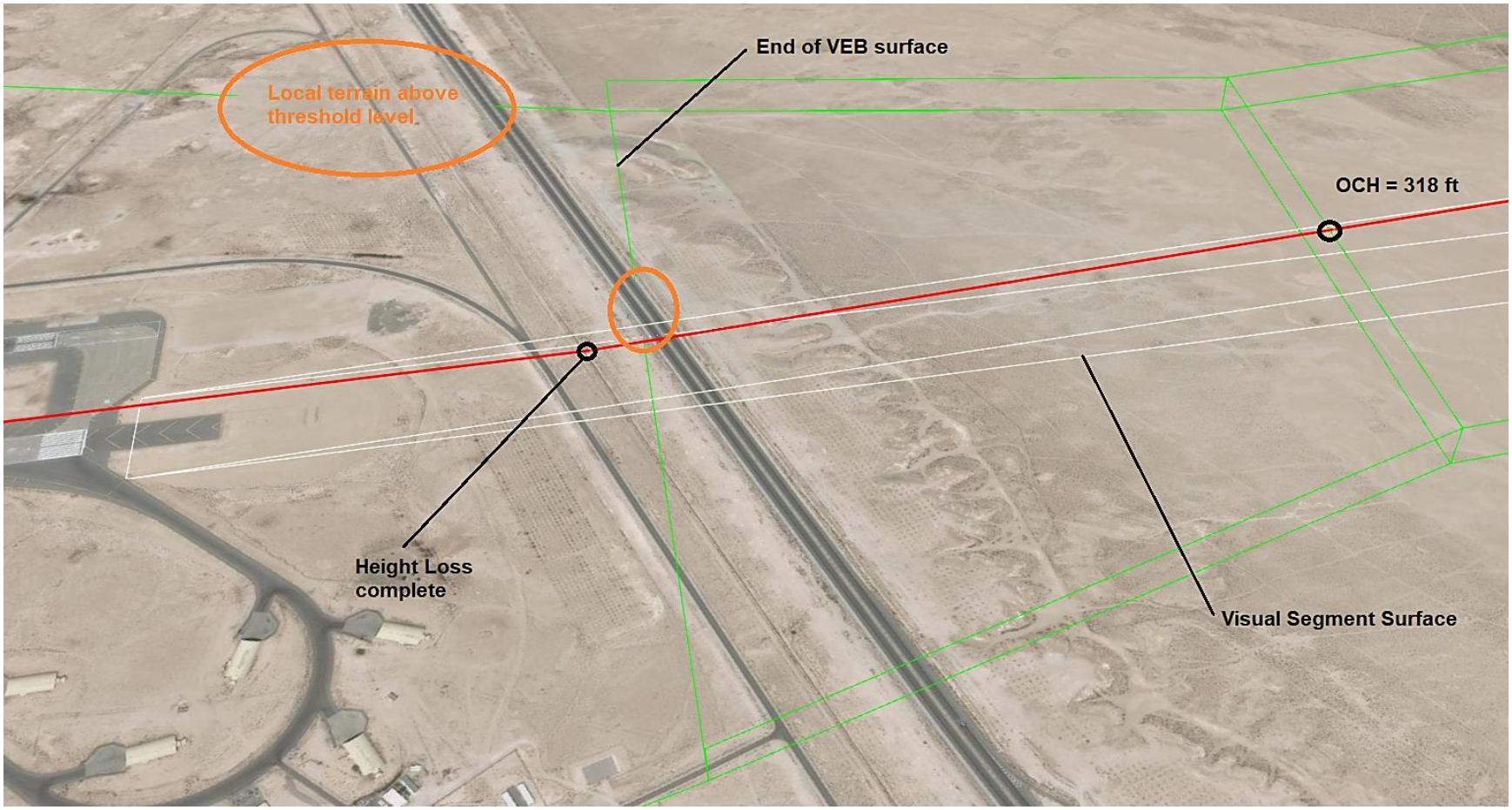

b) VEB-protected area and initial horizontal surface

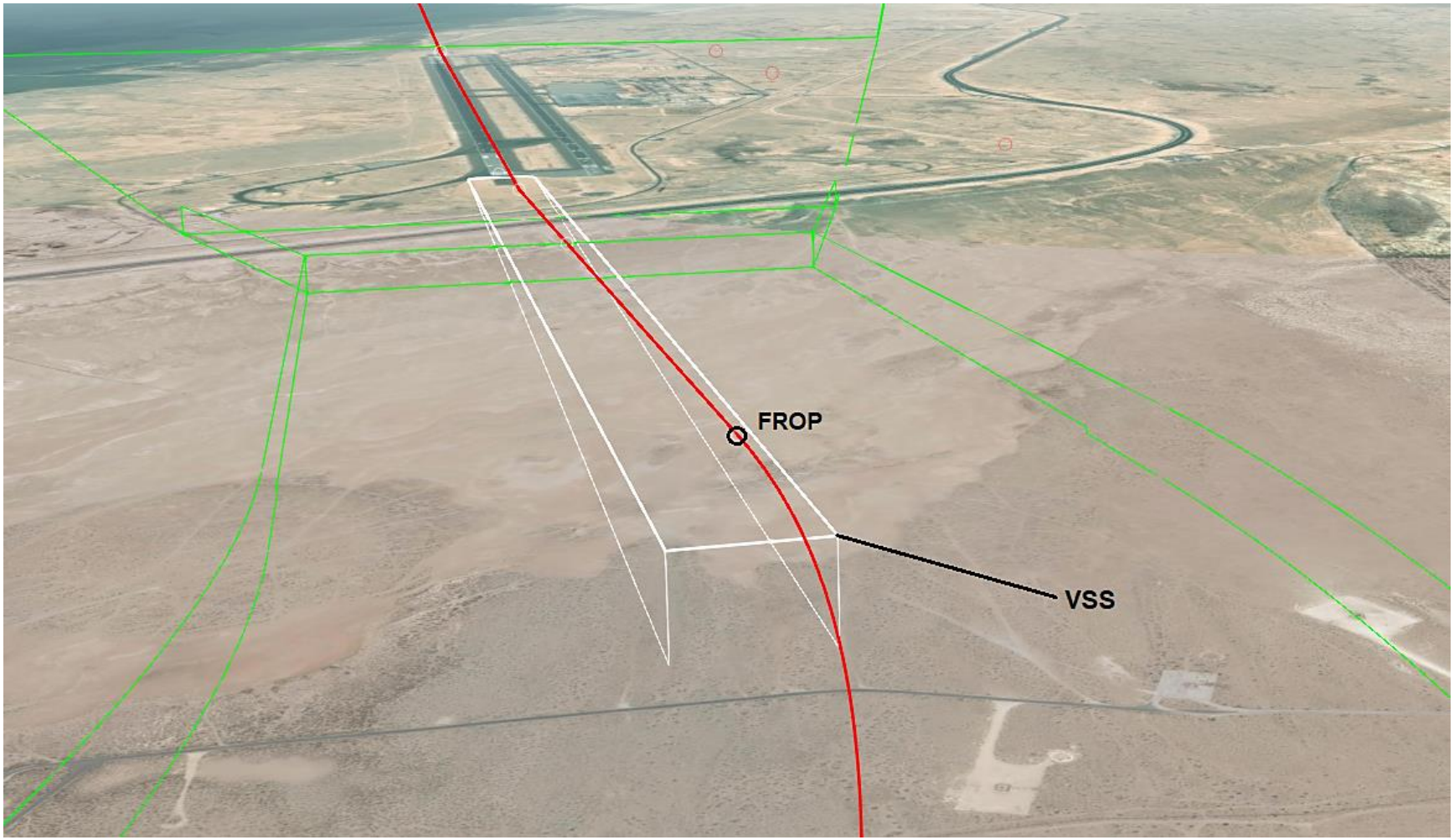

c) Visual segment surface

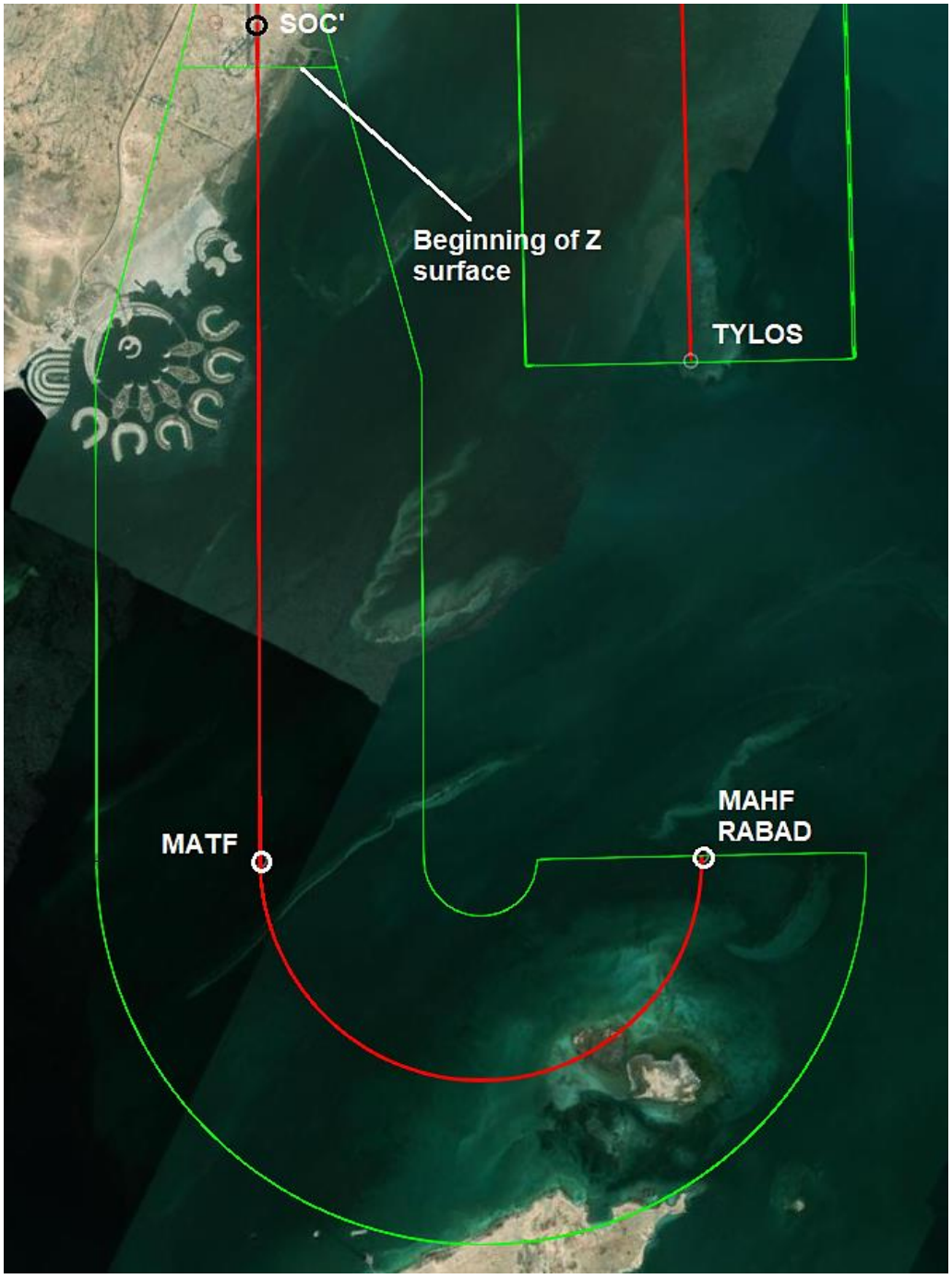

d) Z surface

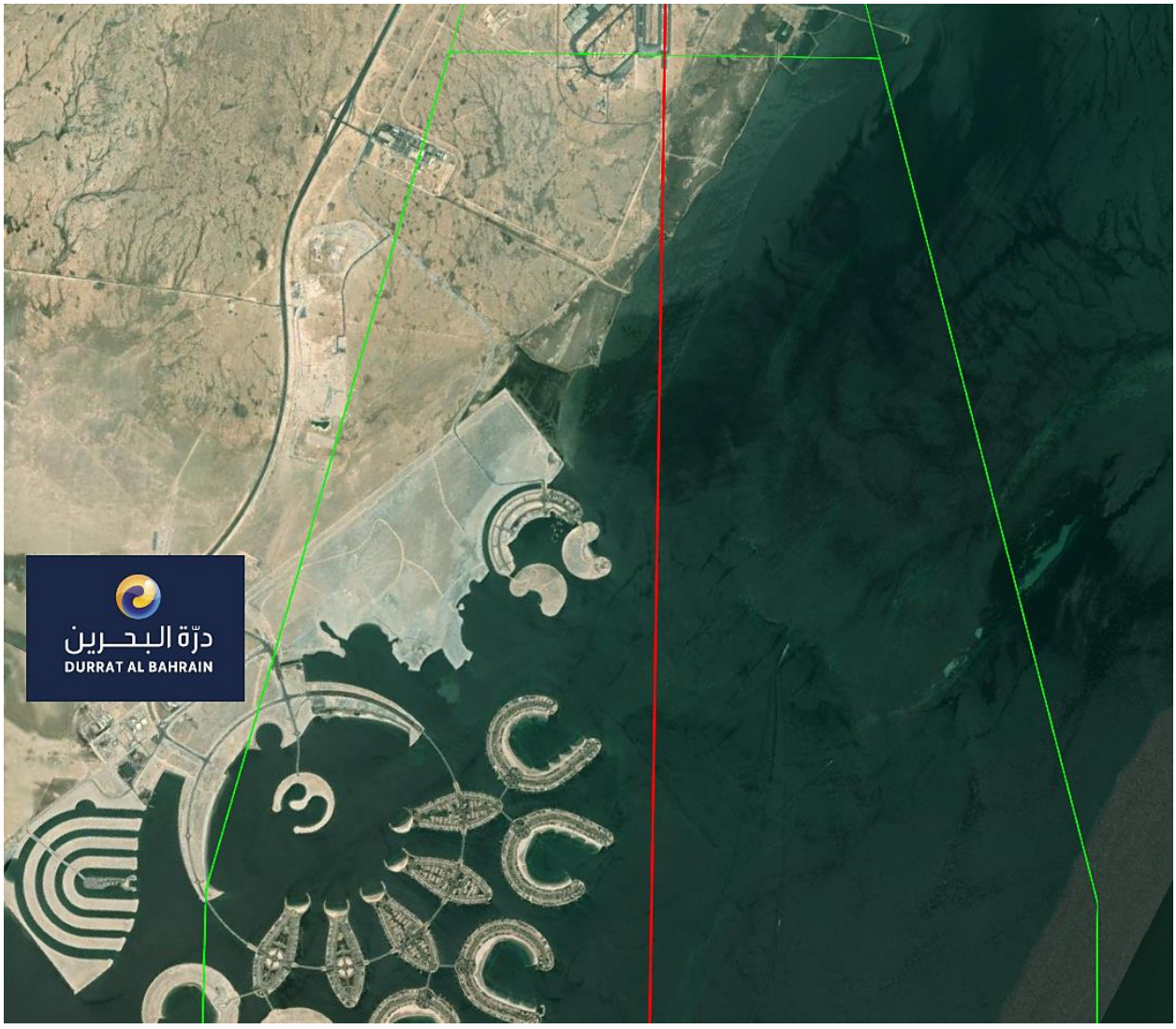

e) Initial Z surface

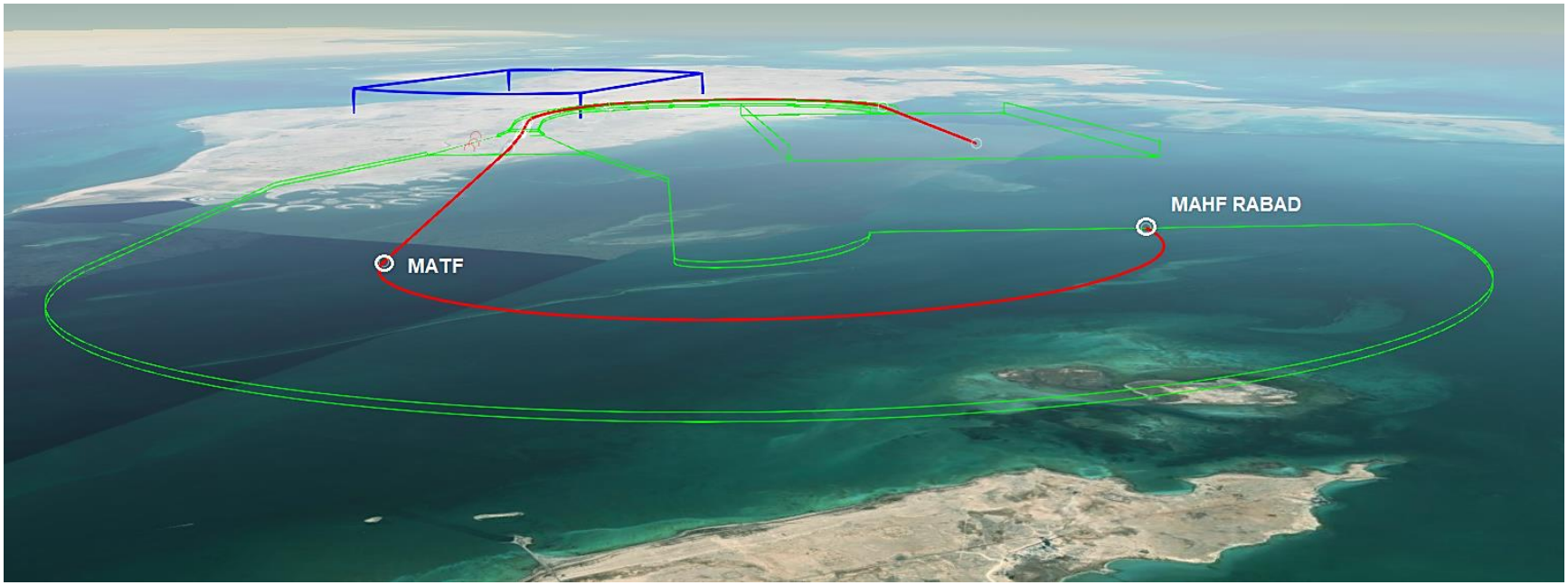

f) MAS turn

Fig. F5 Missed approach segment

Appendix G

Simulator test: Deviations and flight parameters

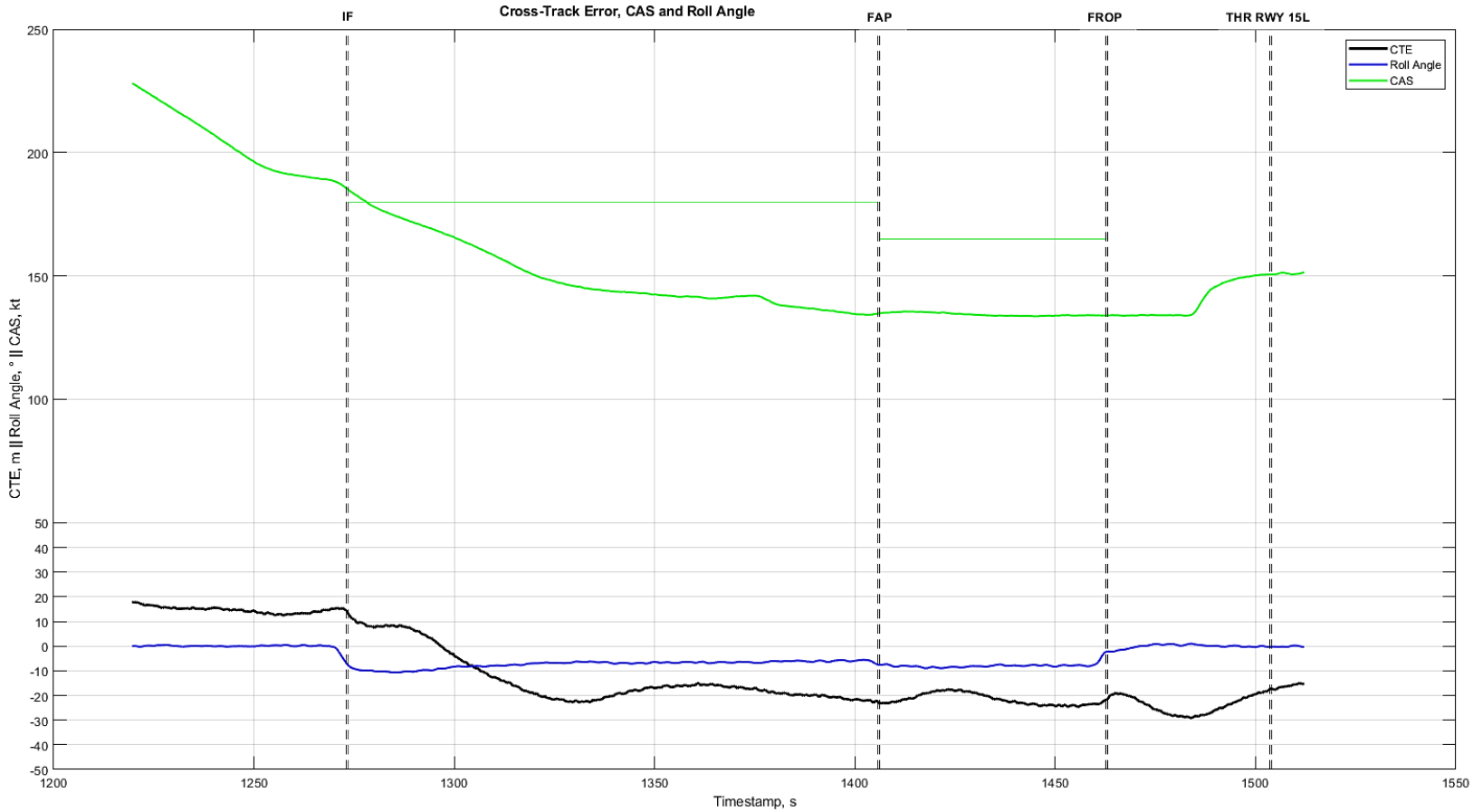

a) CTE, CAS, Roll Angle [#1]

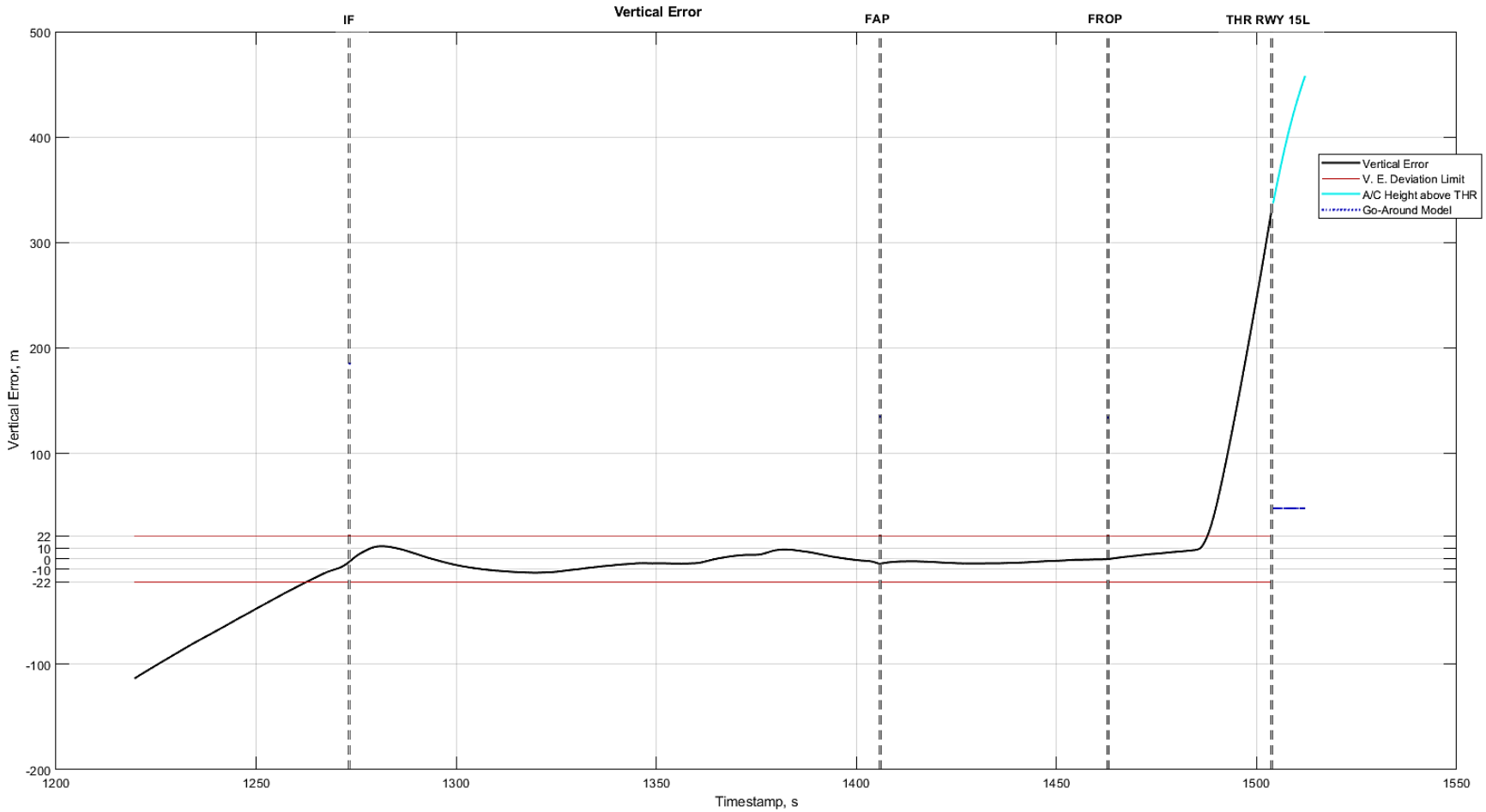

b) Vertical Error [#1]

Fig. G1 Scenario 1

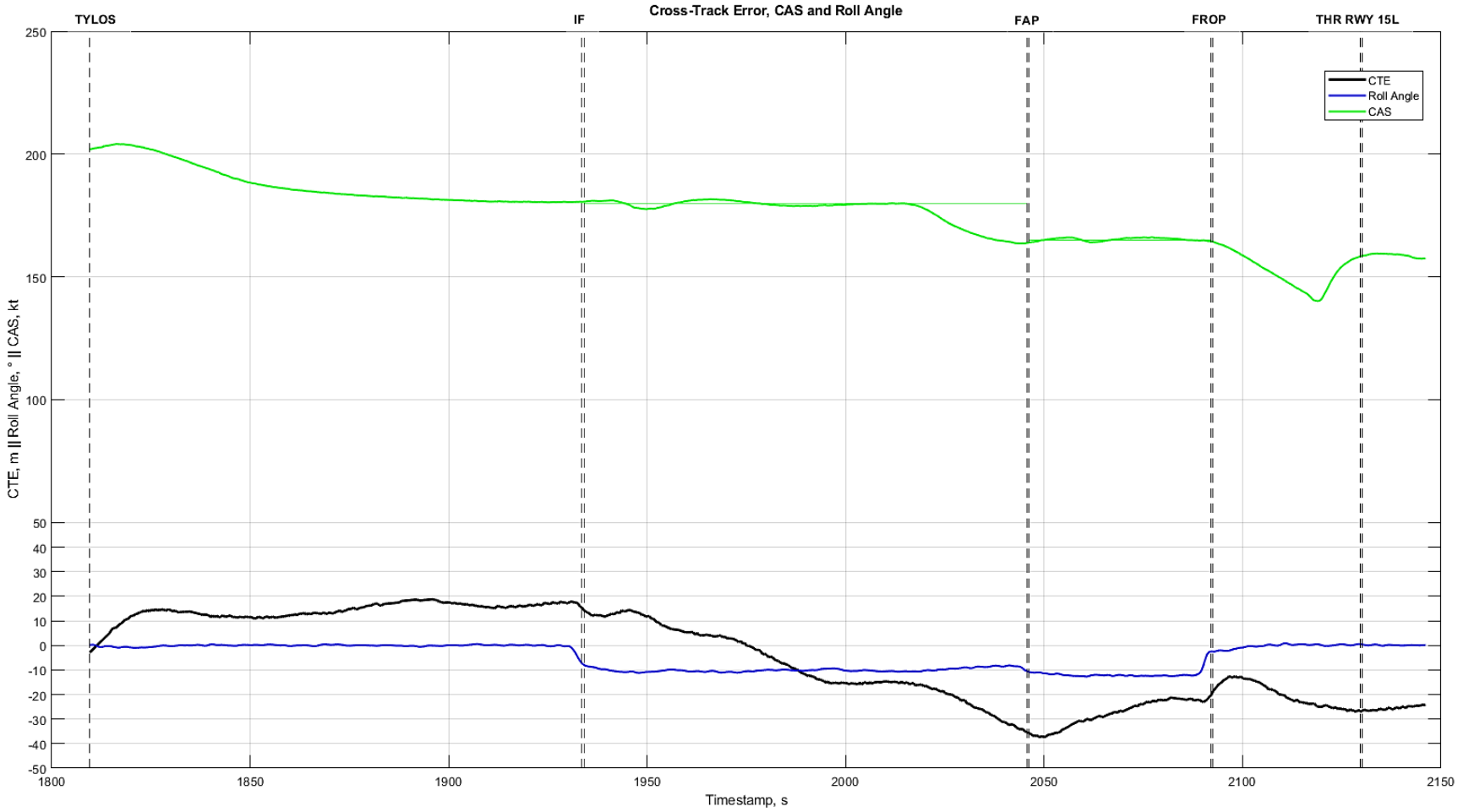

a) CTE, CAS, Roll Angle [#2]

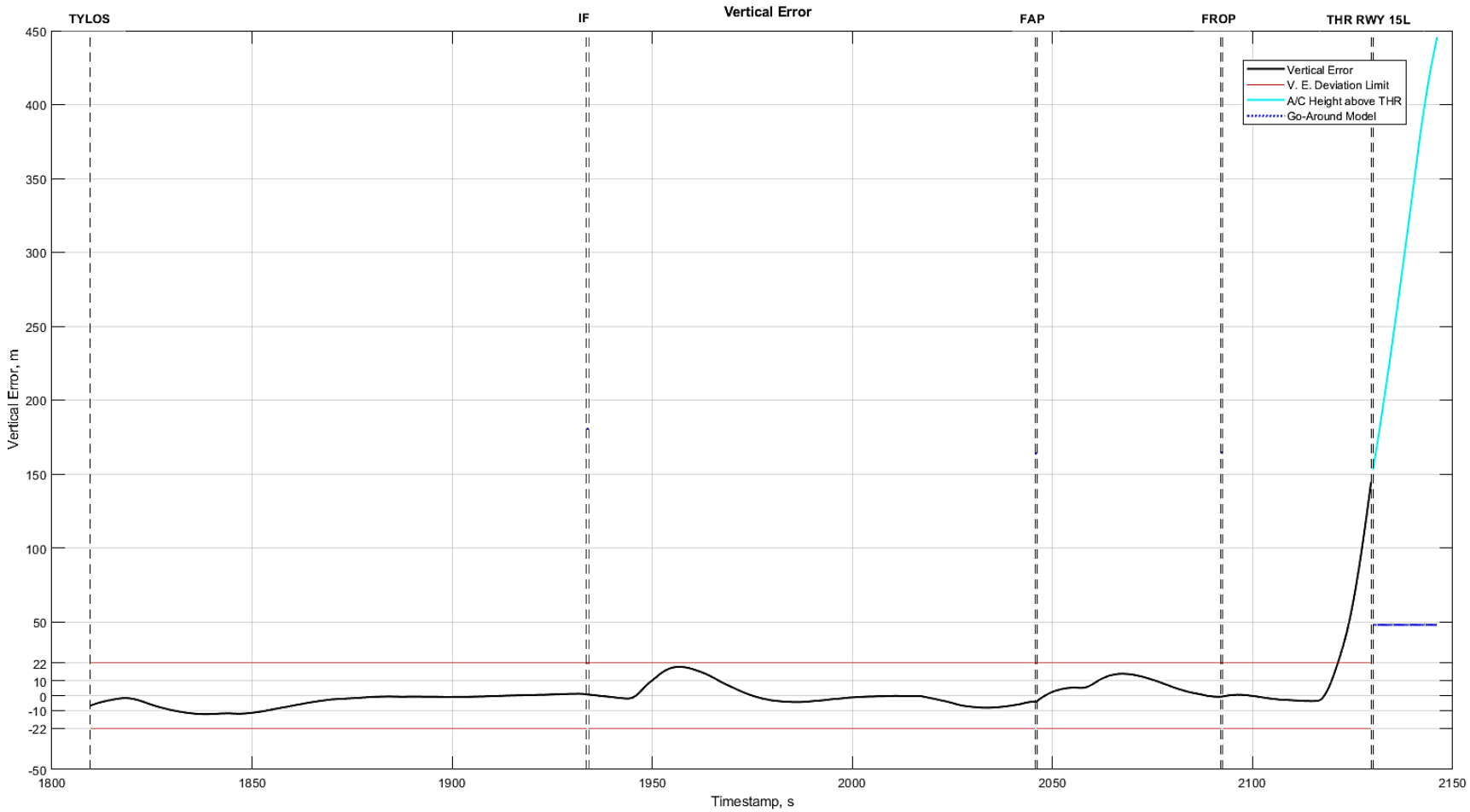

b) Vertical Error [#2]

Fig. G2 Scenario 2

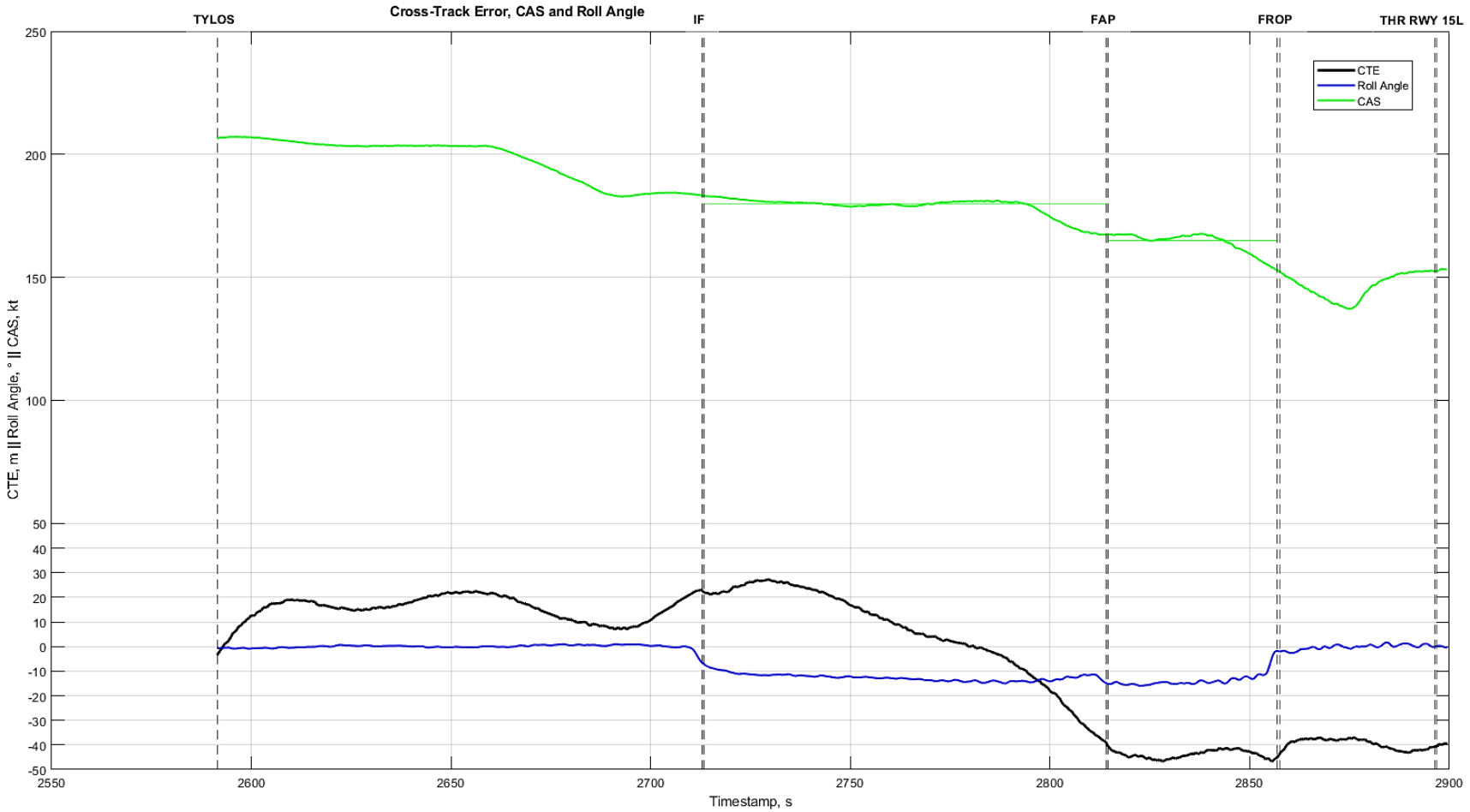

a) CTE, CAS and Roll Angle [#3]

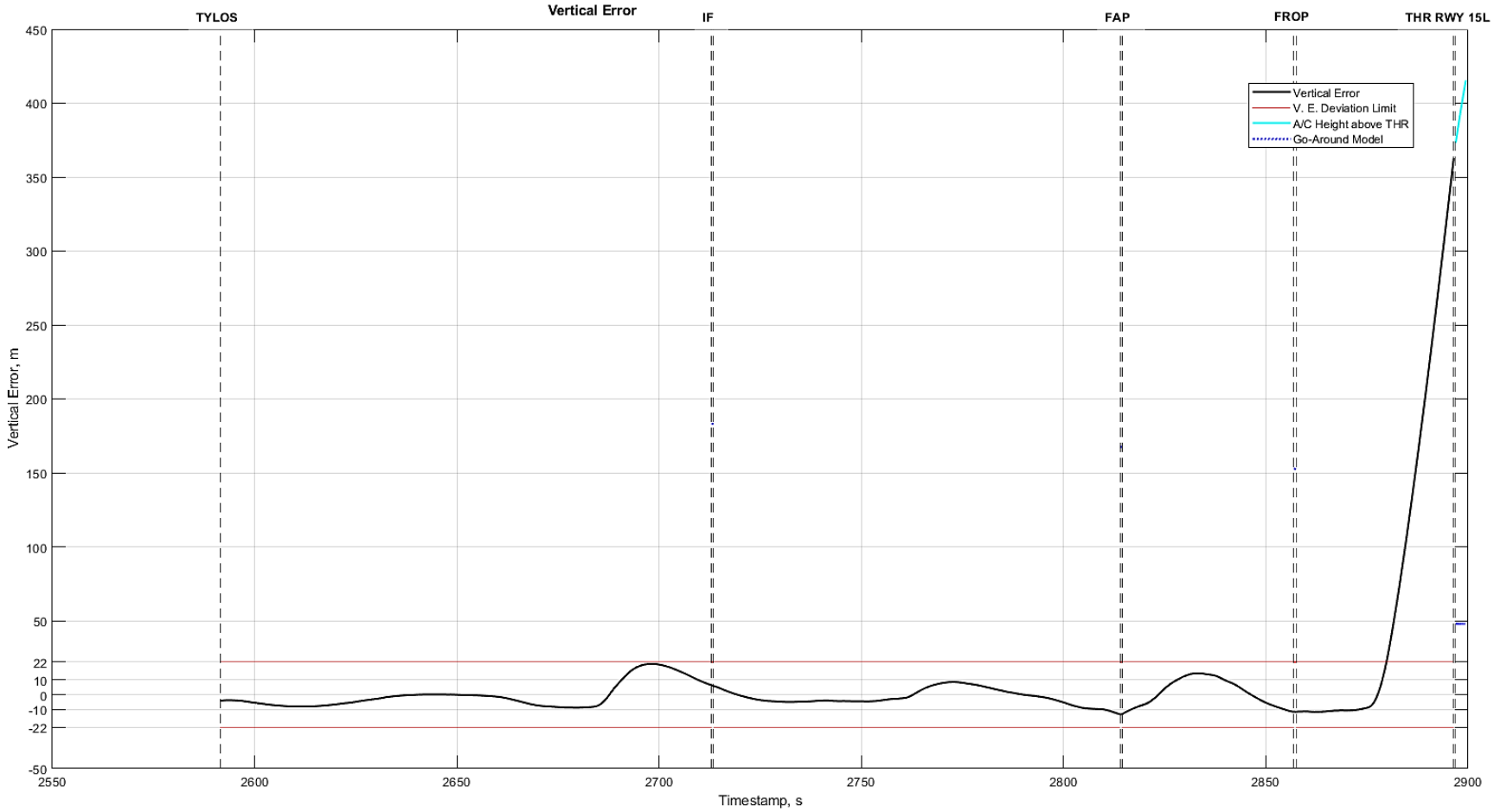

b) Vertical Error [#3]

Fig. G3 Scenario 3

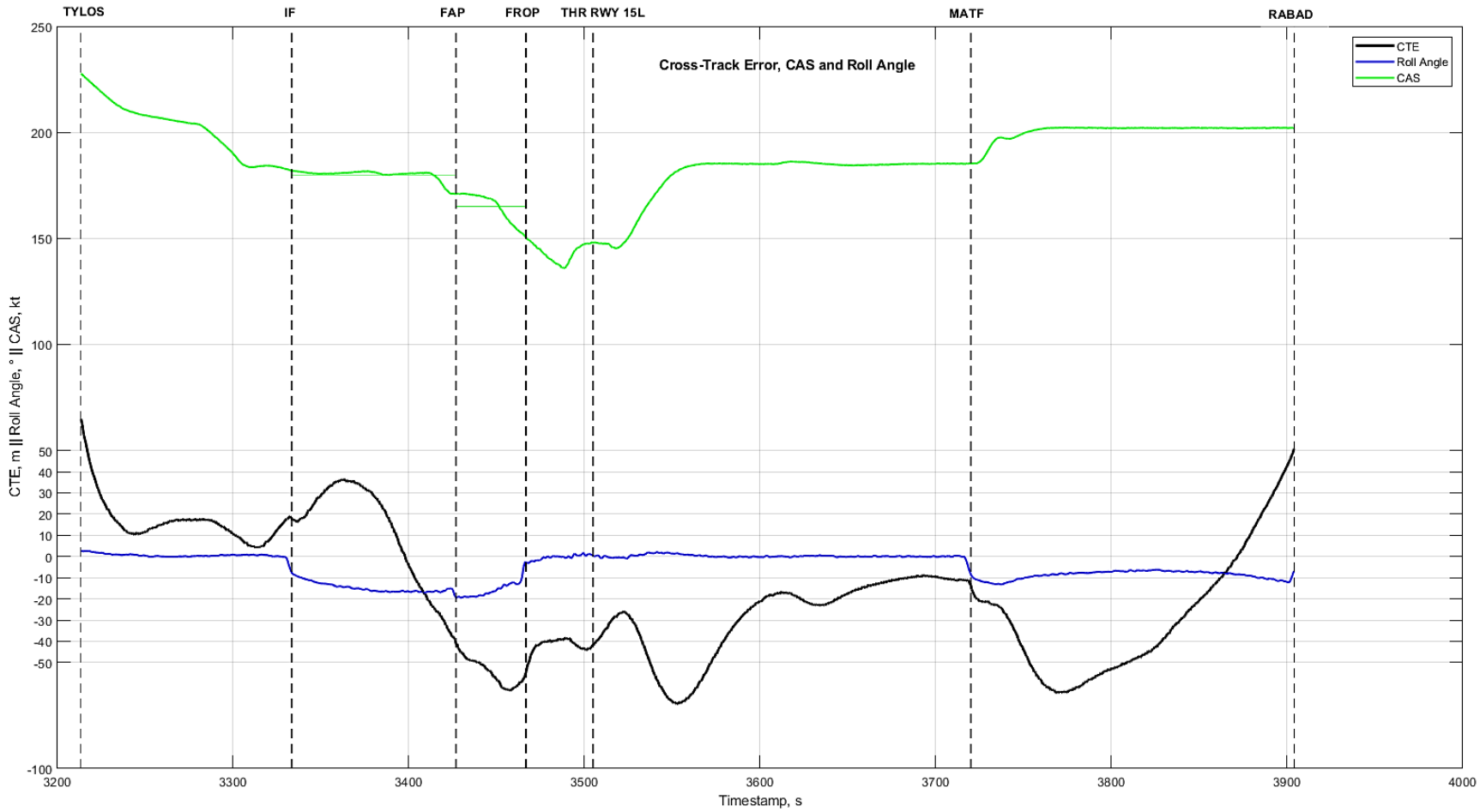

a) CTE, CAS and Roll Angle [#4]

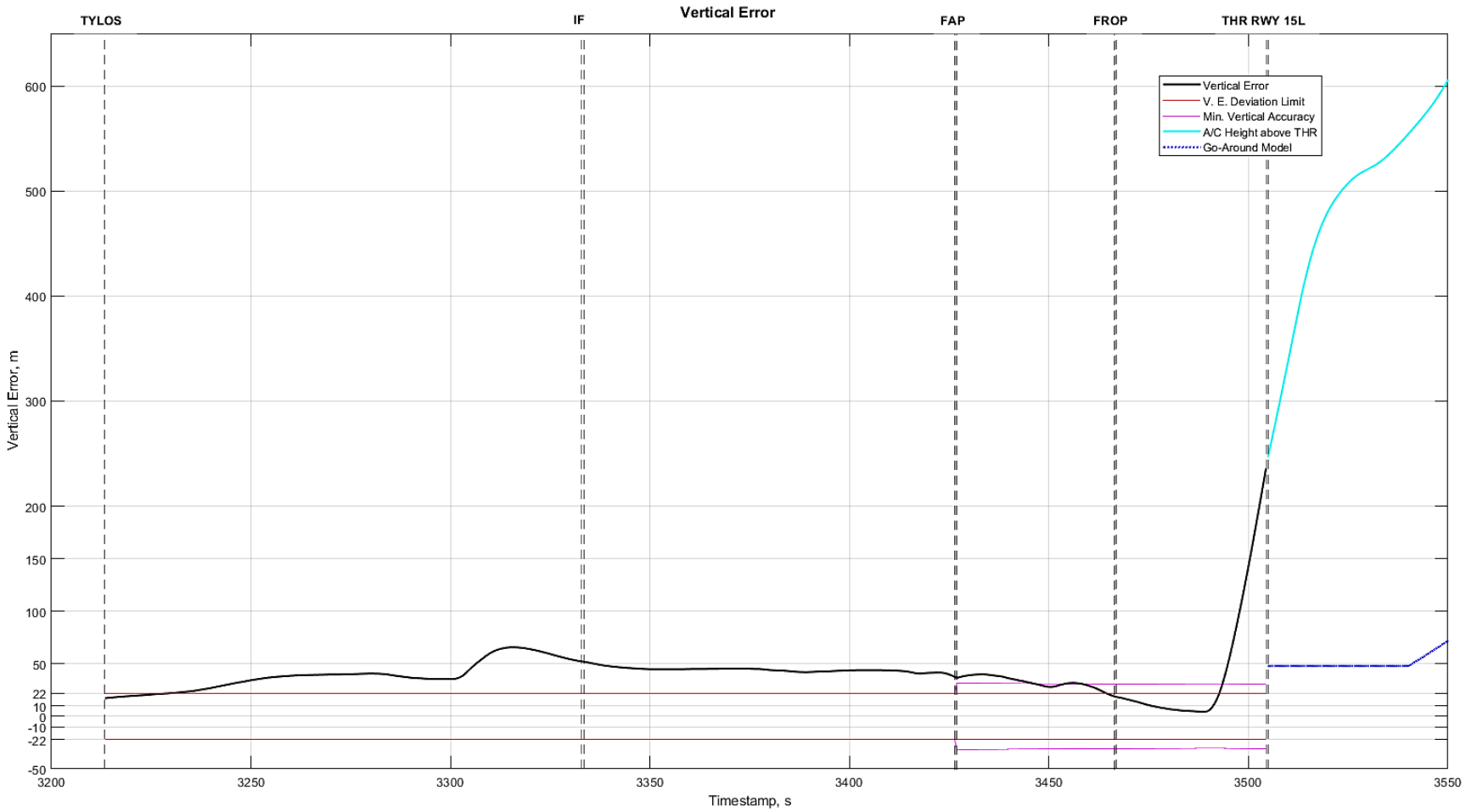

b) Vertical Error Approach [#4]

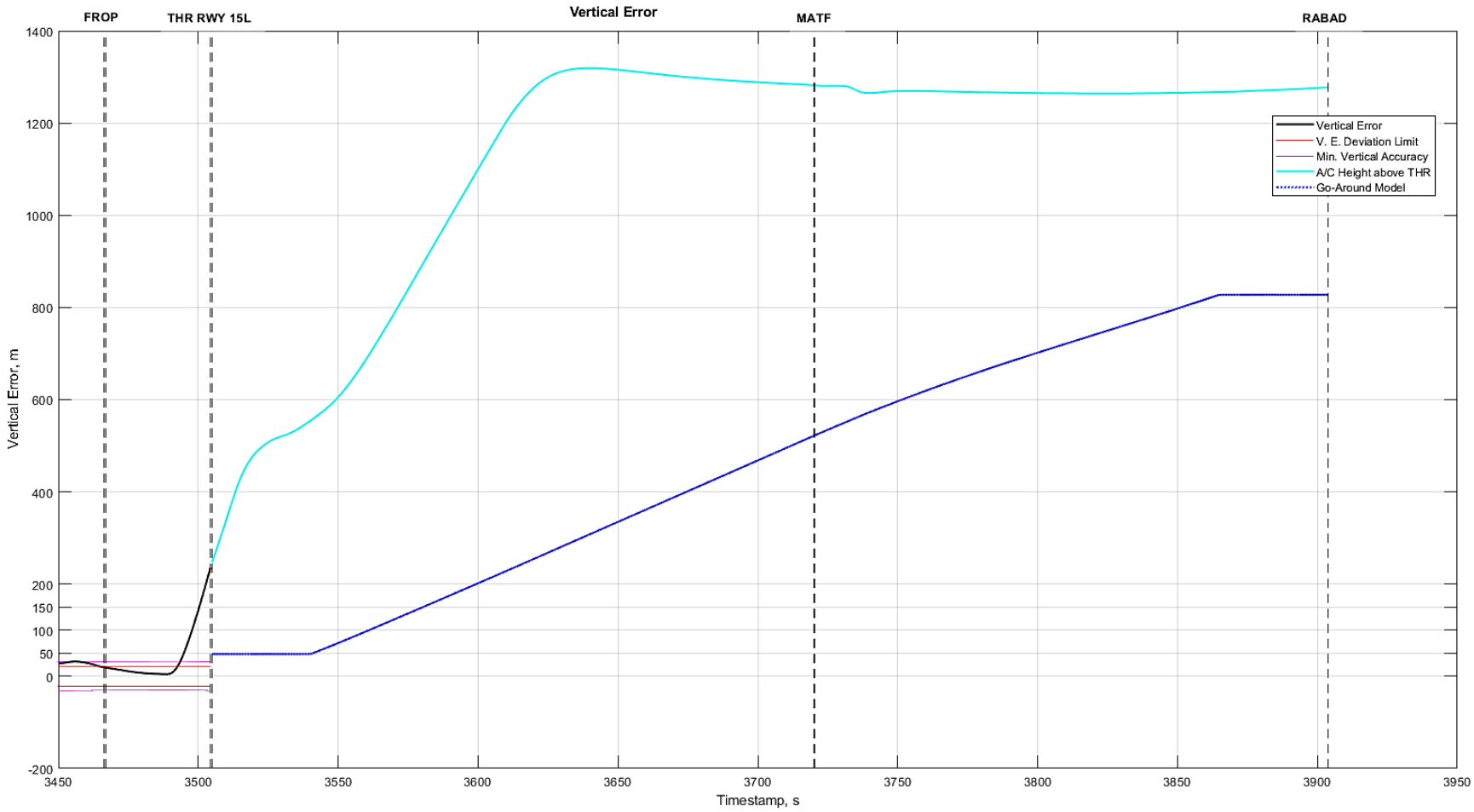

c) Vertical Error MAS [#4]

Fig. G4 Scenario 4

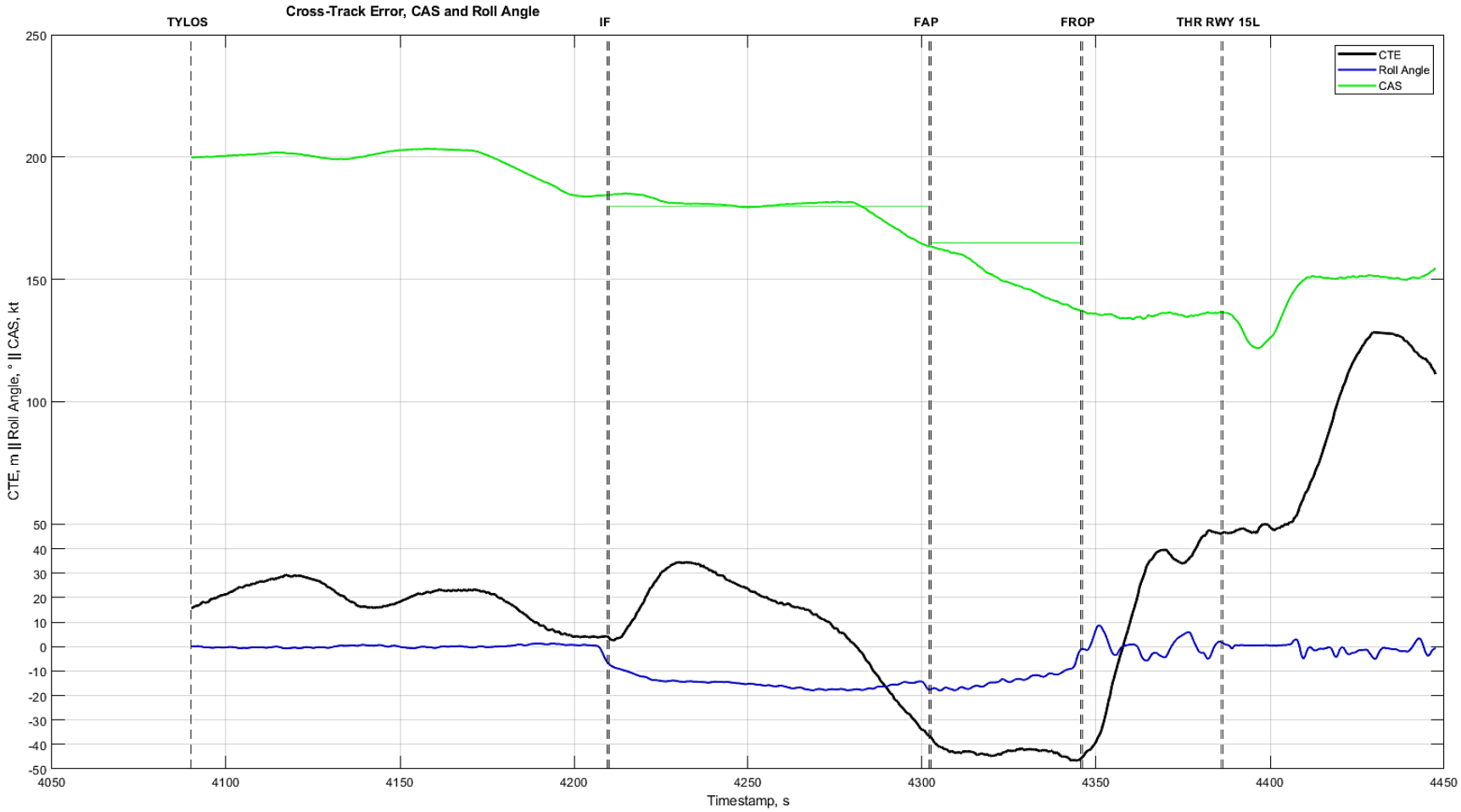

a) CTE, CAS and Roll Angle [#5]

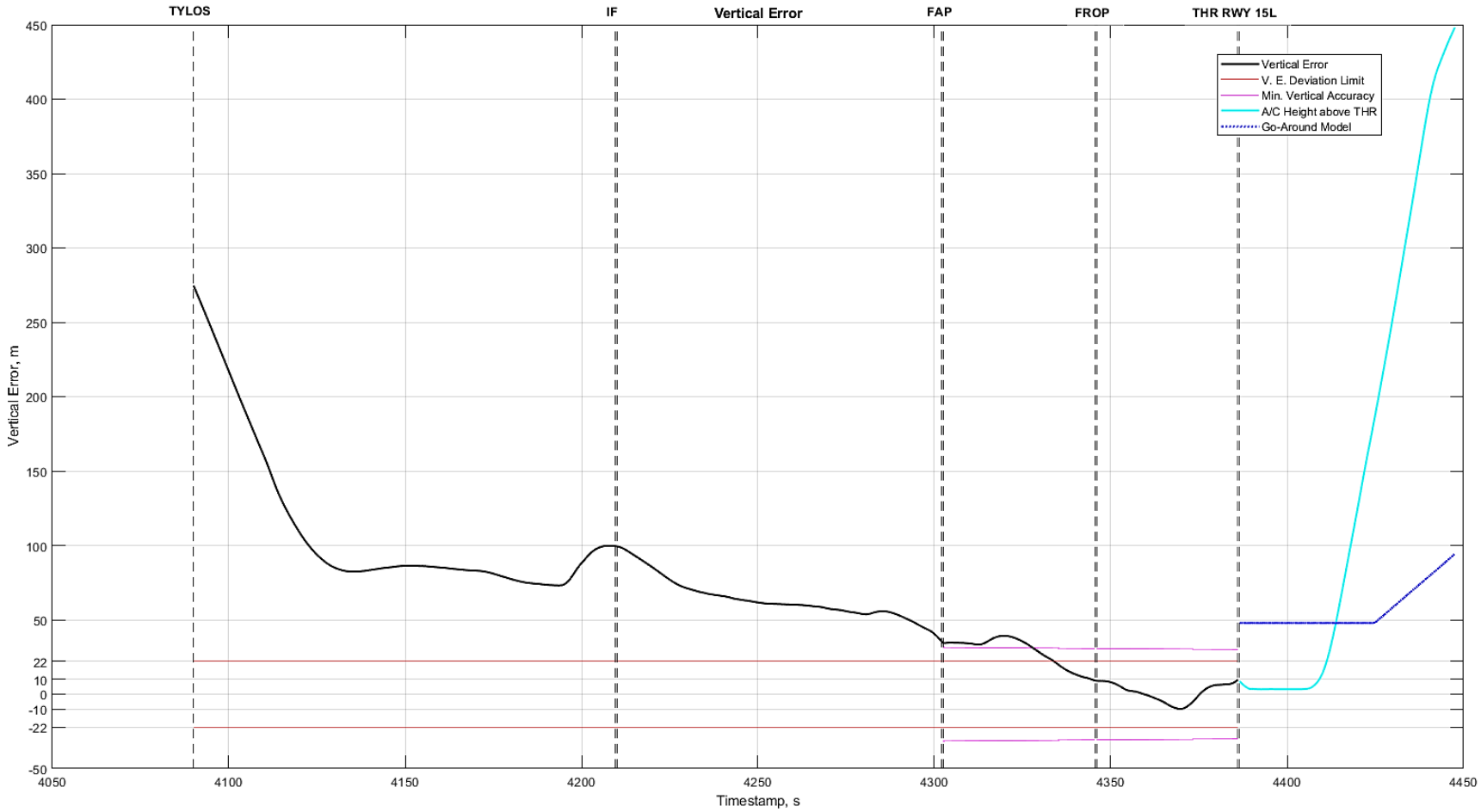

b) Vertical Error [#5]

Fig. G5 Scenario 5

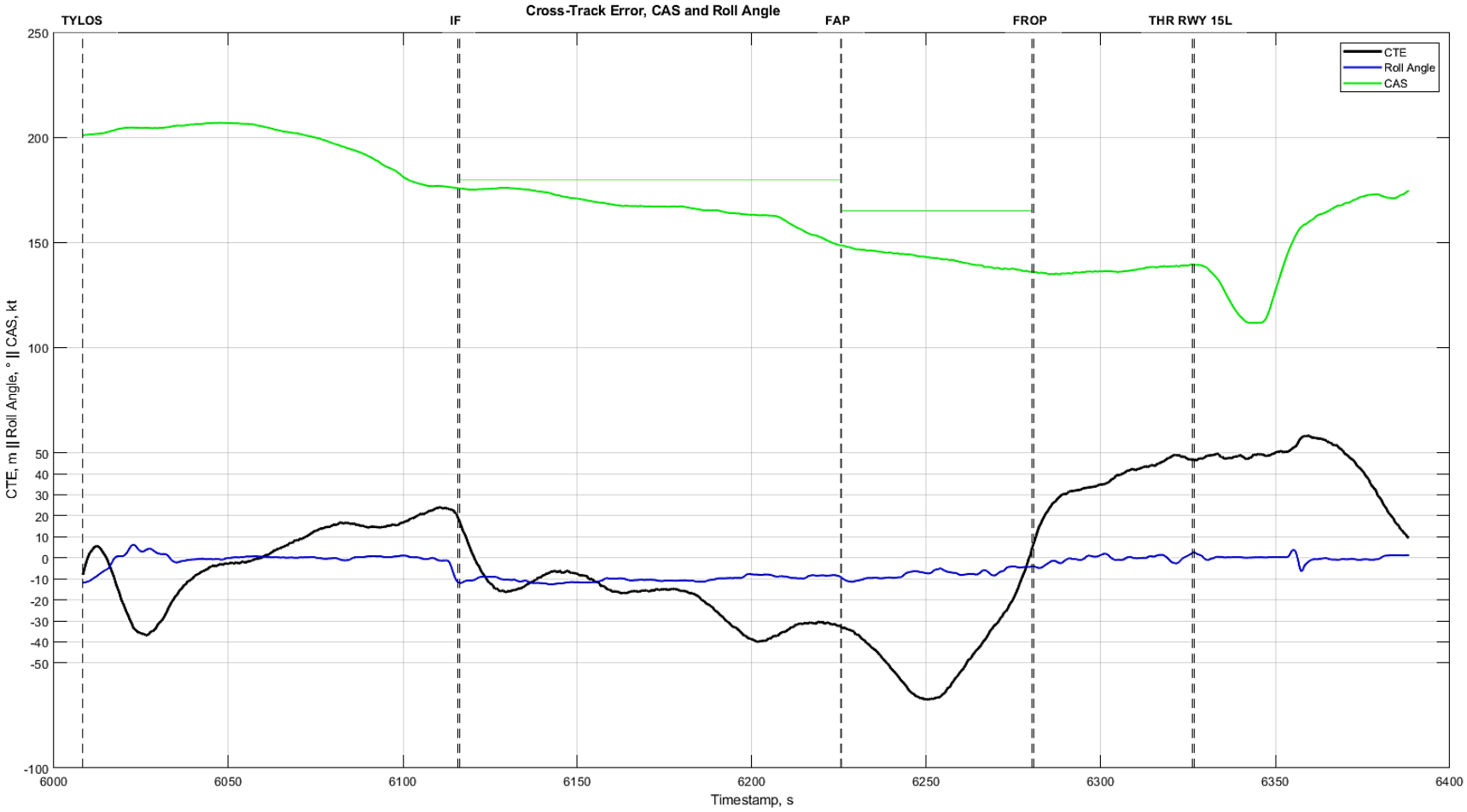

a) CTE, CAS and Roll Angle [#6]

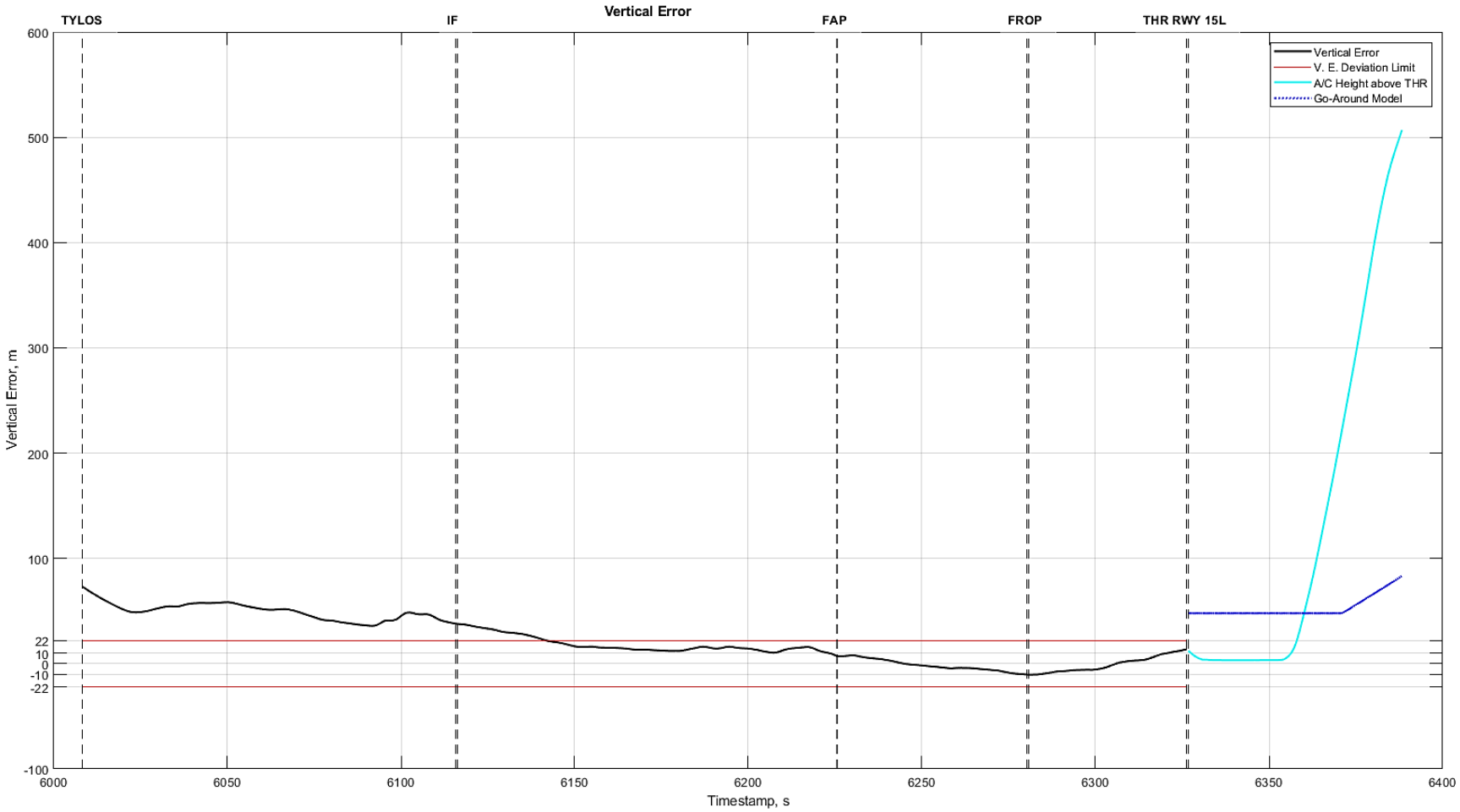

b) Vertical Error [#6]

Fig. G6 Scenario

List of literature

[1] Jackson, N., "Difficult landings part 2", *BALPA Blog*, 2017.
[2] Skrypnik, O., *Radio Navigation Systems for Airports and Airways*, Singapore: Springer Nature Singapore Pte Ltd., 2019, pp. 131ff.
[3] Dautermann, T., Ludwig, T., Geister, R., and Ehmke, L., "Extending access to localizer performance with vertical guidance approaches by means of an SBAS to GBAS receiver", *GPS Solutions*, Vol. 24, No. 2, 2020.
[4] ICAO, *Doc 9905, Required Navigation Performance Authorization Required (RNP AR) Procedure Design Manual, Second Edition*, Montreal: International Civil Aviation Organization, 2016.
[5] Civil Aviation Affairs, Qatar Civil Aviation Authority, *AIP BAHRAIN FIR*, Al Hidd: Civil Aviation Authority, 2020.
[6] NAV Portugal, *AIP PORTUGAL*, Lisbon: NAV Portugal, 2020, p. [LPMA AD 2.24.12-5].
[7] Austro Control, *AIP AUSTRIA*, Vienna: Austro Control, 2020, p. [LOWI AD 2.24-6-5-1].
[8] ICAO, *Doc 9613, Performance-based Navigation (PBN) Manual, Fourth Edition*, Montreal: International Civil Aviation Organization, 2013.
[9] ICAO, *Doc 8168, Procedures for Air Navigation Services - Aircraft Operations Volume II, Construction of Visual and Instrument Flight Procedures, Sixth Edition*, Montreal: International Civil Aviation Organization, 2014.
[10] *Commission Implementing Regulation (EU) 2018/1048*, Official Journal of the European Union L 189, 2018, pp. 3-8.
[11] EASA, *Certification Specifications and Acceptable Means of Compliance for Airborne Communications, Navigation and Surveillance CS-ACNS, Issue 2*, Cologne: European Aviation Safety Agency, 2019.
[12] Civil Aviation Affairs, *Civil Aviation Publication CAP 11 Volume 1 PBN Technology*, Al Hidd: Civil Aviation Affairs, 2017.
[13] Civil Aviation Affairs, *Civil Aviation Publication CAP 11 Volume 2 PBN Operational Approval*, Al Hidd: Civil Aviation Affairs, 2017.
[14] Civil Aviation Affairs, *Civil Aviation Publication CAP 11 Volume 3 PBN Specification Job Aids*, Al Hidd: Civil Aviation Affairs, 2017.
[15] Aimar, J., "Alaska Airlines Pioneers RNP RNAV Operation", *AERO*, No. 12, 2000, p. 37.
[16] FAA, *Advisory Circular 90-101, Approval Guidance for RNP Procedures with SAAAR*, Washington, D.C.: Federal Aviation Administration, 2005.
[17] FAA, *Order 8260.52, United States Standard for Required Navigation Performance (RNP) Approach Procedures with Special Aircraft and Aircrew Authorization Required (SAAAR)*, Washington, D.C.: Federal Aviation Administration, 2005.
[18] FAA, *Roadmap for Performance-Based Navigation*, Washington, D.C.: Federal Aviation Administration, 2006, pp.8-10.

[19] ICAO, *Doc 9613, Performance-based Navigation (PBN) Manual, Third Edition*, Montreal: International Civil Aviation Organization, 2008, p. [I-A-1-5].
[20] "What is SBAS?", *Gsa.europa.eu* Available: https://www.gsa.europa.eu/european-gnss/what-gnss/what-sbas.
[21] ICAO, *Annex 6: Operation of Aircraft: Part II – International General Aviation – Aeroplanes, Tenth Edition*, Montreal: International Civil Aviation Organization, 2018, p. [1.1-5].
[22] Kushwaha, P., "GAGAN-Extension to the Gulf Region - Joint ACAC/ICAO MID Workshop on GNSS 7th & 8th November 2017", 2017.
[23] ICAO, *Guide for Ground Based Navigation System Implementation*, Montreal: International Civil Aviation Organization, 2013, p. 11f.
[24] Drake, S., *DSTO–TN–0432, Converting GPS Coordinates (ϕλh) to Navigation Coordinates (ENU)*, Edinburgh, South Australia: DSTO Electronics and Surveillance Research Laboratory, 2002.
[25] Evans, P., "Rotations and rotation matrices", *Acta Crystallographica Section D*, Vol. 57, No. 10, 2001, pp. 1355-1357.
[26] "Transform local east-north-up coordinates to geodetic - MATLAB enu2geodetic- MathWorks Deutschland", *De.mathworks.com* Available: https://de.mathworks.com/help/map/ref/enu2geodetic.html.
[27] "Activities, Courses, Seminars & Webinars - ALC_Content - ALC-481: Student Pilot VFR Navigation Planning - Speed!", *Faasafety.gov* Available: https://www.faasafety.gov/gslac/ALC/course_content.aspx?cID=481&sID=784&preview=true.
[28] "July in Bahrain was hottest July since 1902", *https://www.bna.bh/en/* Available: https://www.bna.bh/en/JulyinBahrainwashottestJulysince1902.aspx?cms=q8FmFJgiscL2fwIzON1%2BDgKQvpLQ2cjjOtJ3XSamd84%3D.
[29] "Geographic globe plot - MATLAB geoplot3- MathWorks Deutschland", *De.mathworks.com* Available: https://de.mathworks.com/help/map/ref/geoplot3.html.
[30] "Create geographic globe - MATLAB geoglobe- MathWorks Deutschland", *De.mathworks.com* Available: https://de.mathworks.com/help/map/ref/geoglobe.html.
[31] "Jabal ad Dukhan, Bahrain", *peakbagger.com* Available: https://www.peakbagger.com/peak.aspx?pid=10475.
[32] ICAO, *Annex 14: Aerodromes, Volume I, Eighth Edition*, Montreal: International Civil Aviation Organization, 2018, p. [4-8].
[33] "Durrat Al Bahrain", *Durratbahrain.com* Available: http://www.durratbahrain.com/.
[34] "Bahrain's tallest buildings - Top 20", *Emporis.com* Available: https://www.emporis.com/statistics/tallest-buildings/country/100014/bahrain.
[35] "AIRAC", *Icao.int* Available: https://www.icao.int/safety/information-management/pages/airacadherence.aspx.

[36] "Lufthansa Aviation Training // FFS Airbus A320-200 ESS (FT76)", *Lufthansa-aviation-training.com* Available: https://www.lufthansa-aviation-training.com/training-devices/flight-training-devices/ffs-airbus-a320-200-ess-ft76/.
[37] ICAO, *Annex 3: Meteorological Service for International Air Navigation*, Montreal: International Civil Aviation Organization, 2018, p. [APP 3-2].
[38] Airbus, "A318/A319/A320/A321 Flight deck and systems briefing for pilots", 2007, pp. [10.4]ff..
[39] "Control your Speed… During Descent, Approach and Landing | Safety First", *Safetyfirst.airbus.com* Available: https://safetyfirst.airbus.com/control-your-speed-during-descent-approach-and-landing/.
[40] FAA, *Flight Standardization Board (FSB) Report: Airbus A318/A319/A320/A321/A330/A340 (5th revision)*, Washington, D.C.: Federal Aviation Administration, 2016, p.13.
[41] Data Access | National Centers for Environmental Information (NCEI)" [ISD search results for 'Bahrain'], *Ncei.noaa.gov* Available: https://www.ncei.noaa.gov/access/search/data-search/global-hourly?bbox=26.394,50.222,25.710,50.906&pageNum=6.
[42] "3-D point or line plot - MATLAB plot3- MathWorks Deutschland", *De.mathworks.com* Available: https://de.mathworks.com/help/matlab/ref/plot3.html.